

**Hydrogenolysis of biomass-derived furfural to 1,5-pentanediol
catalyzed by Ni-Y₂O₃**

January 2018

HUSNI WAHYU WIJAYA

Graduate School of Engineering

CHIBA UNIVERSITY

(千葉大学審査学位論文)

**Hydrogenolysis of biomass-derived furfural to 1,5-pentanediol
catalyzed by Ni-Y₂O₃**

January 2018

HUSNI WAHYU WIJAYA

Graduate School of Engineering

CHIBA UNIVERSITY

DEDICATION

This thesis work and research are dedicated to
The sake of Allah, the Sustainer of the worlds,
The last prophet Muhammad (blessings and peace of Allah be upon him),
My great parents who have always loved, supported, and blessed me unconditionally,
My beloved family, for encouraging and nursing me with affection and love and their
dedicated partnership for success in my life,
All my respected teachers and mentors, for without their inspiration, teaching, and
enthusiasm none of this would be achieved,
My friends who encourage and support me,
All the people in my life who touch my heart,

Abstract

This thesis deals with studies on the development of nickel catalyst for selective hydrogenolysis of biomass-derived furfurals to 1,5-pentanediol. The addition of yttrium or lanthanum into nickel formed a nickel-metal oxide catalyst which had a critical role for selective hydrogenolysis of furfural compounds in a different manner. The present thesis holds four chapters.

The author surveyed the background of 1,5-pentanediol production from biomass-derived furfurals compound in Chapter 1. A number of researchers designed the heterogeneous catalysts, M-MO_x catalyst system, for that reaction which achieved the highest selectivity of 1,5-pentanediol. Finally, the author pointed out the M-MO_x catalyst consisting of metal (M) and metal oxide (MO_x) is suited to promote the hydrogenolysis reaction of furfurals.

In Chapter 2, the preliminary study continued the addition of lanthanum to nickel catalyst which is prepared by coprecipitation, hydrothermal and subsequent hydrogen treatment. The catalyst has been evaluated in hydrogenolysis of furfural, furfuryl alcohol, and tetrahydrofurfuryl alcohol giving 1,5-pentanediol at mild reaction condition. The addition of yttrium instead of lanthanum provided similar catalytic performance.

In Chapter 3, focusing on the addition of yttrium into nickel catalyst (nickel-yttrium oxide) has been done utilizing the calcination as a pretreatment before the hydrogen treatment procedure which enhanced its acidity amount and catalytic activity. The hydrogenolysis of furfural, furfuryl alcohol, and tetrahydrofurfuryl alcohol on that catalyst produced 1,5-pentanediol at modest yield. The hydrogenation

of aldehyde group and furan ring initially proceeded then ring opening of tetrahydrofuran ring to pentanediols. The proposed mechanism of tetrahydrofurfuryl alcohol as a model compound revealed why the catalyst selectively produces 1,5-pentanediol.

The last chapter represented the addition of ruthenium on nickel-yttrium oxide catalyst accelerating the ring opening of tetrahydrofuran ring as a crucial key to obtaining 1,5-pentanediol. This approach has put forward new ideas to enhance the number of hydride species on catalyst surface while keeping the acidic site. The hydrogen uptake property and acidity amount analysis corroborated with that idea. The high yield of 1,5-pentanediol has been achieved from tetrahydrofurfuryl alcohol substrate at the optimized reaction conditions using nickel-yttrium oxide catalyst containing ruthenium.

CONTENTS

Abstract
Thesis structure

Chapter 1 Introduction

Abstract	1
1.1 General introduction	2
1.2 Development of nickel-based catalyst for hydrogenolysis of furfurals	7
1.2.1 Modified nickel catalyst for hydrogenolysis of furfural	8
1.2.2 Lanthanum and yttrium modified nickel catalyst	9
1.2.3 Ruthenium on Ni-M (M = Y or La) catalyst	10
1.3 Objective study	11
References	11

Chapter 2 Hydrogenolysis of furfural to 1,5-pentanediol over Ni-La and Ni-Y catalyst

Abstract	17
2.1 Introduction	17
2.2 Experimental procedure	20
2.2.1 Catalyst preparation	20
2.2.2 Catalyst characterization	21
2.2.3 Hydrogenolysis catalytic reaction	21
2.3 Result and discussion	22
2.3.1 XRD measurement of catalysts	22
2.3.2 Catalytic hydrogenolysis of furfurals	24
2.3.3 Study of reaction pathway	27
2.4 Conclusion	31
References	32

Chapter 3 Development of Ni-Y₂O₃ catalyst for producing 1,5-pentanediol from furfural and its hydrogenated compounds

Abstract	35
3.1 Introduction	36
3.2 Experimental procedure	37
3.2.1 Catalyst preparation	37
3.2.2 Catalytic hydrogenolysis reaction	38
3.2.3 Characterization of Ni-Y ₂ O ₃ catalyst	39
3.3 Properties of Ni-Y ₂ O ₃ catalyst	40
3.4 Catalytic hydrogenolysis of furfural (FFR)	44
3.4.1 Hydrogenolysis of FFR in various Ni-Y ₂ O ₃ catalysts	44
3.4.2 Investigation of reaction conditions	46

3.4.3 Time profile and reaction pathway	47
3.5 Catalytic hydrogenolysis of furfuryl alcohol (FFA)	49
3.5.1 Hydrogenolysis of FFA in various Ni-Y ₂ O ₃ catalysts	49
3.5.2 Evaluation of reaction conditions	51
3.5.3 Investigation of time course and reaction pathway	53
3.5.4 Reusability test	54
3.5.5 Hydrogenolysis of furanic compounds	56
3.6 Catalytic hydrogenolysis of tetrahydrofurfuryl alcohol (THFA)	57
3.6.1 Hydrogenolysis of THFA in various Ni-Y ₂ O ₃ catalysts	57
3.6.2 Evaluation of reaction conditions	59
3.6.3 Effect of solvent	61
3.6.4 Time course	62
3.6.5 Reusability test	63
3.6.6 Ring opening of cyclic ether to terminal diols	64
3.7 Investigation of THFA hydrogenolysis mechanism	66
3.7.1 Dependency of substrate and catalyst	67
3.7.2 Poisoning experiment	68
3.7.3 Proposing a mechanism of the ring opening of THFA	69
3.8 Surface catalyst characterization	72
3.9 Conclusion	74
References	75

Chapter 4 Improvement of Ni-Y₂O₃ catalyst by the addition of ruthenium to accelerate the C-O bond cleavage

Abstract	79
4.1 Introduction	80
4.2 Experimental procedure	81
4.2.1 Preparation of ruthenium modified Ni-Y ₂ O ₃ catalyst	81
4.2.2 Catalytic hydrogenolysis of THFA	82
4.2.3 Characterization of ruthenium modified Ni-Y ₂ O ₃ catalyst	82
4.3 Result and discussion	83
4.3.1 Screening of the third metal addition on the Ni-Y ₂ O ₃ catalyst	83
4.3.2 Ruthenium modified Ni-Y ₂ O ₃ catalyst properties	85
4.3.3 Catalytic hydrogenolysis of THFA	90
4.3.4 Time course	95
4.3.5 Reusability test	96
4.3.6 FT-IR study of the absorbed THFA	97
4.3.7 XPS analysis of Ru/Ni-Y ₂ O ₃ catalysts	98
4.3.8 Ring opening of cyclic ether to terminal diols	101
4.4 Conclusion	101
References	102

Chapter 5 Summary 105

Bibliography

Acknowledgment

In the Name of Allah, the Most Gracious and the Most Merciful.

I would like to express my gratitude to Professor Shogo Shimazu for outstanding advice, guidance, encouragement, and support throughout the present work and my doctoral degree. I deeply thanks and grateful to Professor Nobuyuki Ichikuni and Associate Professor Takayoshi Hara for valuable advice, numerous discussion, and encouragement. Hearty thanks to the committee members, Prof. Satoshi Sato and Prof. Masami Sakamoto, for their helpful and useful suggestion.

My sincerely to all members of the members of Shimazu Laboratory. Thanks a lot, to Wahyu S. Putro for helping to settle in trial experiment stuff. My deeply indebted to Dr. Takashi Kojima for taking TEM analysis and JEOL company for taking XPS analysis.

I acknowledge to Ministry of Education, Culture, Sports, Science, and Technology (MEXT) Scholarship for conducting Doctor Program in Graduate School of Engineering, Chiba University.

Finally, I extend my thanks to my wife (Viruzi Axellina), my daughter (Hikari Nixel Azzahra), my parents, my brothers, and Prof. Effendy for *do`a* and cheerful encouragement. Thanks to Civitas Faculty of Mathematics and Science, State University of Malang (*Universitas Negeri Malang*) for supporting my study.

Husni Wahyu Wijaya

2018

Chapter 1

Introduction

ABSTRACT. In recent years, development of heterogeneous catalysts to obtain 1,5-pentanediol from biomass derived-furfurals has turned fascinating research and the modified noble metal with reducible metal oxide has been a suitable candidate catalyst for that organic transformations. Those catalysts ease the hydride and proton formation in their catalytic system which is critical to ring opening furan ring giving pentanediol. Dealing with such properties, the addition of metal oxide into nickel catalyst is challenging effort since nickel metal is inactive in this reaction. In this study, we have been developed the addition of lanthanum or yttrium into nickel catalyst and evaluated in catalytic hydrogenolysis of furfural, furfuryl alcohol, and tetrahydrofurfuryl alcohol to 1,5-pentanediol. Then, we propose to take the further approach gaining the high yield of 1,5-pentanediol by calcining and adding ruthenium of nickel-yttrium oxide catalyst.

1.1 General introduction

Biomass as renewable and abundant resources is an alternative option to supersede fossil fuels for sustaining energy and chemicals. Lignocellulosic feedstock as a second-generation biofuel from non-edible resources like agricultural wastes (straw, corn stover, and bagasse) has been evaluated in biorefinery system to supply biomass-derived compound and fuels.^{1,2} Based on U.S. Department of Energy recommendation of the potential top 30 building block candidates from sugar compounds, furfural (FFR) is one of the promising starting compounds to produce fuels and chemicals.³ Many researchers have been reported the utilization of FFR to obtain valuable fine chemicals and fuels, including.⁴⁻⁶

Transformation of FFR as biomass derived compound and its hydrogenation products such as furfuryl alcohol (FFA) and tetrahydrofurfuryl alcohol (THFA), and then terminal pentanediol or 1,5-pentanediol (1,5-PeD) outlines in Figure 1.1.⁷ The 1,5-PeD with an uneven aliphatic carbon chain and terminal diols has been used as a building block in producing polyesters, thermoplastics, polyurethanes, and as a plasticizer monomer.⁸ Among pentanediols, the 1,5-PeD is the demanding product for substituting 1,6-hexanediol (1,6-HDO) as a monomer while it obtains from petrochemical fuel.⁹ The polyesters from 1,5-PeD are safer than from 1,4-butanediol, especially in children's toys.¹⁰ For that reason and demand, the production of 1,5-PeD through the hydrogenolysis of biomass furfural and its derivative is a paramount challenge from the scientific, economic, environmental, and industrial aspect.

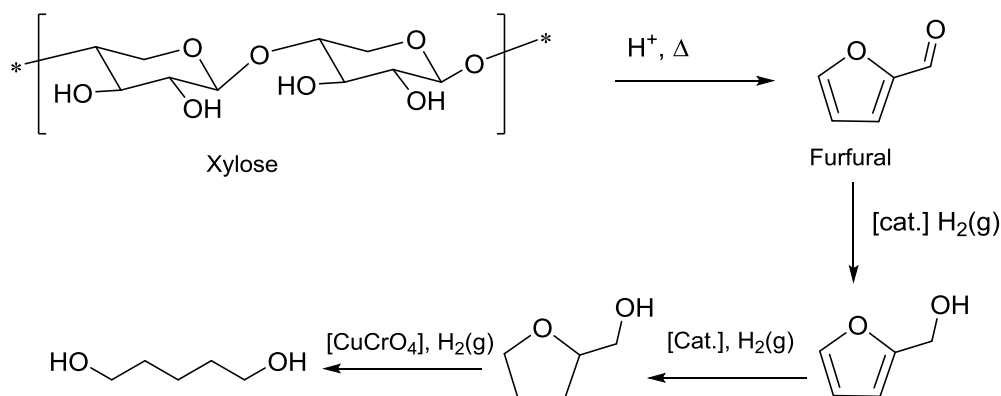


Figure 1.1 Pathway for the conversion of xylose (hemicellulose) to 1,5-pentanediol. (Reproduced from ref. [7] with permission from The Royal Society of Chemistry)

Synthesis of 1,5-PeD starting from THFA through 3,4-dihydro-2H-pyran formation step has been established firstly in 1945's employing $\gamma-Al_2O_3$ and copper chromite as illustrated in Figure 1.2.¹¹ The environmental point of view infer that designing of the heterogeneous catalyst using transition and noble metals is crucial as an alternate catalyst regarding the high demand of 1,5-PeD especially from non-edible biomass compounds. The activation of the hydrogen molecule is essential before H inserting step which leads to C-O bond cleavage of furan or tetrahydrofuran ring giving the desired product, 1,5-PeD. For that reason, the heterogeneous catalysts of hydrogenation reaction which include noble metal (Pd, Pt, Rh, Ir, Ag, or Ru) and non-noble metal (Cu or Ni) are the candidate for this reaction. Collaboration with metal oxide support and a modifier as well could be challenged for new catalyst development.

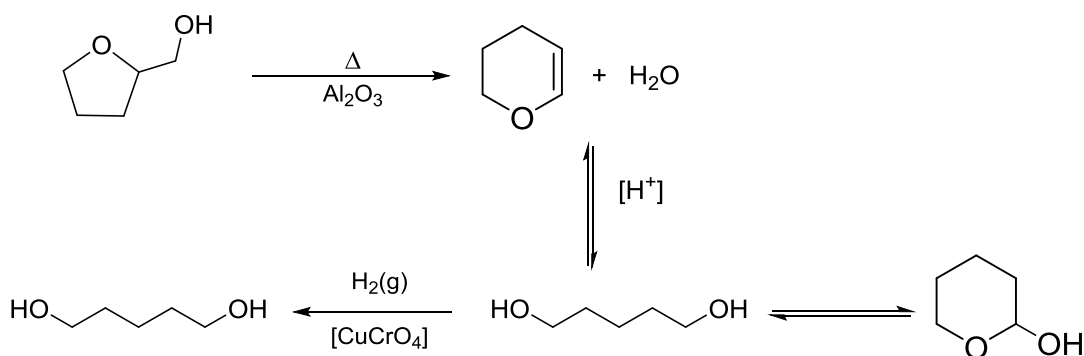


Figure 1.2 Showed three-step process for transformation of tetrahydrofurfuryl alcohol to 1,5-pentanediol (1,5-PeD). (Reproduced from ref. [7] with permission from The Royal Society of Chemistry).

Seeking the non-toxic catalyst to obtain 1,5-PeD has been conducted and development of Noble based catalyst is great alterability from the point of view of activity and predictability. Monometallic noble metal (Rh or Ru) supported SiO_2 or C firstly reported giving 1,5-PeD (< 20% selectivity) from THFA under 8 MPa pressurized H_2 gas and drastically enhanced up to 94.2% selectivity by adding ReO_x as a modifier to Rh supported catalyst.¹² Controlling Rh/Re mol ratios allowed to enhance the activity for direct hydrogenolysis of FFR to 1,5-PeD up to 91.3% selectivity with 51.6% conversion.¹³ Alteration of ReO_x with WO_x and MoO_x also experimented and Rh- MoO_x gave a similar catalytic performance. The proposed mechanism in hydrogenolysis of THFA on Rh-based catalyst suggest the attachment of deprotonated THFA molecule on ReO_x surface then the regioselective attack of hydride from the side of CH_2OH group and subsequent protonation of the anion formed 1,5-PeD as illustrated in Figure 1.3.^{14,15} However, Ir- $\text{ReO}_x/\text{SiO}_2$ catalyzed of FFR giving 17% yield of 1,4-pentanediol (1,4-PeD) rather than the other pentanediol for 24 h (6 MPa H_2 , 393 K).¹⁶ Another research group evaluated the addition of

MoO_x instead of ReO_x in various noble metal (Ir, Pd, Pt, Ru, or Rh) supported SiO₂ revealed that Rh-MoO_x/SiO₂ catalyst seemingly resulted in the highest 1,5-PeD from THFA with a similar mechanism.¹⁷ A mechanistic study in Rh-MoO_x/SiO₂ reveals that the ring opening of tetrahydrofuran group of THFA occurred on the acidic molybdate surface (H_xMO₃) giving 1,5-PeD as a preferable product.¹⁸ Up to now, employing the C as a support of Rh-ReO_x/C catalyst achieved the highest yield of 1,5-PeD (96%) with the same reaction mechanism.¹⁹ Briefly, the addition of reducible metal oxide which acts as acidic site into Noble metal is applicable to opening tetrahydrofuran ring, although their activities are found wanting as well.

Alteration of ReO_x and MoO_x as reducible metal oxides support affected by the desired pentanediol product. Dispersing of Pt (1.9%wt.) on CoAlO₄ prepared by coprecipitation provided mild reaction conditions (1.5 MPa H₂, 413 K) obtaining 1,5-PeD (24.6% yield) from furfural along with 1,2- and 1,4-PeD.²⁰ The ring opening of furan ring ascribes to the existence of CoO_x in particular Co³⁺ ion on that catalyst. Exploration of the basic support such as hydrotalcite (HT) for noble metals (Pd, Pt, Ir, Ag, Rh, and Ru) turned the product selectivity of FFR hydrogenolysis and only Pt/HT afforded to give 1,2-PeD (73% yield) using 2-propanol as solvent (3 MPa H₂, 423 K).²¹ Employing MnO_x as a support for dispersing Ru preferentially also directed on the 1,2-PeD formation starting from FFA (1.5 MPa H₂, 423 K) but hardly formed any pentanediol in the case of THFA.²² The recent update in this reaction resulted 1,5-PeD up to 35% yield using 5%Pt/WO₃/ZrO₂ catalyst which elaborated the role of reducible WO_x as an acidic site.²³ The above-reported work seemingly acknowledged the existence of basic site on the support driving the pentanediol selectivity and availability on tuning the targeted diol.

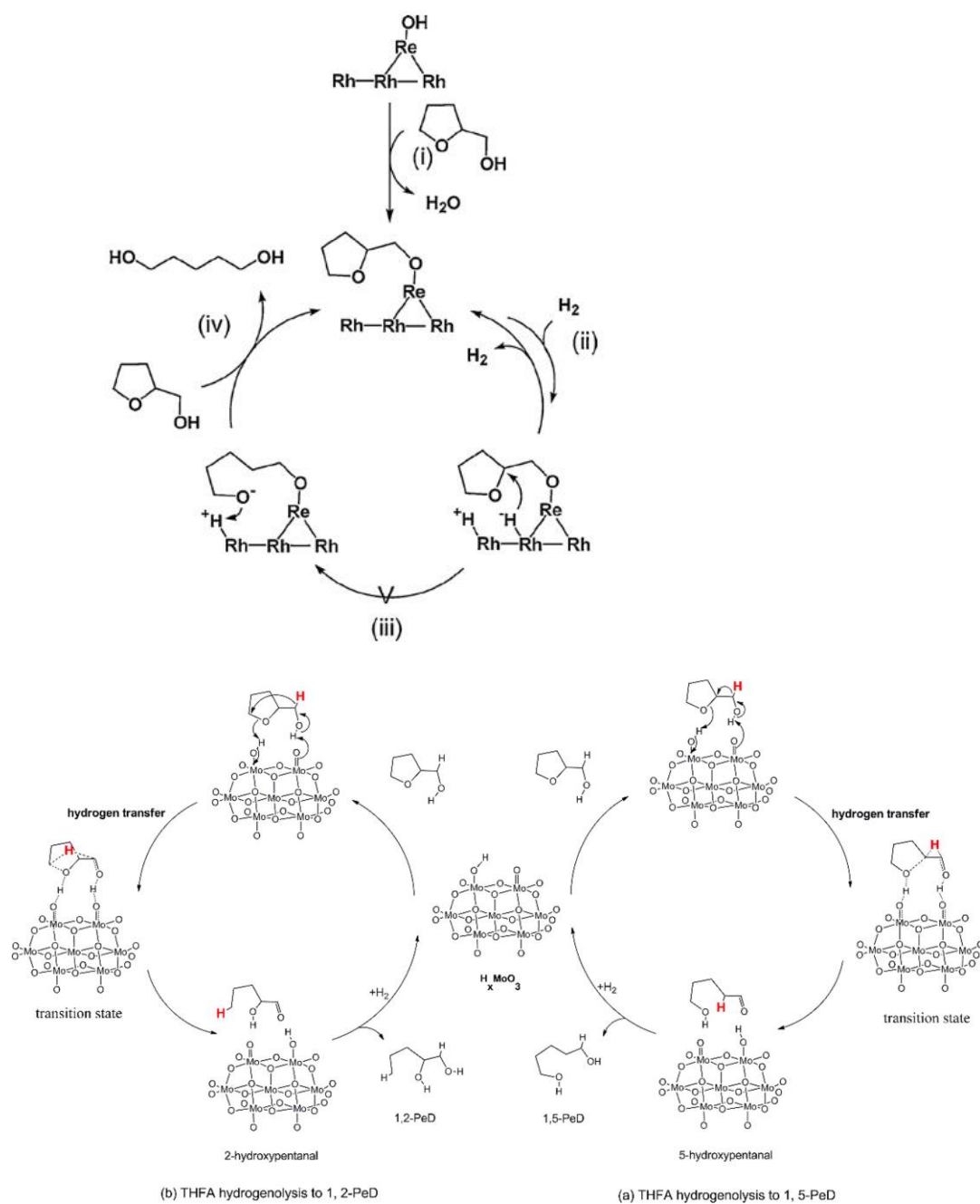


Figure 1.3 (Top) Proposed mechanism of THFA hydrogenolysis over Rh-ReO_x/SiO₂. (Bottom) Possible reaction pathway for the selective C–O bond cleavage from THFA to produce 1,5-PeD and 1,2-PeD over H_xMoO₃ catalyst (Copied from ref. [15] with ACS permission and ref. [18] with Elsevier permission).

Hydrogenolysis of FFR is paramount importance route to achieve a straightforward way producing pentanediol directly in particular of 1,5-PeD. A 2-step together,

hydrogenation and hydrogenolysis reaction, occurs in case of FFR as well as FFA hydrogenolysis and the formation of polymerized-product is delicate matters obviously. The addition of a noble metal such as Rh or Pd into Ir-ReOx/SiO₂ catalyst and applying two-step reaction temperature which expects to suppress polymerization reaction was experimented enhancing the yield of 1,5-PeD up to 65.8%.^{16,24} Up to now, this approach successfully achieves the highest yield 1,5-PeD directly from FFR. Additionally, all those achievements stimulate the search for a non-noble catalyst which enables to open other novelty in this process.

1.2 Development of Ni-based catalyst for hydrogenolysis furfurals

Utilization of Ni-based catalysts in an organic synthesis which is more active than Pd- and Pt-catalyzed requires much more effort to achieve the predicted outcome.²⁰ Modification of nickel as a single component is open a remarkable opportunity to develop a new nickel-based catalyst to meet the activity, selectivity, and stability criteria for targeted catalytic reaction, particularly in the heterogeneous catalyst. Nickel bimetallic catalysts have been developed giving the superior properties and catalytic performances in particular in hydrogenation and reforming reaction compare to their monometallic itself.²⁵ Our group has been reported a novelty of introducing an electropositive metal such as Sn and Fe to nickel forming corresponding Ni alloy which suppresses its activity to be highly selective for hydrogenation α , β -unsaturated aldehyde giving α , β -unsaturated alcohol.²⁶⁻²⁸ Recently, we escalate applying Ni-modified catalyst of an alternate noble metal to hydrogenolysis of furfural giving 1,5-PeD which is one burgeoning research area to obtain α , ω -diol from biomass-derived furfurals.

1.2.1 Modified nickel catalyst for hydrogenolysis of furfurals

Up to now, catalytic hydrogenolysis of furfural and derivatives to pentanediols have been achieved employing the noble metal-based by modifying with the reducible metal oxide as explained earlier. Exploiting of an alternate catalyst such as nickel and copper has been reported for those substrates as reported elsewhere.^{29,30} Ni phyllosilicate catalyst only hydrogenated C=C and C=O bonds of FFR without pentanediol formation.²⁹ The existence of an acidic Al₂O₃ in Cu-Al₂O₃ and Ni-Al₂O₃ catalysts catalyzed FFA (8 MPa H₂, 413 K) giving 1,5-PeD only 13.7% and 1.3% yield, respectively.³⁰ The recent report showed that alloying Ni-Cu on MgAlO support with acidic surface gave 1,2-PeD and 1,5-PeD less than 5% yield.³¹ It means that the modified nickel catalysts particularly inclined to be discontented as they achieved a low yield of 1,5-PeD.

Persevering in the addition of second metal to Ni catalyst to tune its catalytic activity, the addition of lanthanum as non-reducible metal oxide extended employing the Ni-based catalyst for hydrogenolysis of biomass derived-furfurals. Lanthanum oxide is known to act on the decomposition of 4-hydroxy-4-methyl-pentanone and isomerization of 1-butene.³² The unsaturated bond of both substrates may absorb on the La₂O₃ surface during the catalytic reaction. Dehydration of 2-propanol on the surface through a hydrogen bond with the anionic hydroxyl group of La₂O₃ created surface acidic hydroxyl group with acidic character.³³ That acidic character could be acted like HxMoO₃ which is active for ring opening furan ring as mentioned earlier. Lanthanum complexes, ligated by a ferrocene-based-type ligand were highly active for ring opening polymerization of lactide and ϵ -caprolactone.³⁴ Our previous works

proved that the addition of lanthanum formed Ni-La catalyst was active and selective for hydrogenolysis of furfurals to 1,5-PeD under moderate condition.³⁵

Those successful works lead to enhance the ring opening of furan ring as well as tetrahydrofuran ring and achieve the high yield of 1,5-PeD. For that goal, the addition of yttrium oxide (Y_2O_3) instead of La_2O_3 could be secure approach regarding their relationship on Periodic Table. The catalytic activity of Y_2O_3 seemingly active for decomposition of 4-hydroxy-4-methyl-pentanone and isomerization of 1-butene,³² dehydration 2-propanol to acetone,³⁶ and highly active for ring opening polymerization of ϵ -caprolactone,³⁷ in which run with the similar manner of La_2O_3 . Finally, the addition of lanthanum or yttrium into Ni catalyst could be offered a remarkable opportunity achieving the high yield of 1,5-pentanediol from furfurals as the main concern for this research.

1.2.2 Lanthanum and yttrium modified nickel catalyst

Modification nickel with Y_2O_3 and La_2O_3 has been used as support or additive in reforming reaction. Ethanol steam reforming to hydrogen production on Ni/ La_2O_3 and Ni/ Y_2O_3 catalysts have been reported possessing a good stability and high catalytic activity and selectivity of hydrogen formation compared to Ni/ Al_2O_3 .³⁸ The surface oxygen mobility in particular on the Y_2O_3 support is a key factor for its better catalytic activity than Ni/ Al_2O_3 catalyst.³⁹ Crystallite size of Y_2O_3 support affects that property, not dispersion and particle size of a nickel.⁴⁰ The addition of Y_2O_3 as a modifier to Ni/ Al_2O_3 affected for enhancing catalytic activity and catalyst stability in the autothermal reforming of methane than Ni/ Al_2O_3 and Ni/ Y_2O_3 .⁴¹ They proposed an intermediate surface compound between Ni and Y_2O_3 which reduced the coke

formation. Besides that, dehydrogenation and hydrogenolysis rate for cyclohexane dehydrogenation at 533 K gave an analogous manner.

The addition of La_2O_3 as a modifier in $\text{Ni}/\text{Al}_2\text{O}_3$ catalyst has its eminence for steam reforming reaction. The addition of La at optimized control (1.78%wt.) had that superior activity and stability in the CO_2 reforming of methane corresponds to a higher dispersion of Ni, stability on the cooking formation, and chemical effect of La on the catalyst.⁴² Preparation Ni-Al-La catalyst by coprecipitation has positive effect expressing better in metal dispersion, cook resistance, and slightly high conversion.⁴³ Preparation through hydrotalcite route enhanced the catalytic performance of Ni-Al-La catalyst giving an excellence yield hydrogen.⁴⁴ The addition of La or Y into Ni-based catalysts mostly enhance their catalytic activity expressing in good metal dispersion and cook resistance which may present a great benefit in the biomass-derived furfural conversion.

1.2.3 Ruthenium on Ni-M (M = La or Y) catalyst

Previously, Ni catalyst has the highest catalytic activity compared to Pd and Pt catalysts.²⁰ The high efficiency of Ni catalyst to alloy with all noble metals, in particular, make easier to develop nickel bimetallic catalysts provide a distinct property and excellent in catalytic reaction than its monometallic counterpart.²⁵ I case of the hydrogenation reaction, bimetallic Ni-Noble metal catalyst performed an excellent catalytic activity. That review inspires an exploration on bimetallic Ni-noble metal particularly ruthenium to achieve a high yield of 1,5-PeD from hydrogenolysis THFA because attacking of the formed hydride species is a key for ring opening of tetrahydrofuran ring based on reaction mechanism in Figure 1.4 (top). Our hypothesis, enhancing the hydride formation on catalyst surfaces could be

accelerated the C-O bond cleavage of tetrahydrofuran ring leading to the higher yield of pentanediol. To that extent, the addition of ruthenium to Ni-Y₂O₃ and Ni-La₂O₃ catalysts will be included in this study.

1.3 Objective study

Transformation of biomass-derived FFR and its hydrogenation product such as FFA and THFA through hydrogenolysis reaction under atmospheric hydrogen gas to obtain 1,5-PeD by employing Ni-based catalyst is the focus of this Thesis. To achieve that goal, development Ni-based catalyst with the addition of lanthanum or yttrium has experimented both catalyst preparation and catalytic reaction. Evaluation of catalytic behavior includes the optimum reaction condition, effect of solvent, time course, and reaction mechanism studies. To enhance the yield of 1,5-PeD, the presenting of ruthenium on yttrium added Ni catalyst has been carried out in this study.

ABBREVIATIONS

FFR: furfural	1,2-PeD, 1,2-pentanediol
FFA: furfuryl alcohol	1,4-PeD: 1,4-pentanediol
THFA: tetrahydrofurfuryl alcohol	1,5-PeD: 1,5-pentanediol

REFERENCES

- 1 S. N. Naik, V. V. Goud, P. K. Rout and A. K. Dalai, *Renew. Sustain. Energy Rev.*, 2010, **14**, 578–597.
- 2 R. A. Sheldon, *Green Chem.*, 2014, **16**, 950–963.
- 3 T. Werpy and G. Petersen, *Top Value Added Chemicals from Biomass Volume I - Results of Screening for Potential Candidates from Sugars and Synthesis Gas Top Value Added Chemicals From Biomass Volume I: Results of*

- Screening for Potential Candidates*, 2004, vol. 1.
- 4 S. Dutta, S. De, B. Saha and I. M. Alam, *Catal. Sci. Technol.*, 2012, **2**, 2025–2036.
 - 5 H. G. Bernal, L. Bernazzani and A. M. Raspolli Galletti, *Green Chem.*, 2014, **16**, 3734–3740.
 - 6 D. Sun, S. Sato, W. Ueda, A. Primo, H. Garcia and A. Corma, *Green Chem.*, 2016, **18**, 2579–2597.
 - 7 M. Schlaf, *Dalt. Trans.*, 2006, 4645–4653.
 - 8 P. Werle, M. Morawietz, S. Lundmark, K. Sørensen, E. Karvinen and J. Lehtonen, in *Ullmann's Encyclopedia of Industrial Chemistry*, 2012, vol. 2, pp. 263–284.
 - 9 Markets and Markets, *1,6-Hexanediol Market by Application (Polyurethanes, Coatings, Acrylates, Adhesives, Polyester Resins, Plasticizers), and Region (Europe, North America, Asia-Pacific, South America, and Middle East & Africa) - Global Forecasts to 2021*, 2016.
 - 10 M. Perry, J. Pomfret and R. Crabb, *Reuters*, 2007.
 - 11 L. E. Schniepp and H. H. Geller, *J. Am. Chem. Soc.*, 1946, **68**, 1646–1648.
 - 12 S. Koso, I. Furikado, A. Shima, T. Miyazawa, K. Kunimori and K. Tomishige, *Chem. Commun.*, 2009, 2035.
 - 13 M. Chia, Y. J. Pagán-Torres, D. D. Hibbitts, Q. Tan, H. N. Pham, A. K. Datye, M. Neurock, R. J. Davis, J. A. Dumesic, Y. J. Pag, Y. J. Pagán-Torres, D. D. Hibbitts, Q. Tan, H. N. Pham, A. K. Datye, M. Neurock, R. J. Davis and J. A. Dumesic, *J. Am. Chem. Soc.*, 2011, **133**, 12675–12689.
 - 14 S. Koso, N. Ueda, Y. Shinmi, K. Okumura, T. Kizuka and K. Tomishige, *J.*

- Catal.*, 2009, **267**, 89–92.
- 15 S. Koso, Y. Nakagawa and K. Tomishige, *J. Catal.*, 2011, **280**, 221–229.
 - 16 S. Liu, Y. Amada, M. Tamura, Y. Nakagawa and K. Tomishige, *Green Chem.*, 2014, **16**, 617.
 - 17 Z. Wang, B. Pholjaroen, M. Li, W. Dong, N. Li, A. Wang, X. Wang, Y. Cong and T. Zhang, *J. Energy Chem.*, 2014, **23**, 427–434.
 - 18 J. Guan, G. Peng, Q. Cao and X. Mu, *J. Phys. Chem. C*, 2014, **118**, 25555–25566.
 - 19 K. Chen, S. Koso, T. Kubota, Y. Nakagawa and K. Tomishige, *ChemCatChem*, 2010, **2**, 547–555.
 - 20 V. P. Ananikov, *ACS Catal.*, 2015, **5**, 1964–1971.
 - 21 T. Mizugaki, T. Yamakawa, Y. Nagatsu, Z. Maeno, T. Mitsudome, K. Jitsukawa and K. Kaneda, *ACS Sustain. Chem. Eng.*, 2014, **2**, 2243–2247.
 - 22 B. Zhang, Y. Zhu, G. Ding, H. Zheng and Y. Li, *Green Chem.*, 2012, **14**, 3402–3409.
 - 23 S. Feng, A. Nagao, T. Aihara, H. Miura and T. Shishido, *Catal. Today*, 2017, 3–8.
 - 24 S. Liu, Y. Amada, M. Tamura, Y. Nakagawa and K. Tomishige, *Catal. Sci. Technol.*, 2014, **4**, 2535–2549.
 - 25 S. De, J. Zhang, R. Luque and N. Yan, *Energy Environ. Sci.*, 2016, **9**, 3314–3347.
 - 26 Rodiansono, S. Khairi, T. Hara, N. Ichikuni and S. Shimazu, *Catal. Sci. Technol.*, 2012, **2**, 2139.
 - 27 W. S. Putro, T. Hara, N. Ichikuni and S. Shimazu, *Chem. Lett.*, 2017, **46**, 149–

- 151.
- 28 W. S. Putro, T. Kojima, T. Hara, N. Ichikuni and S. Shimazu, *Catal. Sci. Technol.*, 2017, **7**, 3637–3646.
- 29 X. Kong, Y. Zhu, H. Zheng, X. Li, Y. Zhu and Y.-W. Li, *ACS Catal.*, 2015, **5**, 5914–5920.
- 30 H. Liu, Z. Huang, H. Kang, C. Xia and J. Chen, *Chinese J. Catal.*, 2016, **37**, 700–710.
- 31 J. Wu, G. Gao, J. Li, P. Sun, X. Long and F. Li, *Appl. Catal. B Environ.*, 2017, **203**, 227–236.
- 32 Y. Fukada, H. Hattori and K. Tanabe, *Bull. Chem. Soc. Jpn.*, 1978, **51**, 3150–3153.
- 33 G. A. M. Hussein and B. C. Gates, *J. Chem. Soc. Faraday Trans.*, 1996, **92**, 2425.
- 34 C. Hermans, W. Rong, T. P. Spaniol and J. Okuda, *Dalt. Trans.*, 2016, **45**, 8127–8133.
- 35 H. Tange, Master Thesis, 千葉大学, 2015.
- 36 G. A. M. Hussein and B. C. Gates, *J. Catal.*, 1998, **176**, 395–404.
- 37 X. Wang, J. L. Brosmer, A. Thevenon and P. L. Diaconescu, *Organometallics*, 2015, **34**, 4700–4706.
- 38 J. Sun, X. P. Qiu, F. Wu and W. T. Zhu, *Int. J. Hydrogen Energy*, 2005, **30**, 437–445.
- 39 G. Sun, K. Hidajat and S. Kawi, *Chem. Lett.*, 2006, **35**, 1308–1309.
- 40 G. B. Sun, K. Hidajat, X. S. Wu and S. Kawi, *Appl. Catal. B Environ.*, 2008, **81**, 303–312.

- 41 D. C. R. M. Santos, L. Madeira and F. B. Passos, *Catal. Today*, 2010, **149**, 401–406.
- 42 Å. Slagtern, U. Olsbye, R. Blom, I. M. Dahl and H. Fjellvåg, *Appl. Catal. A Gen.*, 1997, **165**, 379–390.
- 43 R. Martínez, E. Romero, C. Guimon and R. Bilbao, *Appl. Catal. A Gen.*, 2004, **274**, 139–149.
- 44 C. Anjaneyulu, S. Naveen Kumar, V. Vijay Kumar, G. Naresh, S. K. Bhargava, K. V. R. Chary and A. Venugopal, *Int. J. Hydrogen Energy*, 2015, **40**, 3633–3641.

This page intentionally left blank

Chapter 2

Hydrogenolysis of furfural to 1,5-pentanediol over Ni-La and Ni-Y catalyst

ABSTRACT. Catalytic transformation of furfural (FFR) and its hydrogenation product as biomass-derived chemicals into more sustainable chemicals especially 1,5-pentanediol (1,5-PeD) through hydrogenolysis reaction are challenging for the current issue. While the breakthrough in the C-O bond hydrogenolysis of FFR and its derivatives (furfuryl alcohol (FFA) and tetrahydrofurfuryl alcohol (THFA)) to obtain 1,5-PeD by lanthanum- and yttrium-modified Ni catalysts which are known good in the hydrogenation C=C and C=O bonds have experimented in this study. The addition of lanthanum and yttrium into Ni catalyst enhanced the C-O bond cleavage ability to give 1,5-PeD at high yield and selectivity.

2.1 Introduction

Biomass as renewable and abundant resources is an alternative option to supersede fossil fuels for sustaining energy and chemicals. The production of biomass-based

fine chemicals is an important option in the future as competitive and alternative against petrochemical derivatives. Cellulose is known as the most abundant and non-edible biomass feedstock for refineries which can be obtained from agricultural wastes like straw, corn stover and bagasse.^{1,2} The catalytic reaction for transforming a cellulose to glucose and thence to other value-added chemicals such as 5-HMF (5-hydroxymethylfurfural), FFR, etc. have been explored and investigated. Among of the potential top 30 building block candidates from sugar compounds in the DOE recommendation, FFR is one of the promising starting compounds to produce fuels and chemicals.³⁻⁵

The utilization of FFR to give value-added compounds has been produced more than a hundred chemicals involving hydrogenation, rearrangement, and C-C coupling reaction rate.^{6,7} The catalytic hydrogenation of FFR, a substituted furan compound at C(1) with a formyl group, to value-added chemicals such as FFA, THFA, 2-methylfuran (2MF), 2-methyltetrahydrofuran (2MTHF), furan, tetrahydrofuran (THF) and other useful chemicals (e.g. cyclopentanone and cyclopentanol), on the numerous catalysts have been reported so far.⁸ The other potential route is the transformation of FFR and its derivatives such as FFA and THFA giving pentanediols such as 1,2-PeD, 1,4-PeD, and 1,5-PeD through hydrogenolysis reaction, a C-O bond cleavage of furan or tetrahydrofuran ring.⁹ The hydrogenolysis reaction deals with the cleavage of carbon to carbon or carbon to oxygen (or heteroatom) bonds accompanied by the addition of hydrogen.¹⁰ The pentanediols formation especially 1,2- and 1,5-PeD from FFR, FFA, and THFA was reported mostly by using the Noble metal catalyst as active metals.⁹ The review insists that metal-metal oxide catalyst system is responsible for C-C bond cleavage and

hydrogenation C=C bonds as well as C=O bond to give pentanediols. In the metal-metal oxide catalyst system, the metal (Ru, Rh, Pd, Ir, and Pt) have a prominent role as hydride formation and partially reduced metal oxide (ReO_x, MoO_x, or MnO_x) act as Lewis acidic acid to bond C=O or C-O(H) bond.

The use of non-noble metal catalyst instead of noble metal catalyst for producing 1,5-PeD is challenging effort. The hydrogenolysis of FFA over Cu based catalysts such as Cu-Al₂O₃ or Cu-Mg₃AlO_{4.5} were reported to give 1,2- and 1,5-PeD at low selectivity, 48.6-51.2%, and 22.7-28.8%, respectively.^{11,12} Both reports were included Ni-Al₂O₃ and Ni-LDO which is inactive in the 1,5-PeD formation. Instead of Noble metals and Cu-based catalyst, a nickel-based catalyst which has the C=C and C=O bonds hydrogenation ability is the promising candidate for this reaction. Indeed, the modification is essential to accomplish the catalytic performance of the Ni-based catalyst. Our group was successfully added electropositive (such as Sn or Fe) into Ni for altering its catalytic behavior to be highly selective in the C=O bond hydrogenation of unsaturated aldehydes compounds especially FFR to FFA.^{13,14} Both added electropositive metal produced Ni-Sn or Ni-Fe alloy. Alumina supported Ni, Lewis acidic metal oxide, only hydrogenated C=C and C=O bonds of FFR to THFA.¹⁵ It means that the added Lewis acid into Ni catalyst is not an only key factor to improve C-O bond cleavage on the Ni-based catalyst for that reaction. The interaction of C=C bonds furan ring with the vacant 4*d* or 5*d* orbital via π electron donation is essential for enhancing polarization of C-O furan ring then the hydrogenolysis occurs easily. The rare earth oxide (REO) was utilized in the hydrogenation of ethylene and the highest rate of ethane formation was achieved over Y₂O₃ and La₂O₃ other than the investigated REO prior to heterolytically

hydrogen dissociation over REO cation and oxygen anion.¹⁶ Refers to metal-metal oxide catalyst system, the addition yttrium or lanthanum into Ni catalyst is firstly investigated for hydrogenolysis FFR and derivatives to 1,5-PeD.

2.2 Experimental procedure

2.2.1 Catalyst preparation

Ni-Y catalysts were prepared by combining three methods, co-precipitation, hydrothermal, and reduction method. Firstly, the aqueous solution of yttrium nitrate ($\text{Y}(\text{NO}_3)_3$ 0.49 M and aqueous solution nickel nitrate ($\text{Ni}(\text{NO}_3)_2$) 0.86 M were mixed by keeping of metal ions to 12 mmol and then control the Ni/Y mol ratios (1.5, 2.5, or 5.0). The pH of the solution adjusted equal to 13.2 by adding 8 mL NaOH 3.1 M. After stirring for 1 h, the slurry solution transferred into the Teflon vessel of the hydrothermal bomb and aged at 423 K for 24 h. Green precipitate was filtered and washed with distilled water until neutral filtrate then dried in vacuum overnight and denoted as Ni-Y(*n*), *n* is Ni/Y mol ratio. As a reference, Y_2O_3 was prepared with the same condition without nickel ($\text{Y}(\text{NO}_3)_3 \cdot 6\text{H}_2\text{O}$, 1.6551 g, 6.0 mmol). All samples reduced by using hydrogen gas in hydrogen treatment apparatus at 573, 623, and 473 K for 4.5 h before using as a catalyst. The catalysts denoted as Ni-Y(*n*)HTtemp, HTtemp is hydrogen treatment temperature in Kelvin. A similar procedure was employed in the preparation of Ni-La catalysts by using lanthanum aqueous solution instead of yttrium and hydrogen treatment temperatures of 523 K, 573 K, and 623 K. Then, it was denoted as Ni-La(*n*)HTtemp (temp = 523, 573, or 623).

The physical mixture Ni-M(2.5) catalyst was synthesized as follow. The proper amount of Y_2O_3 or La_2O_3 was added to 0.86 M $\text{Ni}(\text{NO}_3)_2$ aqueous solution and then added 3.1 M NaOH to adjust pH 13.2. The similar steps were applied as the Ni-M(*n*)

catalyst preparation, i.e. hydrothermal and later hydrogen treatment. The catalyst was denoted as Ni-Y(2.5)HT573pm and Ni-La(2.5)HT623pm. The monometallic catalysts were also synthesized with the similar procedure.

2.2.2 Catalyst characterization

All catalysts had been characterized by powder X-ray diffraction (Miniflex 600, Rigaku) with Cu as monochromatic source K α radiation ($\lambda = 1.5444$ nm). The XRD worked at 40 kV and 15 mA with 1.25 deg. solar slit, 5 deg./min. scan step and using Ni K β filter.

The *in-situ* Fourier transformation infrared (FTIR) spectra of adsorbed furfural were recorded by using HORIBA FT720 at a resolution of 4 cm⁻¹ and accumulating 16 scans. The Ni-M sample powder was loaded into the sample cell tube, reduced *in situ* at 573 K for Ni-Y and 523 K for Ni-La catalyst for 1 h under a circulating of H₂. Then, the sample was cooled down to room temperature, and then the background spectrum was recorded. Furfural vapor was introduced through the line. The remained FFR vapor was evacuated after 60 min and the adsorbed FFR on the catalyst was recorded at room temperature. The temperature was raised to 423 K and FFR vapor was introduced for 60 min. Finally, adsorbed FFR on the catalyst was recorded at room temperature after evacuating the remaining FFR.

2.2.3 Hydrogenolysis catalytic reaction

Catalytic hydrogenolysis of furfural performed in a 30 mL stainless steel autoclave equipped with a magnetic stirrer, pressure gauge, inserted glass vessel, and automatic temperature control apparatus. The reactor connected to a hydrogen cylinder of the reaction pressure. In typical experiment, catalyst (0.05 g) was put in glass vessel together with a magnetic stirrer, 2-propanol (3 mL), *trans*-decahydronaphthalene

(0.07 g) and substrate (0.1 g). The glass vessel was inserted into the autoclave with 2.0 MPa H₂ and heated at 423 K for 72 h. After the reaction, catalyst was separated from the mixture by centrifugation and the solution containing analyte was injected into GC-FID for analyzing product distributions. The conditions for GC were capillary column Inertcapt 624 (30 m, DF = 1.40 μm, 0.25 mm i.d.) with a flame ionization detector (FID). The temperature program was carried out as follows: the initial temperature and time = 70 °C, 0 min; final temperature = 250 °C, heating rate = 10 °C min⁻¹, temperature of injector = 220 °C, temperature of detector = 250 °C.

2.3 Result and discussion

2.3.1 XRD measurement of catalysts

Preparation and properties of Ni-La catalyst were explained in the previous report.¹⁷ Variation in Ni/La mol ratio clearly produced Ni(OH)₂ and La(OH)₃. The same procedure was used for synthesis Ni-Y catalyst as mentioned in the experimental procedure. Similar with Ni-La catalyst, the hydroxides of nickel and yttrium were obtained during coprecipitation and hydrothermal process as shown in Figure 2.1. The Y(OH)₃ was formed according to the ICSD 24309 having a hexagonal structure. However, the hydroxides of nickel were a mixture of Ni(OH)₂NiOOH (ICSD 202427) and Ni(OH)₂ (ICSD 24015). Some peaks at 2θ = 33, 38, 52, 59, and 63 of Ni(OH)₂ superimposed onto Y(OH)₃ probably because they have same hexagonal structure.

The identity of species in the Ni-M catalysts was established by XRD. The XRD patterns of Ni-Y(2.5) catalysts at various hydrogen treatment temperatures (Figure 2.2(a)) indicate that hydrogen treatment at 573 K was adequate in the Ni⁰ (ICSD 646092) and Y₂O₃ (ICSD 647653) formations. Indeed, the hydrogen treatment

condition transformed hexagonal yttrium hydroxide to Y_2O_3 . This is in line with the studies of Li et al., in which cubic Y_2O_3 was obtained from transformation of hexagonal $Y(OH)_3$, which was produced from precipitation of yttrium nitrate with sodium hydroxide at pH 13 by a hydrothermal method.¹⁸

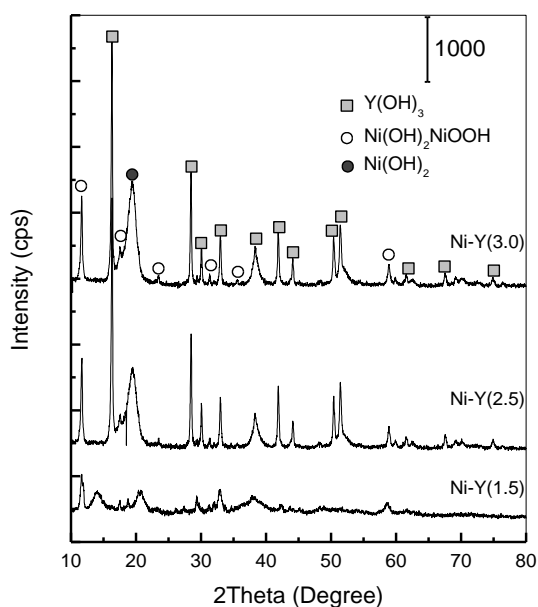


Figure 2.1 XRD patterns of hydroxides of Ni-Y(n), n = Ni/Y mol ratio.

In the case of the Ni-La(2.5) catalysts, hydrogen treatment temperatures of 523 K and 573 K formed Ni^0 and $La(OH)_3$ (ICSD 245669) as shown in Figure 2.2(b). Increasing hydrogen treatment temperatures only resulted in lowering the $La(OH)_3$ crystallinity as a result of the dehydration process. At 673 K, peaks of Ni^0 appeared as dominant peaks. Neuman and Walter reported that dehydration of $La(OH)_3$ to lanthanum oxyhydroxide ($LaOOH$) occurred at approximately 603 K, and increasing the temperature up to 763 K produced La_2O_3 .¹⁹ Therefore, the Ni-La(2.5)HT673 catalyst contains Ni^0 and mixed lanthanum oxide, but the other two Ni-La(2.5) catalysts contain $La(OH)_3$ as well as Ni metal.

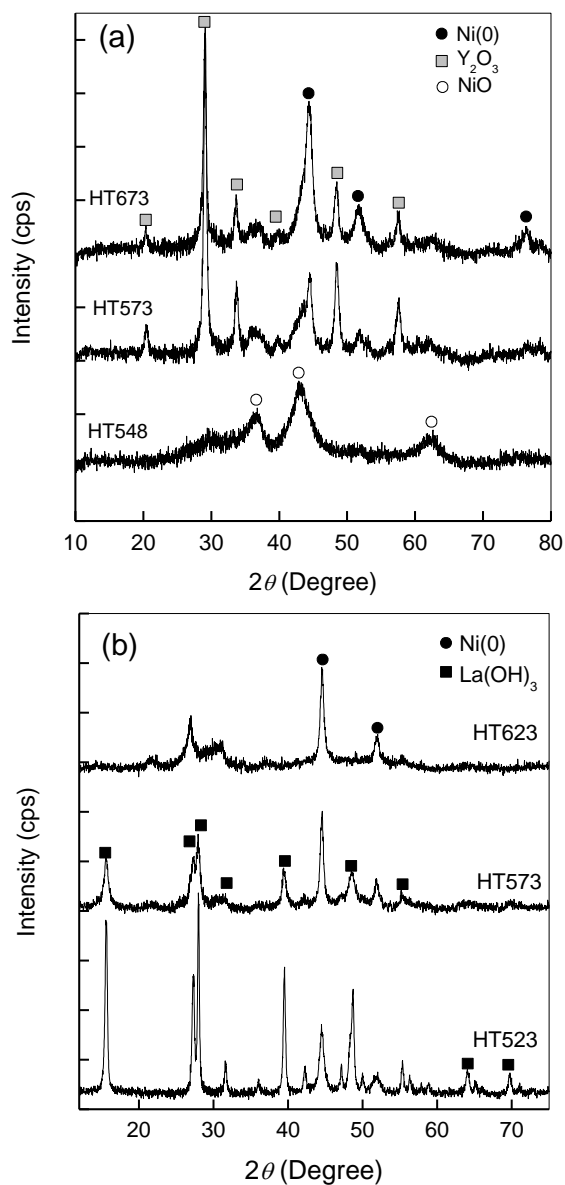
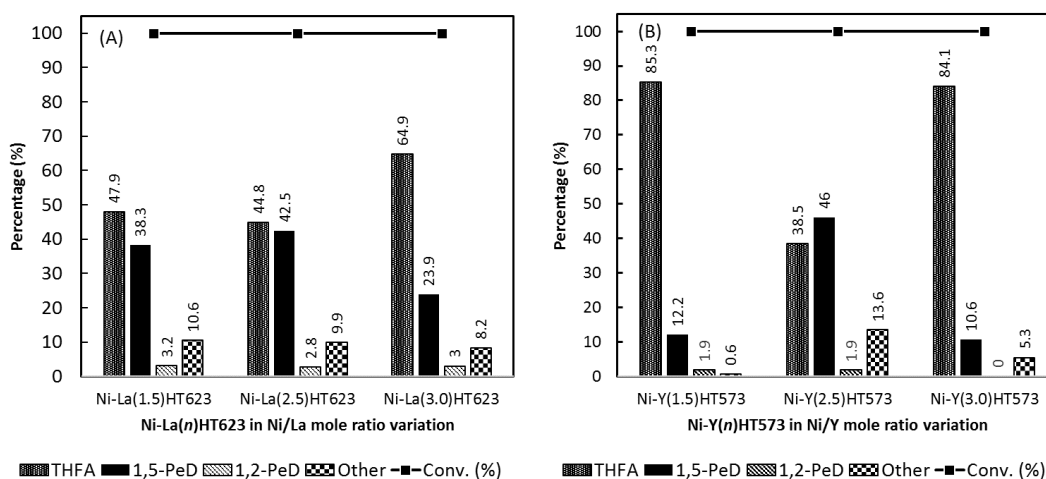


Figure 2.2 XRD patterns of (a) Ni-Y(2.5) and (b) Ni-La(2.5) at various hydrogen treatment temperatures.

2.3.2 Catalytic hydrogenolysis of furfurals

The performance of Ni-M catalysts with various Ni/M molar ratios was investigated to achieve a high yield of 1,5-PeD. The catalytic activities for hydrogenolysis of FFR at different Ni/M mol ratios are displayed in Figure 2.3. All catalysts showed the full conversion of FFR with 1,5-PeD obtained as the predominant hydrogenolysis product along with the by-product, THFA. Variances in

the catalytic activities were clearly observed as a function of the Ni/M mol ratio; the highest yield of 1,5-PeD was obtained at the 2.5 Ni/M mol ratio, with Ni-Y(2.5)HT573 and Ni-La(2.5)HT623 producing 1,5-PeD up to 46% and 42.5%, respectively. Then, both catalysts were used for further investigation.



Reaction conditions: Ni-M catalyst (0.05 g), FFR (1.1 mmol), 2-propanol (3 mL), *trans*-decahydronaphthalene (0.07 g), initial hydrogen pressure (2 MPa) at 423 K for 72 h. Conversion and yield were determined by GC using an internal standard technique.

Figure 2.3 The catalytic activity of (A) Ni-Y(*n*)HT573 and (B) Ni-La(*n*)HT623 (lower) catalysts in *n* (Ni/M mol ratio) function.

Varying the hydrogen treatment temperature for the Ni-Y(2.5) and Ni-La(2.5) catalysts accomplished its catalytic activities. The hydrogen treatment temperature provided distinguishing features of catalysts, as shown in Figure 2.2. The effects on 1,5-PeD yield were noticeable, as seen in Table 2.1 (entries 1-6). The Ni-Y(2.5)HT573 catalyst (entry 2) exhibited the highest yield of 1,5-PeD compared with the other Ni-Y(2.5) catalysts. Surprisingly, the hydrogen treatment at 523 K for Ni-La(2.5), the Ni-La(2.5)HT523 catalyst, produced 1,5-PeD up to 55.8% yield (entry 4). The results indicated that Ni-Y₂O₃ as well as Ni-La(OH)₃ composites are important in hydrogenolysis of the C-O bond, which is essential to obtain 1,5-PeD.

Table 2.1. Hydrogenolysis of FFR over Ni-M catalysts (Ni-M(2.5)HTtemp) at various H₂ treatment temperatures ^a.

Entry	Catalyst	Conv. (%)	Yield (%)		
			THFA	1,5-PeD	1,2-PeD
1	Ni-Y(2.5)HT548	100	77.0	18.4	1.7
2	Ni-Y(2.5)HT573	100	38.5	46.0	1.9
3	Ni-Y(2.5)HT673	100	84.7	12.9	2.4
4	Ni-La(2.5)HT523	100	31.7	55.8	2.8
5	Ni-La(2.5)HT573	100	32.6	53.5	1.9
6	Ni-La(2.5)HT623	100	44.8	42.5	2.8

^a *Reaction conditions*: Ni-M catalyst (0.05 g), substrate (1.1 mmol), *trans*-decahydronaphthalene (0.07 g), 2-propanol (3 mL), initial H₂ pressure (2.0 MPa), 423 K, for 72 h. Conversion and yield were determined by GC using an internal standard technique.

Table 2.2 Hydrogenolysis of FFR in various catalysts ^a.

Entry	Catalyst	Conv. (%)	Yield (%)			
			FFA	THFA	1,5-PeD	1,2-PeD
1	Y ₂ O ₃	98.1	83.2	0.0	0.0	0.0
2	NiO	99.0	77.2	9.3	13.5	0.0
3	Ni ^{0b}	100	0.0	87.2	4.4	0.6
4	Ni-Y ₂ O ₃ (2.5)pm ^c	100	0.0	82.0	12.8	2.2
5	Ni-Y(2.5)HT573	100	0.0	38.5	46.0	1.9
6	La ₂ O ₃ ^b	100	98.1	0.0	0.0	0.0
7	Ni-La ₂ O ₃ (2.5)pm ^c	100	0.0	78.6	9.3	3.5
8	Ni-La(2.5)HT523	100	0.0	31.7	55.8	2.8

^a *Reaction conditions*: catalyst (0.05 g), FFR (1.1 mmol), *trans*-decahydronaphthalene (0.07 g), 2-propanol (3 mL), initial H₂ pressure (2.0 MPa), 423 K, for 72 h. ^b 24 h. ^c pm = physical mixing. Conversion and yield were determined by GC using an internal standard technique.

The catalytic activities of the nickel and lanthanum precursors are shown in Table 2.2 compared with those of Ni-M catalysts in the FFR transformation. NiO, Y₂O₃, and La₂O₃ were inactive in 1,5-PeD production but showed remarkably high performance for the selective hydrogenation of FFR to FFA. The physical mixing of Ni-M catalysts (entries 4,7) and Ni⁰ metal only gave a small amount of 1,5-PeD.

Notably, the yttrium or lanthanum addition enhanced the hydrogenolysis ability of Ni catalysts. This result suggested that the interface of the Ni⁰-Y₂O₃ on the Ni-Y catalysts and Ni⁰-La(OH)₃ and La₂O₃ on the Ni-La catalysts are essential for 1,5-PeD formation.

2.3.3 Study of reaction pathway

To further investigate the reaction mechanism, catalytic reactions using FFA and THFA substrates were carried out under the same reaction conditions to verify that these intermediates could be converted into pentanediols. The hydrogenolysis of FFA was performed over Ni-Y(2.5)HT573 and Ni-La(2.5)HT523 catalyst. At the full conversion, the yield of 1,5-PeD was obtained up to 42.3% and 51.3% which was slightly lower than from the FFR substrate (Table 2.3, entries 1-2). Otherwise, THFA was dominantly obtained from the hydrogenation of C=C bonds, similar to using FFR as substrate. By using THFA as the substrate, as shown in Table 2.3 (entries 3-8), 1,5-PeD was the only hydrogenolysis (or ring opening) product among diols. Ni-Y(2.5)HT573 and Ni-La(2.5)HT523 exhibited the highest yields of 1,5-PeD, up to 77.6% (entry 4) and 92.4% (entry 6), respectively.

The metal oxide precursors exhibited very high selectivity for hydrogenating FFR into FFA, even though they were inactive in C-O bond cleavage (Table 2.4). The employment of N₂ gas instead of H₂ confirmed that the selective transfer hydrogenation reaction proceeded predominantly in N₂ atmosphere with 2-propanol as a hydrogen source (Table 2.4). This result suggested the adsorption of the carbonyl of FFR onto the electropositive metal (Y³⁺ or La³⁺).¹³ The FFR adsorption study would be presented for considering that suggestion.

Table 2.3. Hydrogenolysis of FFA and THFA over Ni-M (M = Y or La) catalysts.

Entry	Catalyst ^a	Conv. (%)	Yield (%)			
			THFA	1,5-PeD	1,2-PeD	1-BuOH
FFA as a substrate						
1	Ni-Y(2.5)HT573	100	47.6	42.3	2.2	2.9
2	Ni-La(2.5)HT523	100	28.3	51.3	0.0	4.8
THFA as a substrate						
3	Ni-Y(2.5)HT548	36.2	–	33.9	0.0	2.4
4	Ni-Y(2.5)HT573	80.5	–	77.6	0.0	3.9
5	Ni-Y(2.5)HT673	78.1	–	71.6	0.0	2.6
6	Ni-La(2.5)HT523 ^b	99.5	–	92.4	0.0	3.4
7	Ni-La(2.5)HT573 ^b	95.3	–	92.1	0.0	3.6
8	Ni-La(2.5)HT623 ^b	76.4	–	64.6	0.0	1.9

^a Reaction conditions: Catalyst (0.05 g), FFA (1.1 mmol), *trans*-decahydronaphthalene (0.07 g), 2-propanol (3 mL), 423 K, initial H₂ pressure (2.0 MPa), for 72 h or ^b 84 h. Conversion and yield were determined by GC using an internal standard technique.

Table 2.4. Effect N₂ gas in the transformation of FFR.

Catalyst ^a	Conv. (%)	Yield (%)			
		FFA	THFA	1,5-PeD	1,2-PeD
Ni ⁰	33.8	16.3	0.0	0.0	0.0
NiO	64.5	41.2	0.0	0.0	0.0
Y ₂ O ₃	39.6	7.7	12.0	0.0	0.0
La(OH) ₃	61.7	7.7	0.0	0.0	0.0
Ni-Y(2.5)HT573 ^b	65.9	39.6	0.0	0.0	0.0
Ni-La(2.5)HT523	46.4	22.7	0.0	0.0	0.0

^a Reaction conditions: Catalyst (0.05 g), FFR (1.1 mmol), *trans*-decahydronaphthalene (0.07 g), 2-propanol (3 mL), 423 K, initial N₂ pressure (1.0 MPa), for 24 h. ^b 15 h. Conversion and yield were determined by GC using an internal standard technique.

The FTIR spectra of the adsorbed FFR vapor on the Ni-Y(2.5)HT573 and Ni-La(2.5)HT523 catalysts and FFR vapor as a reference are shown in Figure 2.4. Gas-phase furfural shows the C=O stretching vibration mode at 1722 cm⁻¹. As shown in Figure 2.4 (left side), the downshifted C=O stretching band in the adsorbed furfural

species appears at around 1698 cm^{-1} on Ni-Y(2.5)HT573 surface at 423 K. Unfortunately, adsorption on Ni-La(2.5)HT523 catalyst, the downshifted C=O hardly distinguished with C=O stretching mode. These lower frequencies indicate a weakening of the C=O bond as a result of the interaction with the surface. The highest downshift on Ni-Y(2.5)HT573 catalyst surface suggested strong interaction via η^2 with the carbonyl O, but only through an interaction η^1 with the carbonyl O on Ni-La(2.5)HT523 catalyst.^{20,21} Hence, the electropositive yttrium or lanthanum ions strongly interact with the C=O bond of FFR and otherwise weakly interacts with the oxygen furan ring. Consequently, FFA was produced at the beginning of the reaction, and then a small amount of FFA converted to 1,2-PeD (Figure 2.5-2.6). FFR was hydrogenated into FFA. Further hydrogenation to THFA occurred rapidly, followed by hydrogenolysis of FFA to 1,2-PeD with the assistance of the adsorption of the CH₂OH functional group onto the metal surface.²² Hydrogenolysis of THFA selectively produced 1,5-PeD. In addition, 1-butanol was suggested through C-C bond cleavage of the pentanediols. Moreover, a study of the adsorption of ethanol on Ni metal surface at temperatures of 100 – 400 K suggested that Ni⁰ might promote C–C bond breaking of the ethanol molecule, leading to the emergence of hydrogen and methane.²³ On the presumption that their catalytic reaction occurs at the Ni-Y(2.5) or Ni-La(2.5) boundaries, the cleavage of the C-O bond of tetrahydrofuran ring proceeded selectively on it. Based on the above results, a possible reaction pathway is proposed in Scheme 2.1. Therefore, the Ni⁰-Y₂O₃ or Ni⁰-La(OH)₃ composites had a prominent role in the 1,5-PeD formation from FFR and FFA with THFA as an intermediate.

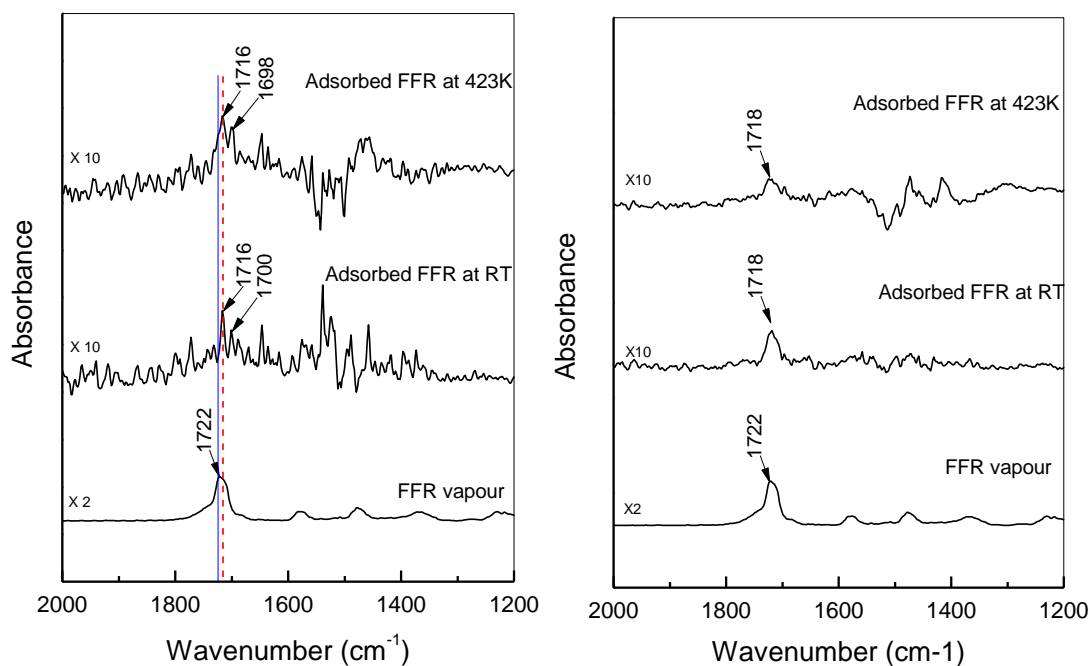
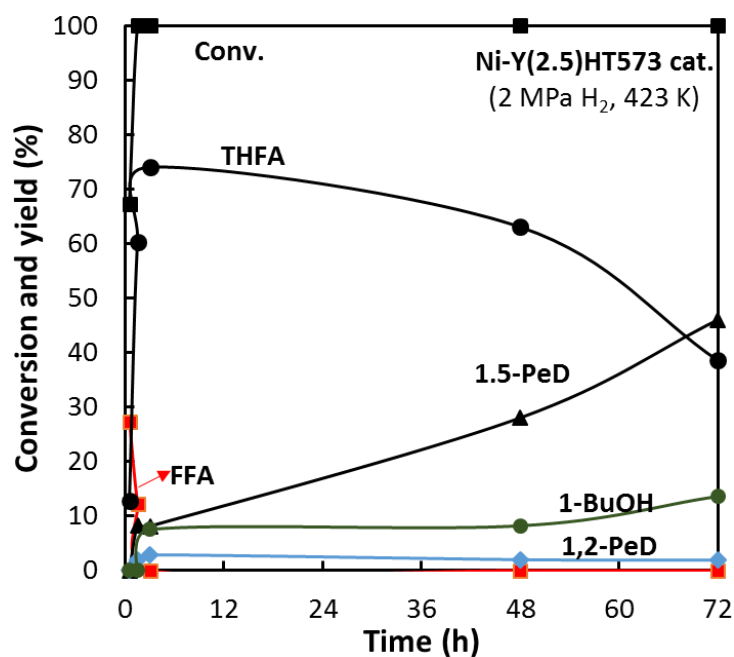
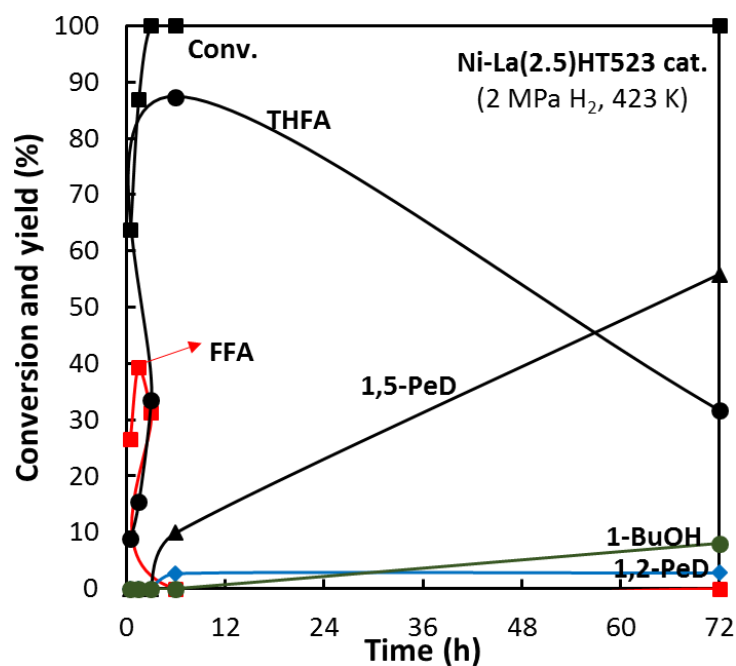


Figure 2.4 FTIR of absorption FFR gas on the surface of Ni-Y(2.5)HT573 and Ni-La(2.5)HT523 catalysts.



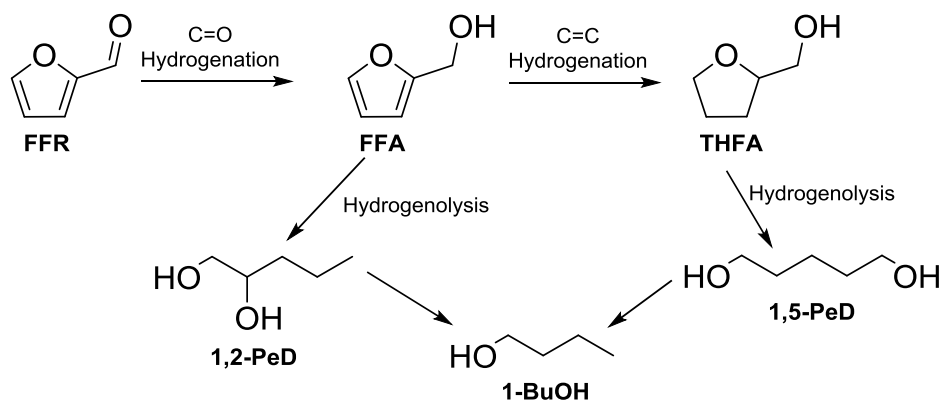
Reaction conditions: Ni-Y(2.5)HT573 catalyst (0.05 g), FFR (1.1 mmol), *trans*-decahydronaphthalene (0.07 g), 2-propanol (3 mL), 423 K, and initial H₂ pressure (2.0 MPa). Conversion and yield were determined by GC using an internal standard technique.

Figure 2.5 Time profile for hydrogenolysis of FFR over Ni-Y(2.5)HT573.



Reaction conditions: Ni-La(2.5)HT523 catalyst (0.05 g), FFR (1.1 mmol), *trans*-decahydronaphthalene (0.07 g), 2-propanol (3 mL), 423 K, and initial H₂ pressure (2.0 MPa). Conversion and yield were determined by GC using an internal standard technique.

Figure 2.6 Time profile for hydrogenolysis of FFR over Ni-La(2.5)HT523.



Scheme 2.1. Possible reaction pathways for the hydrogenolysis of FFR.

2.4 Conclusion

The Ni-Y₂O₃ and Ni-La(OH)₃ catalysts were synthesized and showed promise as catalysts for the hydrogenolysis of FFR to 1,5-PeD (423 K, 2.0 MPa H₂). Both catalysts exhibited remarkably high selectivity for producing 1,5-PeD from the hydrogenolysis of FFR, particularly starting from THFA. The results emphasized the

essential role of the Ni⁰-Y₂O₃ or Ni⁰-La(OH)₃ composites in executing C-O bond cleavage selectively as a key step in 1,5-PeD formation.

Notes

All results have been published as follow: H. W. Wijaya, T. Sato, H. Tange, T. Hara, N. Ichikuni and S. Shimazu, Hydrogenolysis of Furfural into 1,5-Pentenediol by Employing Ni-M (M = Y or La) Composite Catalysts, *Chem. Lett.*, 2017, **46**, 744–746.

ABBREVIATIONS

FFR: furfural	1,2-PeD, 1,2-pentenediol
FFA: furfuryl alcohol	1-BuOH: 1-butanol
THFA: tetrahydrofurfuryl alcohol	2-PrOH: 2-propanol
1,5-PeD: 1,5-pentenediol	

REFERENCES

- 1 S. N. Naik, V. V. Goud, P. K. Rout and A. K. Dalai, *Renew. Sustain. Energy Rev.*, 2010, **14**, 578–597.
- 2 R. A. Sheldon, *Green Chem.*, 2014, **16**, 950–963.
- 3 T. Werpy and G. Petersen, *Top Value Added Chemicals from Biomass Volume I - Results of Screening for Potential Candidates from Sugars and Synthesis Gas Top Value Added Chemicals From Biomass Volume I: Results of Screening for Potential Candidates*, 2004, vol. 1.
- 4 S. Dutta, S. De, B. Saha and I. M. Alam, *Catal. Sci. Technol.*, 2012, **2**, 2025–2036.
- 5 H. G. Bernal, L. Bernazzani and A. M. Raspolli Galletti, *Green Chem.*, 2014, **16**, 3734–3740.

- 6 J. P. Lange, E. Van Der Heide, J. Van Buijtenen and R. Price, *ChemSusChem*, 2012, **5**, 150–166.
- 7 R. Mariscal López, P. Maireles-Torres, M. Ojeda, I. Sadaba and M. López Granados, *Energy Environ. Sci.*, 2016, **9**, 1144–1189.
- 8 K. Yan, G. Wu, T. Lafleur and C. Jarvis, *Renew. Sustain. Energy Rev.*, 2014, **38**, 663–676.
- 9 Y. Nakagawa, M. Tamura and K. Tomishige, *Catal. Surv. from Asia*, 2015, **19**, 249–256.
- 10 R. Connor and H. Adkins, *J. Am. Chem. Soc.*, 1932, **54**, 4678–4690.
- 11 H. Liu, Z. Huang, F. Zhao, F. Cui, X. Li, C. Xia and J. Chen, *Catal. Sci. Technol.*, 2016, **6**, 668–671.
- 12 H. Liu, Z. Huang, H. Kang, C. Xia and J. Chen, *Chinese J. Catal.*, 2016, **37**, 700–710.
- 13 Rodiansono, S. Khairi, T. Hara, N. Ichikuni and S. Shimazu, *Catal. Sci. Technol.*, 2012, **2**, 2139.
- 14 W. S. Putro, T. Hara, N. Ichikuni and S. Shimazu, *Chem. Lett.*, 2017, **46**, 149–151.
- 15 S. Sang, Y. Wang, W. Zhu and G. Xiao, *Res. Chem. Intermed.*, 2017, **43**, 1179–1195.
- 16 K. M. Minachev, Y. S. Khodakov and V. S. Nakhshunov, *J. Catal.*, 1977, **49**, 207–215.
- 17 H. Tange, 千葉大学, 2015.
- 18 N. Li and K. Yanagisawa, *Mater. Res. Bull.*, 2011, **46**, 428–431.
- 19 A. Neumann and D. Walter, *Thermochim. Acta*, 2006, **445**, 200–204.

- 20 M. Mavrikakis and M. A. Barteau, *J. Mol. Catal. A Chem.*, 1998, **131**, 135–147.
- 21 J. L. Davis and M. A. Barteau, *Surf. Sci.*, 1990, **235**, 235–248.
- 22 Y. Nakagawa, H. Nakazawa, H. Watanabe and K. Tomishige, *ChemCatChem*, 2012, **4**, 1791–1797.
- 23 T. Kratochwil, M. Wittmann and J. Küppers, *J. Electron Spectros. Relat. Phenomena*, 1993, **65**, 609–617.

Chapter 3

Development Ni-Y₂O₃ catalyst for producing 1,5-pentanediol from furfural and its hydrogenated compounds

ABSTRACT. The hydrogenolysis of biomass-derived furfural (FFR) to obtain 1,5-pentanediol (1,5-PeD) was carried out by employing Ni-Y₂O₃ catalyst under mild reaction conditions (2.0 MPa of initial H₂, 423 K) prepared using a subsequent coprecipitation-calcination-hydrogen treatment. The hydrogenation of C=C and C=O bonds of furfural simultaneously came first to forming furfuryl alcohol (FFA) and tetrahydrofurfuryl alcohol (THFA), the hydrogenolysis of THFA was selectively proceeded to give 1,5-PeD (28.3% yield). The hydrogenolysis of FFA proceeded at the similar pathway giving 41.9% yield of 1,5-PeD with THFA as an intermediate. Employing THFA as a substrate corroborated with those results giving 54.7% yield of 1,5-PeD with 59.8% conversion and Ni⁰-Y₂O₃ boundaries had a prominent role for

that. This chapter highlights the hydrogenolysis of FFR, FFA, THFA and their mechanistic study of C-O bond cleavage of tetrahydrofuran ring to 1,5-PeD.

3.1 Introduction

The catalytic conversion of biomass-derived FFR and its derivatives to valuable chemicals and fuels by hydrogenation and hydrogenolysis have received increasing attention in recent years.¹ Upgrading FFA includes the hydrogenation of its furan ring into THFA,² reductions of its hydroxyl group into 2-methylfuran (2MF),³ and hydrogenolysis of the C-O-C bond of the furan ring into pentanediols.^{4,5} For FFA hydrogenolysis, 1,2-PeD was produced in higher yield and selectivity than 1,5-PeD if supported Ru, Pt/HT, or Cu-based catalysts are used.⁶⁻⁹ A Ru/MnOx catalyst system produced 1,2-PeD with 42.1% yield at 1.5 MPa H₂ and 423 K.⁶ Employing basic support on Pt, Pt/HT catalyst directly transformed FFR giving 1,2-PeD up to 73 % yield with a small amount of 1,5-PeD (8 % yield) at full conversion.⁷ Ru-supported carbon catalyzed the aqueous solution of FFA with 20 % selectivity to produce 1,2-PeD at 473 K and 1 MPa H₂.⁸ Cu-LDO with basic support also gave 1,2-PeD up to 51.2 % yield and 28.8 % yield of 1,5-PeD (413 K and 6 MPa H₂).⁵ Another report on the use of nonprecious-metal-based Cu-Al₂O₃ catalyst produced comparable selectivity of 1,2-PeD (48.6 %) and 1,5-PeD (22.7 %) at 6 MPa H₂ and 413 K.⁹ Therefore, the production of 1,5-PeD selectively from FFA hydrogenolysis is an interesting and challenging route toward renewable fine chemicals production. 1,5-PeD with an uneven aliphatic carbon chain and terminal diols has been used as a building block in producing polyesters, thermoplastics, polyurethanes, and as a plasticizer monomer.¹⁰ Employing Ni-based catalysts to transform the biomass-based chemical FFA into 1,5-PeD by hydrogenolysis is a worthwhile investigation.

Transformation of THFA to 1,5-PeD is a challenging route owing to the high yield of 1,5-PeD can be achieved from 2-hydroxytetrahydropyran (2-HY-THP) over Ru/C catalyst up to 80% yield from FFR.¹¹ The direct modification of a noble metal with metal oxide species especially Rh-ReOx and Rh-MoOx exhibited the best selectivity in hydrogenolysis of THFA to 1,5-PeD to 70–87% selectivity.^{12,13} The Brønsted acidic on the catalyst surface of ReOx, as well as MoOx, is essential to bind the oxygen atoms (ether and hydroxyl groups) of THFA and loose a C-O bond to give pentanediol products.^{14,15} Development of nickel-based catalyst instead of modified noble metal is demanding from economic, environmental, as well as scientific aspect for this reaction. Utilization of nickel catalyst which is known good for hydrogenation for this reaction after adding yttrium had been evaluated in this chapter as part of hydrogenolysis of FFR and FFA. In which, THFA is an intermediate product from both substrates by employing a Ni-Y₂O₃ catalyst.

3.2 Experimental procedure

3.2.1 Catalyst preparation

Ni-Y₂O₃ catalyst was prepared in the following steps: co-precipitation, hydrothermal, calcination, and reduction methods. Typically, an aqueous solution of Y(NO₃)₃ 0.49 M was added Ni(NO₃)₂ 0.86 M with Ni/Y mmol ratios (*n*) of 1.5, 2.5, and 3.0. NaOH 3.1 M solution was added dropwise until it achieved pH = 13.2. After stirred for 1 h, the slurry solution was transferred into a Teflon vessel (100 mL) of a hydrothermal bomb and aged at 423 K for 24 h. Then, the precipitate was filtered and washed with distilled water until the pH of the filtrated mother liquor was 7. Afterwards, the green hydrogel was dried in vacuum overnight and then calcined at T temperature in Kelvin (T was 623 K, 773 K, 923 K, or 1073 K). The temperatures

inside the furnace were gradually increased from room temperature to the target temperature with a heating rate of $5 \text{ K}\cdot\text{min}^{-1}$. After the target temperature was reached, the powders were annealed for 5 h in air and were denoted as Ni-Y₂O₃(*n*)T. Before used as a catalyst, All Ni-Y₂O₃(*n*)T catalysts were reduced by using H₂ gas at 673K for 3-4 h in the hydrogen treatment apparatus. A similar procedure was applied to prepare the Ni-Y₂O₃ catalyst with Ni/Y mole ratios of 3.0 and 1.5 at same total of metal ions i.e., 12 mmol. As a reference, Y₂O₃ was prepared with the same condition without nickel nitrate.

The physical mixture Ni-Y₂O₃(2.5) catalyst briefly synthesized as follow. The proper amount of Y₂O₃ was added to 0.86 M Ni(NO₃)₂ aqueous solution and then added 3.1 M NaOH to adjust pH 13.2. The similar steps were applied as the Ni-Y₂O₃(*n*)T catalyst preparation, i.e. hydrothermal, calcination (623 K) and subsequent hydrogen treatment (673 K). The catalyst was denoted as Ni-Y₂O₃(2.5)623pm. The monometallic catalysts also synthesized with the similar procedure.

3.2.2 Catalytic hydrogenolysis reaction

Catalytic hydrogenolysis of furfural performed in a 30 mL stainless steel autoclave equipped with a magnetic stirrer, pressure gauge, inserted glass vessel, and automatic temperature control apparatus. The reactor connected to a hydrogen cylinder of the reaction pressure. In a typical experiment, catalyst (0.05 g) put in glass vessel together with a magnetic stirrer, 2-propanol (3 mL), *trans*-decahydronaphthalene (0.07 g) and substrate (FFR, FFA or THFA) (0.1 g). The glass vessel inserted into the autoclave with 2.0 MPa H₂ and heated at 423 K for 24 h. After the reaction, autoclave cooled, gas released slowly, centrifuged mixture solution, and analyzed filtrate by using GC with *trans*-decahydronaphthalene as an internal standard. The

conditions for GC were capillary column Inertcap 624 (30 m, DF = 1.40 μm , 0.25 mm i.d.) with a flame ionization detector (FID). The temperature program was carried out as follows: initial temperature and time = 70 $^{\circ}\text{C}$, 0 min; final temperature = 250 $^{\circ}\text{C}$, heating rate = 10 $^{\circ}\text{C min}^{-1}$, temperature of injector = 220 $^{\circ}\text{C}$, temperature of detector = 250 $^{\circ}\text{C}$.

3.2.3 Characterization of Ni-Y₂O₃ catalyst

All catalysts had been characterized by Powder X-ray diffraction (XRD) Miniflex 600 Rigaku with Cu as monochromatic source K α radiation ($\lambda = 1.5444$ nm). The XRD was operated at 40 kV and 15 mA with 1.25 deg. solar slit, 5 deg./min. scan step and using Ni K β filter. The particle sizes of yttrium oxide and Ni⁰ were estimated by using Scherrer equation after analyzing some parameters of XRD data such as slit correction, Lorentz polarization correction, background subtraction, and K α 2 elimination by using Integral Intensity Calculation program. TEM micrographs were obtained using Hitachi High-tech H-7650 microscopy with field emissive gun at 150 kV. TEM image analyses of the best catalyst (Ni-Y₂O₃(2.5)623 catalyst) were taken on Hitachi High-Tech H7650 with an emissive gun, operated at 150 kV. The XPS analysis of Ni-Y₂O₃(2.5)623 catalyst was performed on JPS-9030, JEOL using a monochromatic Mg-K α X-Ray source and operated at 12 kV and 25 mA with a base pressure in the XPS analysis chamber of 7×10^{-8} Pa at room temperature. The pass energy was held at 10 eV with energy step at 0.1 eV for each region. Each region was integrated using the SpecSurf of version 2.0 for determination of surface composition.

Isotherm N₂ adsorption-desorption measurements were performed using a Belsorp Max (BEL Japan). The samples were outgassed by evacuation at 473 K for 2 h prior

to analysis. Data were collected at liquid nitrogen boiling temperature (77 K). Surface area was calculated by the BET (Brunauer-Emmett-Teller) method of which data were collected at relative pressures between 0.06 and 0.2. Total pore volume, average pore diameter, and pore size were calculated via the BJH (Barrett-Joyner-Halenda) method and DA method using the adsorption isotherm. Thermogravimetric analysis was performed on Thermo plus EVO2 TG-DTA machine under N₂ gas flow at a 5 °C/min heating rate. The modified FTIR Horiba that was connected with glassware line for introducing THFA vapor was used to study adsorption with 4 cm⁻¹ resolution. The NH₃-TPD was performed on BELCAT-M machine under He gas flow, mixture of 5.23 vol.% NH₃/He gas and a thermal conductivity detector for gas analysis.

3.3 Properties of Ni-Y₂O₃ catalyst

In a typical preparation of Ni-Y₂O₃, nickel and yttrium hydroxides were formed by coprecipitation and later hydrothermal treatment similar to the previous procedure (Chapter 2). Calcination as a pretreatment was conducted at 623 K in various Ni/Y mol ratio and variation calcination temperature from 573 to 1073 K for 2.5 Ni/Y mol ratio as shown in Figure 3.1. Lowering the amount of Ni ratios was indicated by increasing the crystallinity on Y₂O₃ (Figure 3.1(A)). Calcination at 573 K, 623 K, 773 K, 923 K, or 1073 K for 5 h with 5 K/min. elevation step from room temperature transformed nickel and yttrium hydroxides (Ni/Y = 2.5) into their oxides as shown in Figure 3.1(B). The XRD patterns of calcined Ni-Y₂O₃ samples contained peaks at $2\theta=37.2, 43.3, 62.9, 75.3, \text{ and } 79.4^\circ$, which was identified as NiO (ICSD 53931). Cubic yttrium oxide also formed according to ICSD 647653 after calcination at 923 K and 1073 K, although calcination 623 K and 773 K produced amorphous yttrium

oxide in particular at 573 K. The crystallinity of Y_2O_3 decreased with lower calcination temperatures. The results were consistent with the experiment by Liu et al., in which cubic Y_2O_3 in $\text{Ni}/\text{Y}_2\text{O}_3$ was formed after calcination at a temperature higher than 773 K.^{16,17}

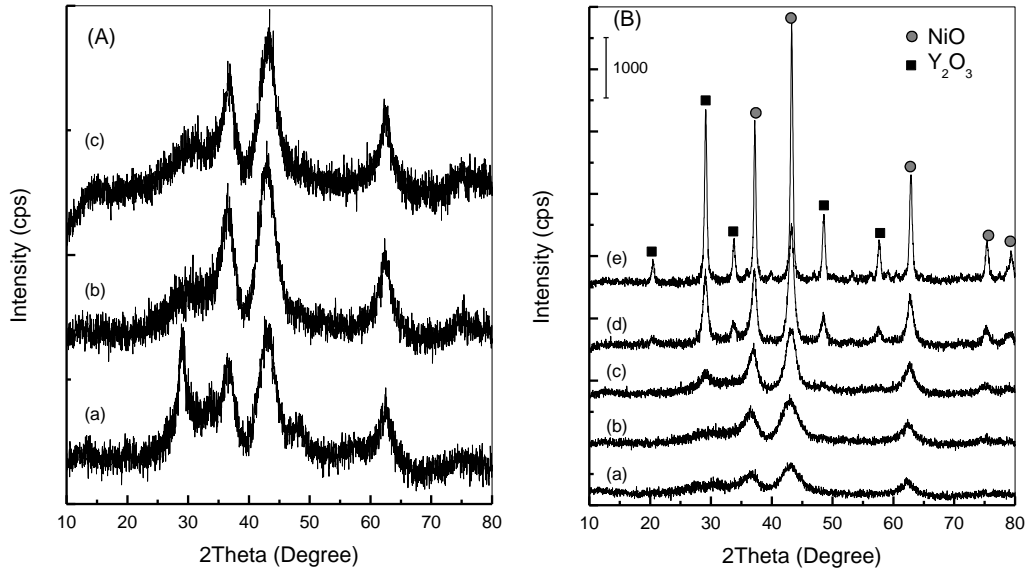


Figure 3.1. XRD patterns of calcined (A) (a) $\text{Ni}-\text{Y}_2\text{O}_3(1.5)623$, (b) $\text{Ni}-\text{Y}_2\text{O}_3(2.5)623$, (c) $\text{Ni}-\text{Y}_2\text{O}_3(3.0)623$; (B) (a) $\text{Ni}-\text{Y}_2\text{O}_3(2.5)623\text{pm}$, (b) $\text{Ni}-\text{Y}_2\text{O}_3(2.5)573$, (c) $\text{Ni}-\text{Y}_2\text{O}_3(2.5)623$, (d) $\text{Ni}-\text{Y}_2\text{O}_3(2.5)773$, (e) $\text{Ni}-\text{Y}_2\text{O}_3(2.5)923$, (f) $\text{Ni}-\text{Y}_2\text{O}_3(2.5)1073$.

Calcination as a pretreatment at 623 K was conducted prior to hydrogen treatment at 673 K on the $\text{Ni}-\text{Y}_2\text{O}_3$ in various Ni/Y mol ratios ($\text{Ni}/\text{Y} = 1.5, 2.5, \text{ or } 3.0$). Their XRD pattern as depicted in Figure 3.2(A) and diffraction peaks of $\text{Ni}(0)$, as well as Y_2O_3 , was obviously noticed based on ICSD 646092 and 53931, respectively. The hydrogen treatment at 673 K only reduced NiO to be Ni^0 and $\text{Ni}-\text{Y}_2\text{O}_3(n)$ (the number in parenthesis indicates the Ni/Y mole ratio) catalyst will be evaluated in the further study due to its catalytic activity.

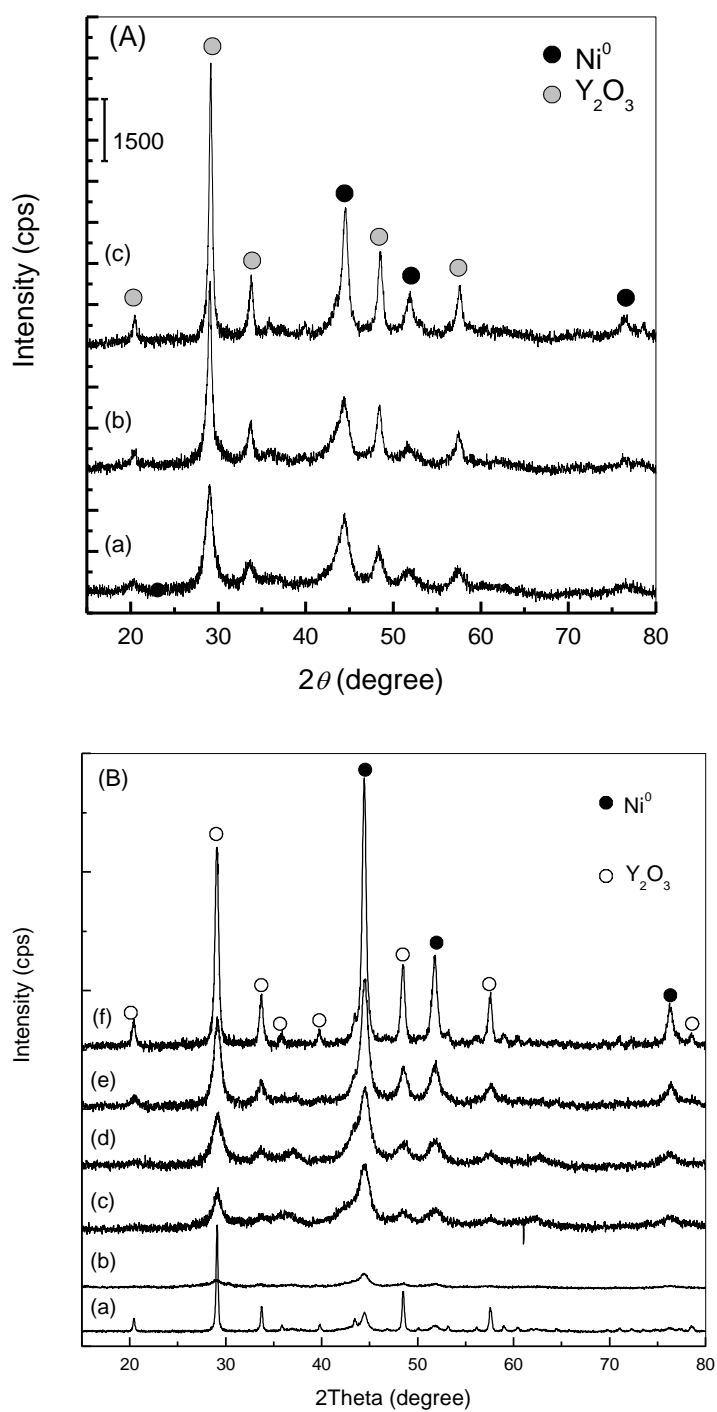


Figure 3.2. XRD patterns of the reduced catalyst by H_2 treatment at 673 K (A) $\text{Ni-Y}_2\text{O}_3(n)623$ ($n = 1.5, 2.5, \text{ and } 3.0$, respectively). (B) (a) $\text{Ni-Y}_2\text{O}_3(2.5)623\text{pm}$, (b) $\text{Ni-Y}_2\text{O}_3(2.5)573$, (c) $\text{Ni-Y}_2\text{O}_3(2.5)623$, (d) $\text{Ni-Y}_2\text{O}_3(2.5)773$, (e) $\text{Ni-Y}_2\text{O}_3(2.5)923$, (f) $\text{Ni-Y}_2\text{O}_3(2.5)1073$.

The XRD patterns of calcined Ni-Y₂O₃(2.5) after hydrogen treatment at 673 K are shown in Figure 3.2(B). Two kinds of peak series are present, which correspond to Ni⁰ and Y₂O₃. The hydrogen treatment only reduced NiO to Ni⁰. This agrees with previous studies that hydrogen treatment at 673 K was the proper procedure for producing Ni⁰. Sun et al. reported that the temperature-programmed reduction (TPR) profile of Ni/Y₂O₃ showed a single peak at 658 K in the reduction of NiO.¹⁸ Pospisil and Kanokova experiment showed that NiO appeared to be only reducible component in the mixed NiO-Y₂O₃ at 683 K.¹⁹ The crystallite sizes of Ni⁰ and Y₂O₃ estimated from Scherrer equation decreased with decreasing calcination temperature as shown in Table 3.1. BET surface area lowered aside from the increasing pre-treatment temperature caused by the agglomeration of both constituents occurred and consequently lowered its surface area. The H₂ chemisorption property of Ni-Y₂O₃(*n*)623 catalysts (*n* = 1.5, 2.5, and 3.0) was dominantly influenced by the Ni/Y mol ratios at the highest yttrium amount and the crystallite sizes of both constituents at the highest nickel amount. The Ni-Y₂O₃(2.5)623 possessed the highest H₂ uptake probably owing to the lowest crystallite size and the highest surface area. Both properties perceive the fused of Ni⁰ and Y₂O₃ on it is much better than the others investigated catalysts. The highest H₂ uptake properties could be used as an indication of the better Ni-H species formation which is critical for attacking C-O bond of tetrahydrofuran ring to triggering the C-O bond cleavage in further catalytic hydrogenation.

Calcination temperature as a pre-treatment impacted the hydrogen uptake property of the reduced Ni-Y₂O₃ catalyst as listed in Table 31. It lowered by increasing the calcination temperature as well as crystallite size of nickel and yttrium oxide at the

same Ni/Y mol ratio i.e. 2.5. Altering Ni/Y mol ratio in this case 1.5 and 3.0 gave a lower H₂ uptake than that of 235.2 $\mu\text{mol/g}_{\text{cat}}$. The acidity amount of Ni-Y₂O₃ catalysts from NH₃-TPD measurement revealed three peaks around 450 K, 620 K, and 929 K which indicated a difference acidity strength and the total was listed in Table 3.1. A Ni-Y₂O₃(2.5)623 catalyst featured the highest total acidity by using this method. It means the distinguished attributes in crystallite size, surface area, H₂ uptake, and acidity amount of Ni-Y₂O₃(2.5)623 catalyst has a promise of a greater candidate for hydrogenolysis of FFR and THFA achieving the highest yield 1,5-PeD compared to the reported Ni-based catalysts.

Table 3.1 Physicochemical properties of Ni-Y₂O₃ catalysts.

Catalyst ^[a]	Crystallite Size (nm) ^[b]		BET (m ² /g)	H ₂ uptake ^[c] ($\mu\text{mol/g. catalyst}$)	Acidity ^[d] (mmol/g)
	Ni ⁰	Y ₂ O ₃			
Ni-Y ₂ O ₃ (2.5)1073	24.2	23.9	17.57	25.4	0.140
Ni-Y ₂ O ₃ (2.5)923	11.8	10.3	37.53	89.6	0.489
Ni-Y ₂ O ₃ (2.5)773	5.3	7.2	52.34	125.1	0.788
Ni-Y ₂ O ₃ (2.5)623	4.5	5.6	74.14	235.2	1.103
Ni-Y ₂ O ₃ (2.5)623pm ^[c]	15.0	93.3	20.39	89.0	0.376
Ni-Y ₂ O ₃ (3.0)623	11.0	13.0	35.5	76.1	0.512
Ni-Y ₂ O ₃ (1.5)623	5.3	6.4	73.1	92.4	1.055

[a] After hydrogen treatment at 673 K. Catalyst is denoted as Ni-Y₂O₃(x)-t; x indicates the Ni/Y mole ratio and t are the calcination temperature. [b] Determined by using the Scherrer equation. (pm = physical mixing). [c] after corrected with H₂ physisorption. [d] Calculated from NH₃-TPD measurement as a total amount of NH₃ desorption at elevated temperature from 373-1073 K.

3.4 Catalytic hydrogenolysis of furfural (FFR)

3.4.1 Hydrogenolysis of FFR in various Ni-Y₂O₃ catalysts

The catalytic hydrogenolysis of FFR over Ni-Y₂O₃ catalysts was firstly evaluated in different Ni/Y mol ratios at a similar calcination pre-treatment as shown in Table 3.2 (entries 1,2 and 6). The addition of yttrium at higher mol ratio (Ni/Y = 1.5) gave 1,5-PeD of below 15 % otherwise the THFA was obtained as the major

hydrogenation product. Decreasing yttrium mol ratio increased the yield of 1,5-PeD up to 28.3 % yield (Ni/Y = 2.5) and only THFA as a sole product at the enrichment of Ni (Ni/Y mol ratio was 3.0). The data showed that the 1,5-PeD was produced at the highest yield over Ni-Y₂O₃(2.5)623 catalyst and would be employed for further investigation.

Table 3.2 Catalytic hydrogenolysis of FFR

Entry	Catalyst ^a	Conv. (%)	Yield (%)			
			THFA	1,5-PeD	1,2-PeD	1-BuOH
1	Ni-Y ₂ O ₃ (3.0)623	> 99	90.5	0.0	0.0	0.0
2	Ni-Y ₂ O ₃ (1.5)623	> 99	84.5	14.5	0.0	1.1
3	Ni-Y ₂ O ₃ (2.5)1073	> 99	86.2	10.4	3.4	0.0
4	Ni-Y ₂ O ₃ (2.5)923	> 99	79.6	9.7	2.4	0.4
5	Ni-Y ₂ O ₃ (2.5)773	> 99	62.6	12.6	2.9	0.4
6	Ni-Y ₂ O ₃ (2.5)623	> 99	56.7	28.3	2.3	2.9
7	Ni-Y ₂ O ₃ (2.5)623pm	> 99	73.9	11.6	2.0	0.3
8	Ni-Y ₂ O ₃ (2.5)HT673 ^b	> 99	66.3	9.8	1.7	0.0
9	Ni(0)	> 99	11.8	9.1	0.0	0.0
10	Y ₂ O ₃	> 99	7.5	0.0	0.0	0.0
11	NiO ^{b,c}	99.0	7.7	11.1	0.0	0.0

^a Reaction conditions: Reduced Ni-Y₂O₃ catalyst (0.05 g), FFR (1.1 mmol), *trans*-decahydronaphthalene (0.07 g), 2-propanol (3 mL), 423 K, initial H₂ pressure (2.0 MPa), for 24 h. Conversion and yield were determined by GC using the internal standard technique. ^b HT was Hydrogen treatment. ^c FFA was formed up to 63.4%.

Calcination as pre-treatment not only impacted by catalyst properties (Figure 1) but also their catalytic performance (Table 2, entries 3-6). For all Ni-Y₂O₃ catalysts, THFA was obtained as a predominant hydrogenation product along with the 1,5-PeD preferentially. Differences in the yield of 1,5-PeD were clearly observed whereby at the same hydrogen treatment temperature, the higher calcination temperature than 623 K gave the lower 1,5-PeD. The catalytic activity decreases due to the increasing crystallite size of Ni⁰ and Y₂O₃ as well as the lower surface area. Physical mixing of

Ni and Y₂O₃ (Ni-Y₂O₃(2.5)623pm catalyst) and direct reduced Ni-Y sample (Ni-Y₂O₃(2.5)HT673 catalyst) only gave 1,5-PeD at 9.3 % and 15.6 % yield, respectively (entries 7-8). Ni⁰ and NiO gave a low activity for this reaction otherwise Y₂O₃ was not active. It insists that Ni⁰-Y₂O₃ boundaries and catalyst surface acidity facilitated in calcination and H₂ treatment are proposed to have a critical role in the C-O bond cleavage to form 1,5-PeD.

3.4.2 Investigation of reaction conditions

Optimization of the catalytic hydrogenolysis of FFR over Y₂O₃(2.5)623 catalyst has a profound effect on a yield of 1,5-PeD evaluated at different reaction temperatures and initial H₂ pressure as shown in Figure 3.3 Changing the initial H₂ pressure, experimented in the range of 1.5–2.5 MPa (Figure 3.3 left), was expected to increase the solubility of H₂ and hydride formation. However, the full conversion of FFR remained largely unaffected by the initial H₂ pressure, the yield of 1,5-PeD is slightly lower than 28.3% at 2.5 MPa. By means of initial H₂ pressure at 2.0 MPa, the investigated reaction temperature between 413 to 453 K (Figure 3.3 right) showed the yield of 1,5-PeD (28.7%) reached a plateau and slightly increased to 32.9 at 453 K while THFA was decreased gradually by increasing reaction temperature. On the contrary, 1-BuOH periodically formed as the reaction temperature function and assumed the decomposition of the hydrogenolysis products (pentanediols) at high temperature. It insisted that FFR was hydrogenated rapidly to THFA at high temperature as well as hydrogen initial pressure and 1,5-PeD was produced selectively from hydrogenolysis of THFA in our catalytic reaction system.

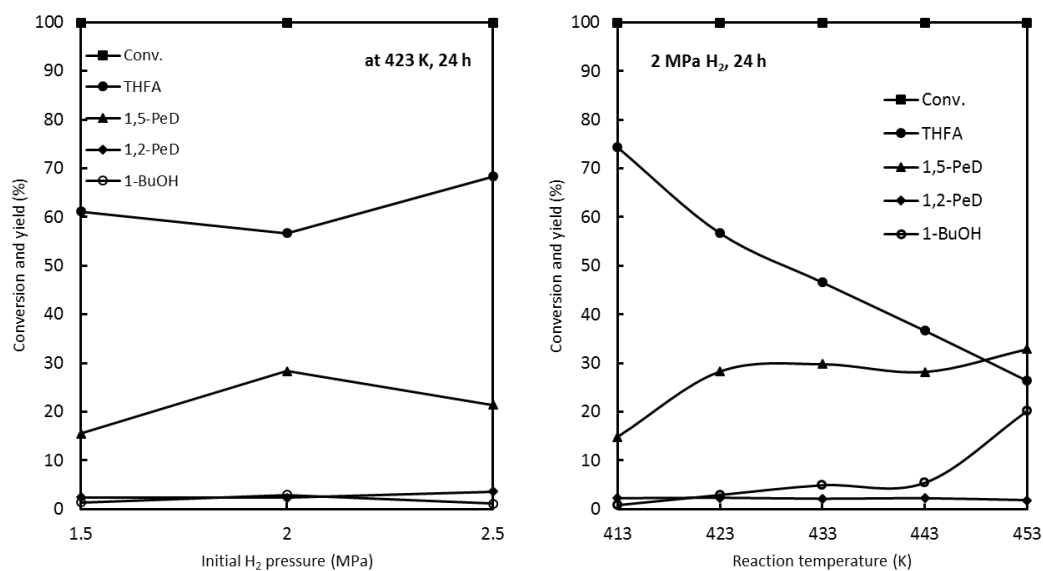
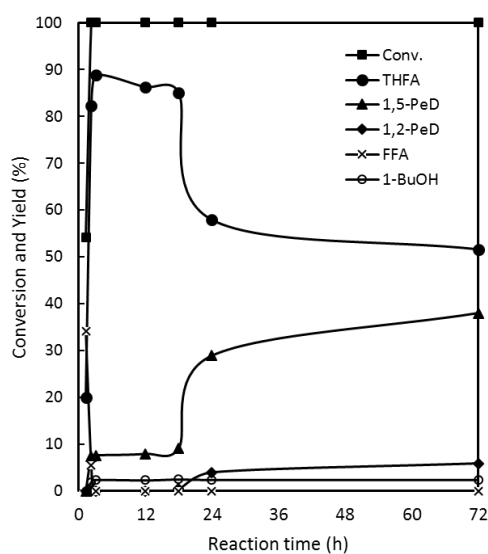


Figure 3.3 Evaluation of initial H₂ pressure dependency (left) and reaction temperature (right) for hydrogenolysis of FFR to 1,5-PeD.

3.4.3 Time profile and reaction pathway

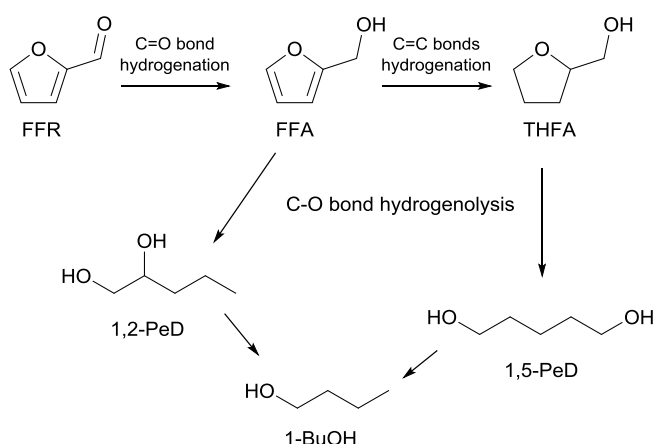
The time course for hydrogenolysis of FFR to 1,5-PeD over Ni-Y₂O₃(2.5)623 catalyst was therefore performed to mitigate a transformation of FFR to 1,5-PeD as shown in Figure 3.4. In the initial period (below 3 h), the hydrogenation of C=C and C=O bonds was concomitantly proceeded to produce the hydrogenation products and only THFA was produced during 3 h. A few pentanediols was initially formed. After 3 h, the hydrogenolysis of THFA dominantly proceeded to 1,5-PeD as reaction time function and the yield of 1,5-PeD did not increase significantly after 24 h. Moreover, 1-BuOH was produced after 18 h and constant with prolonging reaction time to 72 h. Utilizing 1,2-PeD and 1,5-PeD as substrates form 1-BuOH in up to yields of 8.0% and 2.1%, respectively. It suggests that 1-BuOH was produced by owing to the decomposition of pentanediols. These results also inform that the catalyst was deactivated after 24 h.

Based on the time profile result (Figure 3.4), the proposed reaction pathway for hydrogenolysis of FFR was shown in Scheme 3.1. The hydrogenolysis of FFR proceeded with a two-step reaction, hydrogenation giving THFA as an intermediate product and then hydrogenolysis of THFA to form 1,5-PeD. Thus, a study on the hydrogenolysis of FFA and THFA would be presented to comprehend its catalytic properties in our catalyst.



Reaction conditions: Ni-Y₂O₃(2.5)623 catalyst (0.05 g), FFR (1.1 mmol), *trans*-decahydronaphthalene (0.07 g), 2-propanol (3 mL), 423 K, and initial H₂ pressure (2.0 MPa). Conversion and yield were determined by GC using the internal standard technique.

Figure 3.4 Time course for hydrogenolysis of FFR



Scheme 3.1 Reaction route and products distribution in hydrogenolysis of FFR.

3.5 Catalytic hydrogenolysis of furfuryl alcohol (FFA)

The hydrogenolysis of FFR to give 1,5-PeD over Ni-Y₂O₃(2.0)-623 catalyst exhibited the highest yield of 1,5-PeD formation up to 29.8% at the optimized catalytic reaction (423 K and 2.0 MPa initial H₂ pressure). From Scheme 3.1, furfuryl alcohol (FFA) was produced during the transformation of FFR to 1,5-PeD. The investigation of FFA as a substrate will be studied in detail in this section.

3.5.1 Hydrogenolysis of FFA in various Ni-Y₂O₃ catalysts

The first study in hydrogenolysis of FFA was conducted by reduced Ni-Y₂O₃ with different Ni/Y mole ratios, various pretreatment calcination temperatures, a physical mixture of Ni-Y₂O₃, and the corresponding precursors as shown in Table 3.3. FFA was fully converted by all Ni-Y₂O₃ catalysts. At the highest Ni content, THFA was obtained as the predominant hydrogenation product and the yield of 1,5-PeD was less than 7% (entry 1). In contrast, as the Y₂O₃ content increased, 1,5-PeD yield increased slightly to 20% (entry 2). The Ni/Y mole ratio of 2.5 was well-suited for preparing 1,5-PeD as the major product (up to 41.9% yield, entry 6). It suggests that Ni⁰ metal was solely responsible for the C=C bond hydrogenation as confirmed in entry 10.

As mentioned above, the calcination treatment at various temperature affected the physicochemical properties of Ni-Y₂O₃(2.5) catalyst. The catalytic activity at different calcination temperatures was also studied as shown in Table 3.3, entries 3-7. Altering the calcination temperature from 773 K to 1073 K produced 1,5-PeD with yields below 15 % and THFA as the main product. Increasing the crystallite size of Ni⁰ and Y₂O₃ was followed by a lowered BET surface area and surface acidity. Calcination above 673 K was not seemingly effective in the Ni⁰-Y₂O₃ boundaries formation and tuning acidity of catalysts that is essential for the hydrogenolysis of

the C-O bond. The other results (shown in entries 8-11), indicated that the physical mixing of Ni-Y₂O₃ and Ni⁰ produced only 9.3% 1,5-PeD, and the oxides alone were inactive for hydrogenation and hydrogenolysis (entries 11-12). Side products were also detected, i.e., 1,2-PeD at approximately 2.2% and a trace amount of 1-butanol. These results suggest that FFA was converted to THFA at the first step and then THFA was transformed into 1,5-PeD through C-O bond cleavage. Previous reports explained that 1,5-PeD could be obtained selectively from hydrogenolysis of THFA especially over Ir-ReOx/SiO₂ catalysts.⁴ Among the screened Ni-Y₂O₃ catalyst systems, the Ni-Y₂O₃(2.5)623 catalyst was highlighted as a promising catalyst for 1,5-PeD synthesis from FFA hydrogenolysis prior to the best catalyst features.

Table 3.3 Catalytic hydrogenolysis of FFR

Entry	Catalyst ^a	Conv. (%)	Yield (%)			
			THFA	1,5-PeD	1,2-PeD	1-BuOH
1	Ni-Y ₂ O ₃ (3.0)623	> 99	77.3	6.8	1.9	0.0
2	Ni-Y ₂ O ₃ (1.5)623	> 99	52.5	20.0	1.8	1.3
3	Ni-Y ₂ O ₃ (2.5)1073	> 99	77.5	7.5	1.6	0.0
4	Ni-Y ₂ O ₃ (2.5)923	> 99	77.7	12.3	2.0	0.0
5	Ni-Y ₂ O ₃ (2.5)773	> 99	73.6	12.9	2.0	0.0
6	Ni-Y ₂ O ₃ (2.5)623	> 99	30.4	41.9	1.2	1.6
7	Ni-Y ₂ O ₃ (2.5)573	> 99	71.6	11.8	1.9	trace
8	Ni-Y ₂ O ₃ (2.5)623pm	> 99	68.5	7.1	0.0	0.0
8	Ni-Y ₂ O ₃ (2.5)623 ^b	> 99	0.0	0.0	0.0	0.0
9	Ni(0)	> 99	100	0.0	0.0	0.0
10	Y ₂ O ₃	0.0	0.0	0.0	0.0	0.0
11	NiO ^b	0.0	0.0	0.0	0.0	0.0

^a Reaction conditions: Reduced catalyst (0.05 g), FFA (1.1 mmol), *trans*-decahydronaphthalene (0.07 g), 2-propanol (3 mL), 423 K, initial H₂ pressure (2.0 MPa), for 24 h. Conversion and yield were determined by GC using the internal standard technique. ^b without H₂ treatment.

3.5.2 Evaluation of reaction conditions

An investigation to figure out the optimal reaction conditions for the production of 1,5-PeD was performed under a variety of initial hydrogen pressures and reaction temperatures utilizing the Ni-Y₂O₃(2.5)623 catalyst. Results altering the initial H₂ pressure ranging from 1.5 to 3.0 MPa at 423 K are shown in Figure 3.5(A). At low hydrogen pressure (1.5 MPa), THFA was exclusively produced by the hydrogenation of FFA and the C-O bond was hardly cleaved to give pentanediols. Elevation of the hydrogen pressure to 2.0 MPa increased the yield of 1,5-PeD to 41.9% and to 47.8% for a hydrogen pressure of 3.0 MPa. The initial H₂ pressures below 1.5 MPa were insufficient to cleave the C-O bond of THFA. These results are similar to that on the hydrogenation of FFA to THFA over Ru/C (at 403-448 K, 1.03-2.06 MPa), and only the rate of the hydrogenation reaction was increased.²⁰

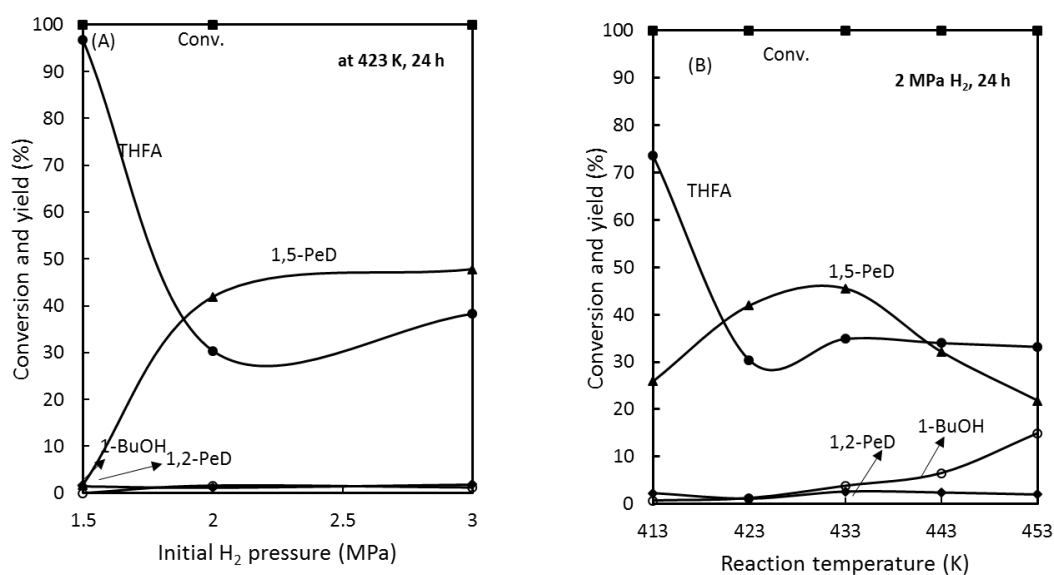


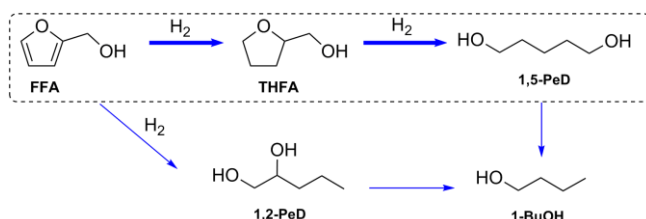
Figure 3.5 (A) Initial H₂ pressure and (B) reaction temperature dependencies.

The effect of reaction temperature (from 413 to 453 K) on the yield of 1,5-PeD is shown in Figure 3.5(B). Using 2-PrOH as the solvent, FFA reacted completely within 24 h at all temperatures. The main hydrogenolysis product was 1,5-PeD rather

than 1,2-PeD; the yields of 1,2-PeD were consistently approximately 2% at all temperatures. It suggests that 1,2-PeD was produced from hydrogenolysis of FFA through the C-O bond cleavage in the furan ring and THFA was converted to 1,5-PeD through C-O bond cleavage in the tetrahydrofuran ring. We also tested the hydrogenolysis of THFA in which 1,2-PeD was not detected. The proposed mechanism of 1,2-PeD formation from FFA was reported by Liu et al.^{5,9} The yield for 1,5-PeD rose steadily to 45.5 % at 433 K and then decreased as the temperature increased. However, the THFA yield became constant at approximately 33% in the range between 423 and 453 K. In contrast, the byproduct 1-BuOH yield rose as the reaction temperature increased (up to a maximum of 14.9% at 453 K). Clearly, these results imply that the formation of 1-BuOH may mainly include the C-C cleavage of 1,5-PeD at higher temperatures. Decomposition of ethanol to methane and CO on a Ni (111) surface was explained in detail by Gates and co-workers.²¹ The β -hydride elimination and C-C bond cleavage occurred to form CO and methane at 400 K. According to this mechanism, 1-BuOH can be formed from 1,5-PeD in an analogous manner. This also implies that other low-molecular-weight alcohols and hydrocarbons must be included in the "others" column in Table 3.3. These results indicate that the optimized temperature for producing 1,5-PeD at high yield and selectivity with the lowest 1-BuOH formation was 423 K.

Over supported Ru and Pt catalysts, the direct C-O bond cleavage of a furan ring followed by the hydrogenation of C=C bonds produced 1,2-PeD from FFA, and a small amount of THFA was also formed.⁶⁻⁸ Cu-Al₂O₃ gave 1,2-PeD and 1,5-PeD with comparable amounts through C-O cleavage of the furan ring and hydrogenation of the ring-opened species to diols.⁹ An alcoholate species was proposed in the

reaction mechanism of basic support of Cu, Cu-LDO catalyst, giving 1,2-PeD and 1,-PeD.⁵ Our results suggest that THFA is one of the hydrogenated products with a ring as shown in Scheme 3.2. The C=C bonds of the furan ring were hydrogenated from FFA and then the tetrahydrofuran ring C-O bond was cleaved selectively to produce 1,5-PeD with remarkably high selectivity (41.9 % yield).



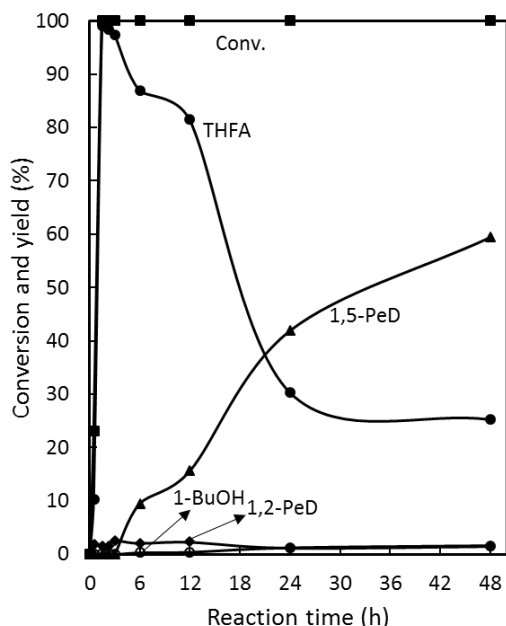
Scheme 3.2 Proposed reaction route in the production of 1,5-PeD from FFA.

3.5.3 Investigation of time course and reaction pathway

The time profile of FFA hydrogenolysis to 1,5-PeD is illustrated in Figure 3.6. First, FFA was converted to THFA with a small amount of 1,2-PeD. FFA was almost fully converted to THFA (99.8%) within 1.5 h. After this initial formation, THFA sharply decreased and formed up to a 41.9% yield of 1,5-PeD over 24 h. On the other hand, the yield of 1,2-PeD decreased to 1.5% over 48 h. A small amount of 1-BuOH was detected and this amount slightly increased to 1.6% owing to the decomposition of 1,2-PeD and 1,5-PeD.

The time course of FFA transformation to 1,5-PeD through hydrogenolysis is fully consistent with the proposed reaction pathway outlined in Scheme 3.2. Under the same reaction conditions over 24 h, using THFA as the substrate produced 1,5-PeD in a 54.7 % yield with a THFA conversion of 59.4% without 1,2-PeD formation. Utilizing 1,2-PeD and 1,5-PeD as substrates yielded 1-BuOH in yields of 8.0% and 2.1 %, respectively. These results also confirm the pathway outlined in Scheme 3.2. Nickel oxide (NiO) and yttrium oxide (Y₂O₃) were inactive towards FFA

hydrogenolysis, and nickel metal (Ni^0) gave only THFA under the same reaction conditions. These results suggest that a boundary of coupled $\text{Ni}^0\text{-Y}_2\text{O}_3$ species plays a prominent role in the C-O bond cleavage of the tetrahydrofuran ring.



Reaction conditions: Ni-Y₂O₃(2.5)623 catalyst (0.05 g), FFA (1.1 mmol), *trans*-decahydronaphthalene (0.07 g), 2-propanol (3 mL), 423 K, initial H₂ pressure (2.0 MPa), for 24 h. Conversion and yield were determined by GC using the internal standard technique.

Figure 3.6 Time course of hydrogenolysis of FFA over Ni-Y₂O₃(2.5)623 catalyst.

3.5.4 Reusability test

The reusability of Ni-Y₂O₃(2.5)623 was conducted at the optimum conditions to evaluate the stability of the catalyst (Table 3.4). Although the conversion of FFA was maintained at 100%, the yield of 1,5-PeD decreased to 15.3% in the second run. Increasing the THFA yield and decreasing the 1,5-PeD might indicate a change of the Ni-Y₂O₃ catalyst components and/or surface poisoning of the catalyst surface. The XRD analyses of fresh and used catalysts are shown in Figure 3.7(A). The fact that no considerable changes were detected may exclude the catalyst component change. Thermogravimetric analysis of used catalyst showed the reduction of mass

(11.15%) at 573 K under N₂ gas flow. Polymerized products were detected by FTIR analysis of the used catalyst (Figure 3.7(B)). Choura et al. reported that homopolymerized products of FFA were formed by a Lewis acid catalyst.²² Polymer products were also observed in the hydrogenolysis of FFA over the Ru-supported catalyst.⁸ These reported results were similar to those of our used catalyst, which might be partially covered with the polymerization product and cause the decrease of 1,5-PeD owing to the decrease in the Ni⁰-Y₂O₃ boundary. We conclude that poisoning of Ni⁰-Y₂O₃ boundary lowered the hydrogenolysis ability of the C-O bond.

Table 3.4. Reusability test of the Ni-Y₂O₃(2.5)623 catalyst.

Run	Conv. (%)	Yield (%)			
		THFA	1,5-PeD	1,2-PeD	1-BuOH
1 ^a	> 99	30.4	41.9	1.3	1.2
2 ^b	> 99	59.0	15.3	4.0	0.0

Reaction conditions: [a] Reduced Ni-Y₂O₃ catalyst (0.05 g), FFA (1.1 mmol), trans-decahydronaphthalene (0.07 g), 2-propanol (3 mL), 423 K, initial H₂ pressure (2.0 MPa), for 24 h. [b] Used catalyst was only washed with 2-propanol three times and then dried. Conversion and yield were determined by GC using the internal standard technique.

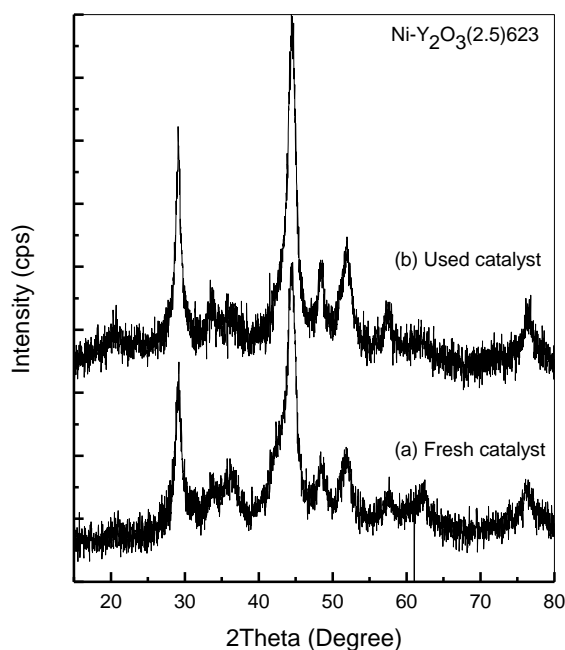
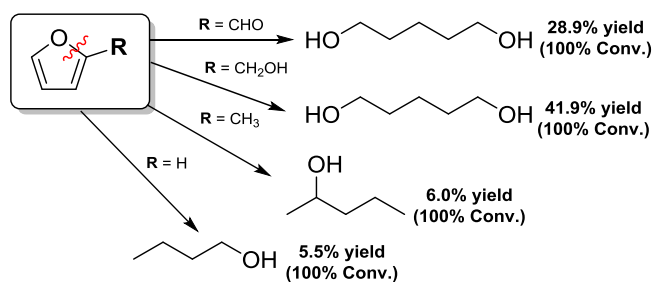


Figure 3.7 XRD pattern of fresh and used Ni-Y₂O₃(2.5)623 catalyst

3.5.5 Hydrogenolysis of furanic compounds

The remarkable selectivity of the 1,5-PeD production from FFA suggested that the C-O bond cleaved selectively on the Ni⁰-Y₂O₃ boundary and Ni-Y₂O₃(2.5)623 had the best catalytic activity. We speculate the following reaction pathway based on the above-mentioned reaction results. Initially, C=C bonds of FFA were hydrogenated and then the C-O bond of the tetrahydrofuran ring cleaved selectively to form 1,5-PeD. On the other hand, the hydrogenolysis of furan derivatives as a substrate such as FFR, 2MF, and furan was also examined by using Ni-Y₂O₃(2.5)623 at the optimized conditions. The reaction summary is illustrated in Scheme 3.3. All substrates gave a full conversion with the furan-ring-hydrogenation product as the main product. The yield of 1,5-PeD to 28.9 % as the major hydrogenolysis product was also produced from using FFR. The major hydrogenolysis product of 2MF and furan was 2-pentanol (6.0% yield) and 1-butanol (5.5% yield), respectively. Those results imply the Ni-Y₂O₃(2.5)623 catalyst demonstrated a similar reaction pathway for hydrogenolysis of FFR, 2MF, and furan to the corresponding diol or alcohol.



Reaction conditions: Ni-Y₂O₃(2.5)623 catalyst (0.05 g), substrate (1.1 mmol), *trans*-decahydronaphthalene (0.07 g), 2-propanol (3 mL), 423 K, H₂ (2.0 MPa), for 24 h. Conversion and yield were determined by GC using the internal standard technique.

Scheme 3.3 Hydrogenolysis products from biomass furanic compound.

3.6 Catalytic hydrogenolysis of tetrahydrofurfuryl alcohol (THFA)

3.6.1 Hydrogenolysis of THFA in various Ni-Y₂O₃ catalysts

The catalytic activity of the Ni-Y₂O₃ catalyst in the hydrogenolysis of FFR and FFA was examined. THFA was produced at a higher yield than the target compound. Indeed, employing THFA as a substrate has been experimented to achieve a comprehensive study of that reaction as shown in Table 3.5. Tuning Ni/Y mol ratios (number in parenthesis) between 1.5 and 3.0 in the catalyst preparation influenced their catalytic performances achieving more than 50% conversion and 32% yield of 1,5-PeD, Ni-Y₂O₃(2.5)₆₂₃ achieving the highest yield of 1,5-PeD up to 54.7 among them (entries 1, 2, 6). Their product distributions were 1,5-PeD solely as a hydrogenolysis product and 1-BuOH as a by-product. Obviously, the Ni-Y₂O₃ catalyst is highly selective in producing 1,5-PeD from THFA. Employing catalysts such as Ni⁰, NiO, Y₂O₃ and unreduced Ni-Y₂O₃ at the same reaction condition, and neither case formed 1,5-PeD (entries 9-12). The results indicated that the C-O bond cleavage of tetrahydrofuran ring of the THFA should proceed on the Ni-Y₂O₃ boundaries as we proposed earlier.

Calcination temperatures as a pre-treatment have been varied in the range of 623 – 1073 K of Ni-Y₂O₃(2.5)_T catalyst with a single H₂ treatment temperature at 673 K and their catalytic performance showed in Table 3.5 (entries 3-7). As mentioned earlier, calcination temperature had a great influence on their crystallinity, surface area, and acidity, an increase in the calcination temperature drastically decreased the conversion of THFA and yield of 1,5-PeD. The pre-treatment at 623 K, Ni-Y₂O₃(2.5)₆₂₃ catalyst, exhibited the highest THFA conversion and 1,5-PeD of up to 59.8% and 54.7%, respectively. While the other pentanediols such as 1,2- and 1,4-

were not observed in all investigated catalysts. An introduction of Y₂O₃ onto Ni⁰ (Ni-Y₂O₃(2.5)-623pm catalyst) was enough for producing around 18 % yield 1,5-PeD (entry 8). Seemingly, in our case, a higher crystallinity of nickel and yttrium oxide is detrimental to Ni-Y₂O₃ interaction by means of Ni⁰-Y₂O₃ boundaries formation and surface acidity which have a prominent role of C-O bond cleavage and effectively formed in Ni-Y₂O₃(2.5)623 catalyst. The optimized variation of Ni/Y mol ratios and calcination temperatures seems to bring out the best in 1,5-PeD formation on Ni-Y₂O₃(2.5)623 catalyst considering an effective formation of Ni⁰-Y₂O₃ boundaries. The ring opening of THFA on Ni⁰-Y₂O₃ boundaries implies a respect for the 1,5-PeD yield.

Table 3.5 Catalytic hydrogenolysis of THFA to 1,5-PeD

Entry	Catalyst ^a	Conv. (%)	Yield (%)	
			1,5-PeD	1-BuOH
1	Ni-Y ₂ O ₃ (3.0)623	53.0	34.9	2.1
2	Ni-Y ₂ O ₃ (1.5)623	51.7	32.0	trace
3	Ni-Y ₂ O ₃ (2.5)1073	13.1	13.1	0.0
4	Ni-Y ₂ O ₃ (2.5)923	27.4	18.6	trace
5	Ni-Y ₂ O ₃ (2.5)773	28.1	21.3	1.0
6	Ni-Y ₂ O ₃ (2.5)623	59.8	54.7	2.3
7	Ni-Y ₂ O ₃ (2.5)573	56.1	35.3	1.1
8	Ni-Y ₂ O ₃ (2.5)623pm	24.3	18.3	0.0
9	Ni-Y ₂ O ₃ (2.5)623 ^b	0.0	0.0	0.0
10	Ni(0)	19.2	0.0	0.0
11	Y ₂ O ₃	15.6	0.0	0.0
12	NiO ^b	7.0	0.0	0.0

^a Reaction conditions: Reduced Ni-Y₂O₃ catalyst (0.05 g), THFA (1.0 mmol), *trans*-decahydronaphthalene (0.07 g), 2-propanol (3 mL), 423 K, initial H₂ pressure (2.0 MPa), for 24 h. Conversion and yield were determined by GC using the internal standard technique. ^b without H₂ treatment.

3.6.2 Evaluation of reaction conditions

The conversion of THFA to 1,5-PeD was conducted in 2-propanol with 2.0 MPa initial H₂ pressure at 423 K for 24 h and Ni-Y₂O₃(2.5)623 catalyst exhibited the highest catalytic activity. We, therefore, investigate the reaction conditions i.e. reaction temperature, initial H₂ pressure, and reaction time dependencies. Alteration in reaction temperature highly impacted both the THFA conversion and 1,5-PeD yield as shown in Figure 3.8(A). Starting from FFR as a substrate, the reaction temperature was increased from 313 to 373 K for enhancing C-O bond hydrogenolysis over rhenium- modified Rh-Ir alloy catalyst.²³ It seems to have a propensity for increasing THFA conversion and 1,5-PeD yield at a higher reaction temperature. Our catalytic system was proceeding in a similar way with FFR and FFA as substrates, at higher reaction temperature than 423 K, which not only increased the yield of 1,5-PeD but also the 1-butanol steadily. Moreover, the selectivity regarding the other pentanediols yield was well maintained by means of increasing the reaction temperature up to 473 K. It suggests that the Ni⁰-Y₂O₃ boundaries cleaved the C-O bond in tetrahydrofuran ring at remarkably high selectivity leading to the 1,5-PeD formation.

Hydrogen pressure is a crucial parameter in hydrogenation as well as hydrogenolysis, which is related to the hydrogen activation or hydride formation on the catalyst surface. Reported works in hydrogenolysis of THFA to 1,5-PeD suggested that the activation of hydrogen is conducted in the form of a rate-determining step in this reaction.^{12,15,24-26} The initial H₂ pressure dependency in the catalytic performance of Ni-Y₂O₃(2.5)623 catalyst was investigated to be between 1.0 and 3.0 MPa as shown in Figure 3.8(B). At the same reaction temperature

(423K), the rising from the initial H₂ pressure from 1.0 to 2.0 MPa enhanced the conversion of THFA and yield of 1,5-PeD. The effect of the initial hydrogen pressure was found to be insignificant at a higher value than 2.0 MPa.

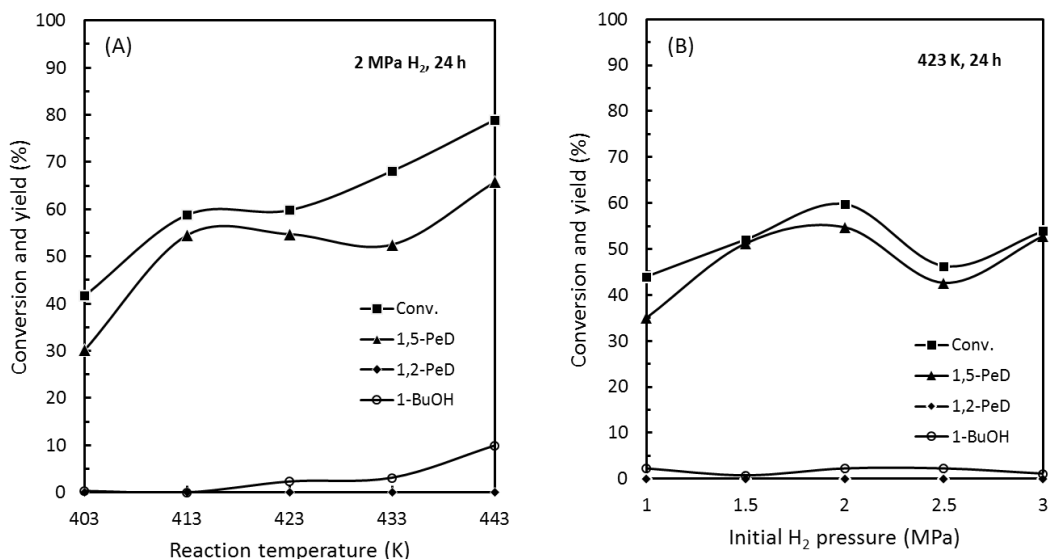


Figure 3.8 Effect of (A) reaction temperature and (B) initial H₂ pressure in hydrogenolysis of THFA over Ni-Y₂O₃(2.5)623 catalyst.

Table 3.6 Effect of composition of pressurized gas on catalytic performance of Ni-Y₂O₃(2.5)623 catalyst.

Entry	Gas ^a Composition	Conv. ^b (%)	Yield (%) ^b	
			1,5-PeD	1-BuOH
1	H ₂	59.8	54.7	2.3
2	H ₂ + N ₂	45.0	19.4	3.7
3	H ₂ ^c	44.0	35.0	2.3
4	N ₂ ^c	0.0	0.0	0.0

Reaction conditions: [a] Reduced Ni-Y₂O₃ catalyst (0.05 g), THFA (1.0 mmol), *trans*-decahydronaphthalene (0.07 g), 2-propanol (3 mL), 423 K, gas pressure (2.0 MPa), for 24 h. [b] were determined by GC using the internal standard technique. [c] without H₂ treatment. [c] 1.0 MPa initial gas pressure.

THFA does not have C=C and C=O bonds, still hydrogen gas is important for C-O bond cleavage of tetrahydrofuran ring. Isopropanol which was employed as a solvent

has an ability for hydrogen source. Our investigation in pressurized gas composition as shown in Table 3.6 proved that pressurized hydrogen gas has a prominent role in C-O bond cleavage. Only isopropanol as hydrogen source was not enough to cleave C-O bond at 1.0 MPa N₂ gas. Moreover, a pressurized of the N₂-H₂ gas mixture (2.0 MPa) lowered the conversion and yield of 1,5-PeD compared with 1.0 and 2.0 MPa H₂. Thus, the reaction temperature at 423 K and the hydrogen pressure of at least 2.0 MPa is adequate for obtaining 1,5-PeD from THFA at high yield and selectivity over that catalyst.

3.6.3 Effect of solvent

The nature of solvent impacted a great influence on the yield of the 1,5-PeD (Table 3.7). The breaking of the C-O bond of furan or tetrahydrofuran ring required proton.^{15,23,27} Effect of solvent was investigated in polar protic and aprotic (1,4-dioxane) solvent. Methanol, ethanol, 2-propanol, and 2-butanol have good H-bond donors and acceptors ($\alpha \neq 0$ and $\beta \neq 0$). For the first time, we used 2-propanol as a solvent in this reaction and exhibited good performance among all investigated solvents. Surprisingly, by employing 1,4-dioxane, higher THFA was converted than in primary alcohol. In fact, 1,5-PeD was obtained up to 15 % yield, which is higher than in methanol, ethanol, and 2-butanol, by employing 1,4-dioxane as a solvent which has H-bond acceptors ($\beta \neq 0$) ability, and less basic (DN = 59.8 kJ/mol) property. Lewis basic solvent ($\beta \neq 0$ and DN > 50 kJ/mol) slanted preferable for C-O bond hydrogenolysis.²⁸ Moreover, in the 2-propanol which possesses the highest H-bond acceptor ($\beta = 0.84$) and donating number (DN = 150.6 kJ/mol) among the investigated solvent exhibited the yield of 1,5-PeD up to 54.7 %. It means that alcohol and 1,4-dioxane as solvent accomplished C-O bond cleavage of

tetrahydrofuran ring for the 1,5-PeD formation and proceeded preferentially in 2-propanol.

Table 3.7 Hydrogenolysis of THFA in various solvents.

Solvent	Parameter				Conv. (%)	Yield (%) 1,5-PeD
	α	β	AN	DN		
2-PrOH	0.76	0.84	140.0	150.6	59.8	54.7
2-BuOH	0.69	0.80	109.0	136.4	36.5	10.9
MeOH	0.98	0.66	172.6	125.5	0.0	0.0
EtOH	0.86	0.75	155.1	133.9	10.0	10.0
Dioxane	0.00	0.37	43.1	59.8	31.1	15.5

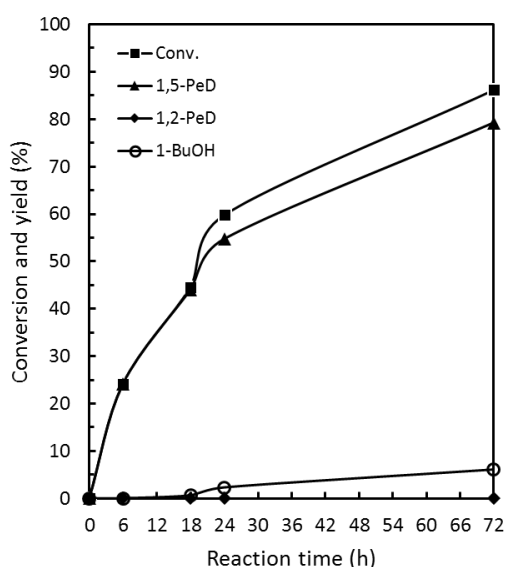
^a Reaction conditions: Ni-Y₂O₃(2.5)623 catalyst (0.05 g), THFA (1.0 mmol), *trans*-decahydronaphthalene (0.07 g), solvent (3 mL), 423 K, initial H₂ pressure (2.0 MPa), for 24 h. Conversion and yield were determined by GC using the internal standard technique.

In the M-M'Ox catalyst system (Tomishige's catalyst), alcohol solvents significantly decrease their catalytic activities because of the competition between the alcohol and substrate for the adsorption on the active site.⁴ A similar manner could occur in our catalytic reaction system, the yield of 1,5-PeD depends likely on the donor proton parameter value and decrease from 54.7 to 0 % yield as the following order 2-PrOH < EtOH < MeOH. It means that the easiest donor proton ability presents the highest competition of THFA to attach on the active site and have a negative impact on the 1,5-PeD yield.

3.6.4 Time course

The time profile in hydrogenolysis of THFA to 1,5-PeD at 423K Ni-Y₂O₃(2.5)623 catalyst was depicted in Figure 3.9. THFA was directly transformed to 1,5-PeD without 1,2-PeD formation and then 1-butanol was seen after 18 h of reaction. Transformation of THFA to 1,5-PeD was increased continuously by prolonging time reaction up to 79.2% yield for 72 h. Meanwhile, 1-butanol was obtained at higher yield during the prolonging time reaction. 1-butanol was detected by using 1,5-PeD

instead of THFA as a substrate. Moreover, a study of the adsorption of ethanol on Ni metal surface at a range of 100 – 400 K suggested that Ni(0) might promote C–C bond breaking of the ethanol molecule lead to the emergence of hydrogen and methane.²⁹ Probably, the 1-butanol formation in our case proceeded in the same manner. Inversely, the 1,2-PeD persisted undetectable, although the reaction time was prolonged to 72 hours at 86.2% THFA conversion. The uncomplete of THFA conversion was suggested due to deactivation of Ni⁰-Y₂O₃ boundaries. The interference from the adsorbed product on catalyst surface also could be contributed to the sluggish 1,5-PeD formation.



Reaction conditions: Ni-Y₂O₃(2.5)623 catalyst (0.05 g), THFA (1.0 mmol), *trans*-decahydronaphthalene (0.07 g), 2-propanol (3 mL), 423 K and initial H₂ pressure (2.0 MPa). Conversion and yield were determined by GC using the internal standard technique.

Figure 3.9 Time course of hydrogenolysis of THFA over Ni-Y₂O₃(2.5)623 catalyst.

3.6.5 Reusability test

The reusability investigation of Ni-Y₂O₃(2.5)623 catalyst, especially which exhibited the best catalytic performance, is shown in Figure 3.10 (left). The catalyst was washed for three times after the first reaction for removing the remaining

organic compounds on the catalyst surface. The thermogravimetric analysis at a temperature below 200 °C under N₂ gas flow for fresh and used catalyst showed a mass loss of 1.69 %wt and 2.17 %wt, respectively. The catalytic activity of spent catalyst lowers the conversion of THFA and yield of 1,5-PeD. The remaining organic compounds on the catalyst surface were contributed for catalyst deactivation. Also, an alteration to the Ni⁰-Y₂O₃ boundary which was proposed as crucial for a C-O bond cleavage is the dominant factor for deactivating the catalyst. The XRD patterns of the used catalyst as displayed in Figure 3.10 (right) revealed the alteration in crystallinity of Ni metal as well as yttrium oxide and most probably due to the leaching of the catalyst. However, it is not yet investigated so far.

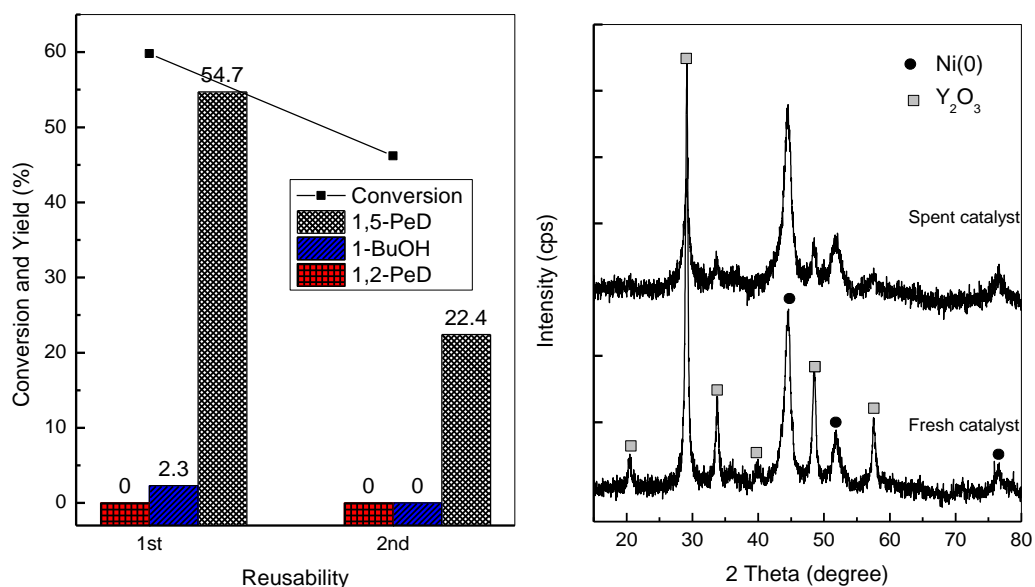


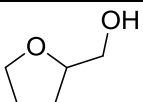
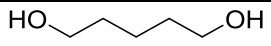
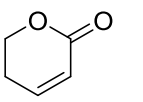
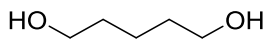
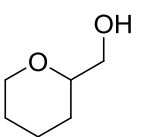
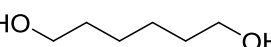
Figure 3.10 Reusability test of Ni-Y₂O₃(2.5)623 catalyst (left) and the XRD patterns of fresh and used catalysts (right).

3.6.6 Ring opening of cyclic ether to terminal diols

Transformation of furfural and its hydrogenation product over Ni-Y₂O₃ catalysts through the C-O bond cleavage of tetrahydrofuran ring selectively proceeds to give 1,5-PeD. At the optimized reaction condition and catalyst (Ni-Y₂O₃(2.5)-623

catalyst) the conversion of THFA which was proposed as an intermediate in hydrogenolysis FFR and FFA produced 1,5-PeD as a sole pentanediol. Recently, Huber and Dumesic have been simulated a multi-step catalytic conversion from furfural feedstock to 1,5-PeD involving hydrogenation and dehydration–hydration–hydrogenation process.¹¹ The conversion of THFA to 2-hydroxytetrahydropyran (2-HY-THP) then hydrogenolysis to 1,5-PeD was suggested as the simple way to obtain 1,5-PeD. Our catalyst was tested in the hydrogenolysis of dihydropyran-2-one (DHP2O) only gave 10.3% yield of 1,5-PeD and the rest was 2-HY-THP (Table 3.18 entry 2). The result gives a view that the conversion of THFA in our catalytic reaction system directly proceeds to give 1,5-PeD.

Table 3.8 The catalytic activity of Ni-Y₂O₃(2.5)623 catalyst for ring opening of cyclic ether to terminal diols.

Entry	Substrate ^a	Conv. ^b (%)	Product	
			diol	Yield (%)
1		59.8		54.7
2		>99		10.2
3		28.2		25.9

Reaction conditions: [a] Ni-Y₂O₃(2.5)623 catalyst (0.05 g), THFA (1.0 mmol), *trans*-decahydronaphthalene (0.07 g), 2-propanol (3 mL), 423 K, gas pressure (2.0 MPa), for 24 h. [b] were determined by GC using the internal standard technique.

Hydrogenolysis of other cyclic ether to terminal diol had been conducted such as 1,6-hexanediol (1,6-HDO) from tetrahydropyran-2-one (THP2M) in our catalysts as listed in Table 3.8 entry 3. THP2M has been reported to be a candidate for obtaining

1,6-hexanediol (1,6-HDO) from biomass-derived compounds.³⁰⁻³² As anyone knows that six-member ring is more stable than five-member, the hydrogenolysis of THP2M gave 1,6-HDO (25.9% yield) as a sole diol at 28.2% conversion over Ni-Y₂O₃(2.5)623 catalyst. The catalytic activity of that substrate was lower than THFA at the same reaction condition. Similarly, the hydrogenolysis of THP2M over Rh-ReO_x/C (Rh/Re = 0.25) gave a lower conversion compare to use THFA as a substrate.³⁰ A lower conversion of THP2M and yield of diol could be assumed as the result of the stability of hexacyclic ether ring toward ring opening reaction. That result confirms the selectivity of the Ni-Y₂O₃ catalyst for hydrogenolysis of THFA as well as THP2M to corresponding terminal diols.

3.7 Investigation of THFA hydrogenolysis mechanism

The best result in the direct conversion of THFA to 1,5-PeD which was conducted in water has been achieved of up to 94 % selectivity using a Rh-ReO_x/C catalyst.³⁰ An acid-catalyzed reaction such as dehydration would effectively occur after giving 1,5-pentanediol on that catalytic system. Authors proposed that the THFA molecule is adsorbed on the metal oxide species, ReO_x, via the -CH₂OH group, and the C-O bond neighboring the -CH₂OH group is attacked by hydride-like species formed from H₂ on the noble metal atom.¹² A similar manner could be proposed in the case of a Ni-Y₂O₃ catalyst, the hydride-like species which is formed on Ni metal surface attacked the C-O bond neighboring the adsorbed CH₂OH group on the acid site of Y₂O₃ giving 1,5-PeD. To understand the reaction mechanism in our catalytic reaction system, several experiments were conducted such as substrate and catalyst dependency including poisoned experiment by presenting 1,5-PeD in the initial

reaction and adsorbed basic compound on catalyst and FTIR study in the adsorption THFA on the catalyst.

3.7.1 Dependency of substrate and catalyst

The hydrogenolysis catalytic reaction experimented in 2-propanol at different molar THFA over Ni-Y₂O₃(2.5)623 catalyst as shown in Figure 3.11(A). With the same catalyst loading amount, an increase in the molar concentration of THFA linearly decreased the conversion of THFA while the yield of 1,5-PeD was likely to show a volcano peak at 0.35 M. At a low concentration, the yield of 1-BuOH obtained at the highest yield (4.1 %) with a high conversion of THFA (62.0 %). The 1-BuOH was formed from the hydrogenolysis of pentanediol as mentioned earlier. Seemingly, the formed 1,5-PeD strongly attached on the catalyst surface which could prevent the adsorption of the unreacted THFA. As a consequence, a higher amount of THFA gave a lower conversion of THFA and yield of 1,5-PeD as well. The thermogravimetric analysis result on the used catalyst at 0.35 M only showed a degradation peak at below 200 °C, and around 2.17 % mass loss which was a little bit higher than fresh catalyst (1.69 %). Therefore, the prolonged reaction time to 72 h enhanced the yield of 1,5-PeD up to 79.2 % (Figure 3.9). The results inferred that covering the catalyst surface with the formed 1,5-PeD could decelerate the ring opening of THFA.

The substrate to catalyst ratio was studied at a constant 0.35 M THFA in the catalyst loading amount variation as illustrated in Figure 3.11 (B). An increase in the amount of Ni⁰-Y₂O₃ boundary by increasing the catalyst loading amount would enhance the hydrogenolysis performance. By product, 1-BuOH was formed as a function of increasing catalyst to substrate ratio. It could be ascribed to further

hydrogenolysis of the formed 1,5-PeD. The highest THFA conversion and 1,5-PeD yield could be obtained at the highest substrate to catalyst ratio (10.8) up to 91.6% and 87.8%, respectively. It is suggested that the attached CH₂OH group of THFA to Ni⁰-Y₂O₃ is crucial to facilitate the ring opening of tetrahydrofuran ring obtaining 1,5-PeD. In addition, the existing hydroxyl group from solvent and product could be ascribed as competitors for attaching THFA on the catalyst surface.

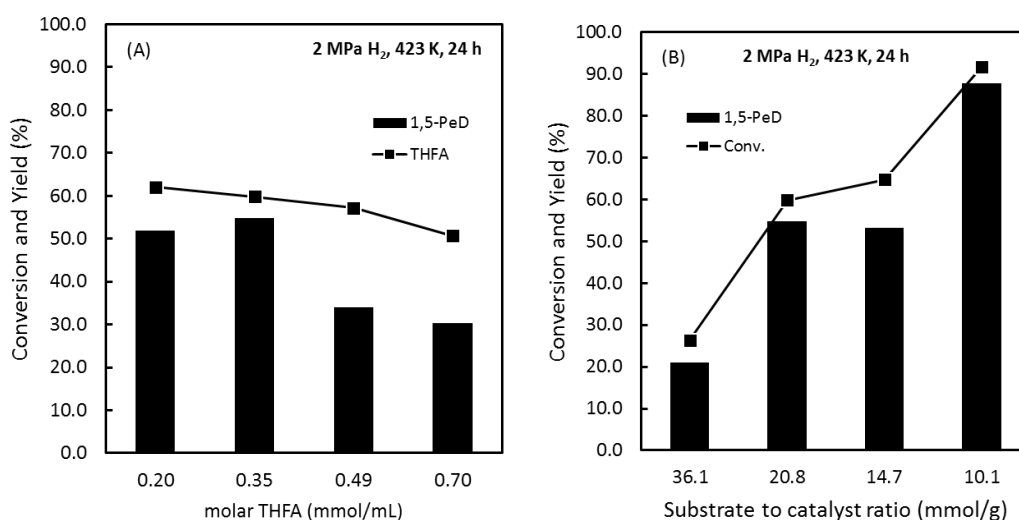


Figure 3.11 (A) Molar THFA dependency at a constant of Ni-Y₂O₃(2.5)623 catalyst loading amount (0.05 g cat.). (B) THFA to Ni-Y₂O₃(2.5)623 catalyst ratio at constant molar THFA (0.35 mmol/mL).

3.7.2 Poisoning experiment

An addition of 1,5-PeD in the initial reaction together with THFA as a substrate which is expected to poison the catalyst active site was performed. At the same catalytic reaction condition, adding 0.5 mmol of 1,5-PeD drastically lowered the conversion of THFA and yield of 1,5-PeD to 19.3 % and 13.3 %, respectively. The adsorption of 2-propanol over Y₂O₃ at 423 K would be ascribed for starting dehydrogenation at 473 K,³³ even the transfer hydrogenolysis could not proceed in our catalyst system (Table 3.4 entry 4). In the case of M-M'Ox catalyst system

(Tomishige's catalyst), alcohol solvents decrease many of their catalytic activities because of the competition between the alcohol and substrate for the adsorption on the active site.⁴ The OH groups of isopropanol, THFA, as well as 1,5-PeD, must compete to attach on the Ni-Y₂O₃ catalyst acidic site. Conducting catalytic reaction in the ethanol and methanol which possess a higher proton donor ability instead of 2-propanol lowered the yield of 1,5-PeD by the order of increasing donor proton ability (Table 3.7). This poisoning experiment could be acted as an evidence that a stronger interaction of the formed 1,5-PeD can interfere in the adsorption of the remained THFA during the catalytic reaction.

On the basis of the reported works, the addition of a reducible metal oxide on Noble metal catalyst is critical facilitating a Bronsted acidic site which is a key role for the ring opening of tetrahydrofuran ring of THFA to form 1,5-PeD. To examine that property, a Ni-Y₂O₃(2.5)623 catalyst exposed to saturated cyclohexylamine vapor for 20 hours at ambient temperature before used it for catalytic hydrogenolysis reaction. It only produced 17.2% yield of 1,5-PeD from THFA at the optimized reaction condition. It suggested the role of the hydroxyl group on the Y₂O₃ surface act as the Bronsted acidic site in our catalytic reaction system.

3.7.3 Proposing a mechanism of the ring opening of THFA

The formation of THFA in the hydrogenolysis of FFR and FFA can be understood in term of consecutive hydrogenation of FFR and FFA. Result in the transformation of THFA to 1,5-PeD without 1,2-PeD formation shows that the ring opening mechanism of THFA on the Ni-Y₂O₃(2.5)623 surface would be an indispensable step to obtain 1,5-PeD. For that goal, the adsorption of THFA molecules on that catalyst surface was experimented using FT-IR as shown in Figure 3.12. Because the

vibrational assignments of THFA vapor were not reported the vibrational spectrum of tetrahydrofuran (THF) was used as references for this study.^{34,35} The authors reported two characteristic vibrations of THF, i.e. the symmetric valence vibration of ether group at 1075 cm^{-1} and the symmetric (pulsating) vibration of tetrahydrofuran ring skeleton at 918 cm^{-1} . In addition, the spectrum of tetrahydrofuran derivatives (the substituted THF) indicated the presence of a five-membered oxygen ring and those bands were antisymmetric valence vibration of C—O—C group (1000-1100 cm^{-1}) and symmetric (pulsating) vibration of the ring (900-950 cm^{-1}). Our results show the absorbed THFA spectra could be assigned to two groups, the tetrahydrofuran ring vibration (983, 1060, 1103 cm^{-1} C—O—C for group and 823, 863, 912 cm^{-1} for symmetric (pulsating) vibration of the ring) and the sp^3 C—H bond stretching (2879, 2969, and 2981 cm^{-1}) in Figure 3.12. The resemblance of all vibrations indicates that tetrahydrofuran ring did not interact with catalyst surface. In addition, a new band at 1270 cm^{-1} which was assigned as δ -OH (Figure 3.12 (b) and (c)) was strongly related with the absorption of THFA molecules on yttrium oxide site of Ni-Y₂O₃(2.5)623 catalyst. The absorption of 2-propanol on the hydroxylated and/or dehydroxylated of Y₂O₃ showed the δ -OH absorption at 1280 cm^{-1} indicating the presence of the coordinated 2-propoxide species.³³ The authors proposed the absorption of 2-propanol on the hydroxylated surface or dehydroxylated yttrium oxide formed water and OH⁻, respectively. Based on Hussein's results³³, we concluded that the yttrium oxide of Ni-Y₂O₃(2.5)623 was coordinated by THFA through hydroxyl group (CH₂OH). Then the absorbed THFA was easily attacked by hydride species from Ni metal surface giving 1,5-PeD with high selectivity (see Figure 3.13). The role of yttrium oxide was also confirmed in the Ni-Y₂O₃(2.5)623 catalyst loading evaluation

(Figure 3.11) and poisoning experiment. The reaction mechanism according to our data for that reaction can be proposed as illustrated in Figure 3.13.

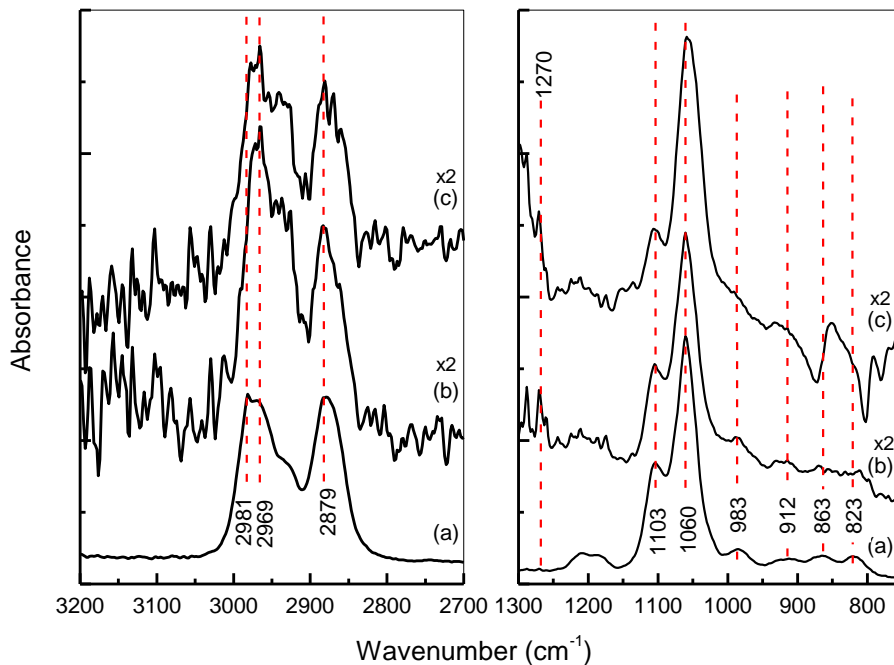


Figure 3.12 Background-substituted FT-IR spectra of (a) THFA vapor, the adsorbed THFA on Ni-Y₂O₃(2.5)623 (b) at ambient temperature and (c) after heated at 423 K.

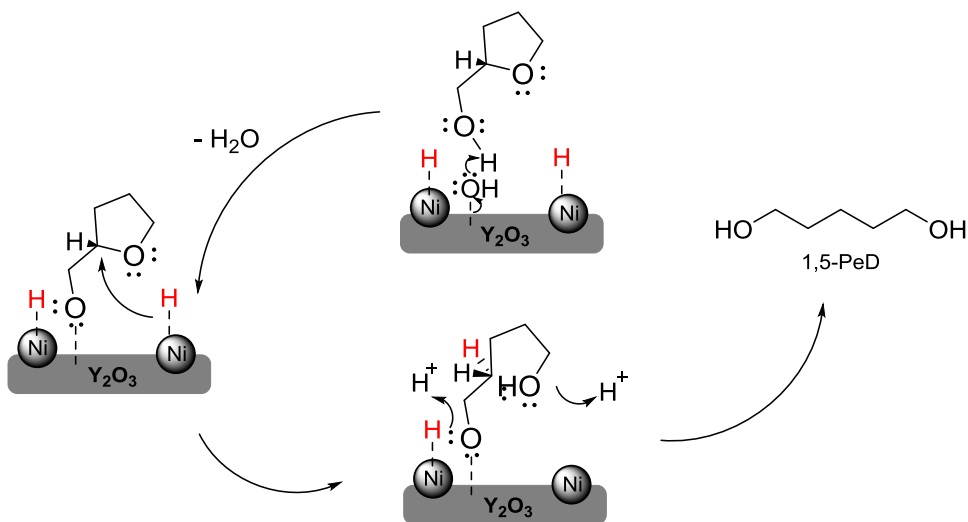


Figure 3.13 Illustrated of the proposed reaction mechanism for selective hydrogenolysis of THFA to 1,5-PeD over Ni-Y₂O₃ catalyst.

3.8 Surface catalyst characterization

The above results underline the Ni-Y₂O₃(2.5)623 catalyst had the best catalytic performance to obtaining 1,5-PeD from FFR, FFA, as well as THFA. The ring opening of THFA is the rate determining step to obtain 1,5-PeD selectively which is studied using FT-IR of the absorbed THFA (section 3.7.3). Further, TEM and XPS analysis were established for that catalyst for understanding the chemistry on the surface. The TEM image of Ni-Y₂O₃(2.5)623 catalyst illustrated a Y₂O₃ rod surrounded with Ni(0) nanoparticles, as shown in Figure 3.14. Similarly, a rod-like Y₂O₃ was observed by Yanagisawa et al.³⁶ When the Ni/Y mole ratio was 2.5, a larger amount of Ni(0) nanoparticles were observed. Following our interest in the oxidation state of nickel and yttrium species on the catalyst surface, we performed XPS (X-ray photoelectron spectroscopy) measurements of Ni-Y₂O₃(2.5)623 catalyst and compared the evaluated binding energies (BE) were with the literature. The BE of Y(3*d*_{3/2}) and Y(3*d*_{5/2}) at 159.6 eV and 157.9 eV indicated the presence of the yttrium oxide species.^{37,38} The O(1*s*) BE at 529.9 eV also confirmed the presence of yttrium oxide. However, carbonate species was found at catalyst surface as shown at 532.0 eV for O(1*s*) and 290.0 eV for C(1*s*). This result was consistent with XRD patterns which were explained earlier.

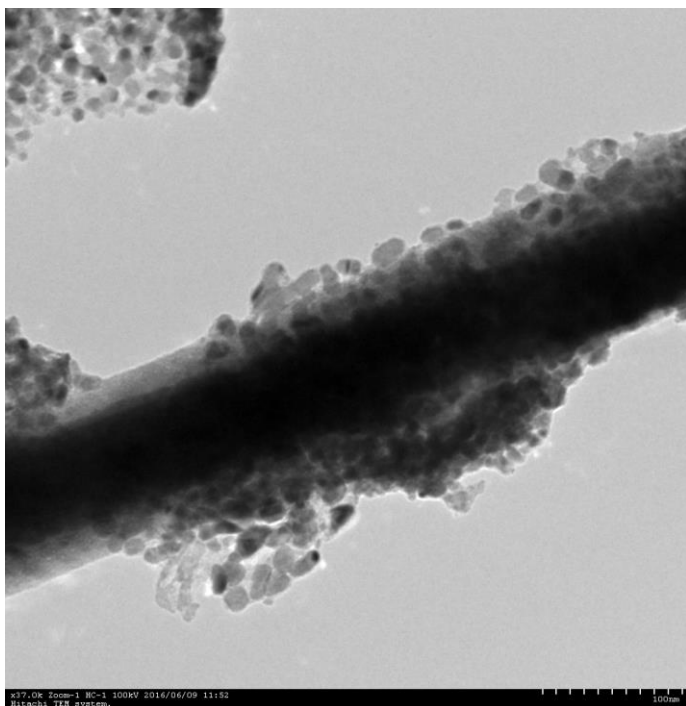


Figure 3.14 TEM image of Ni-Y₂O₃(2.5)623 catalyst.

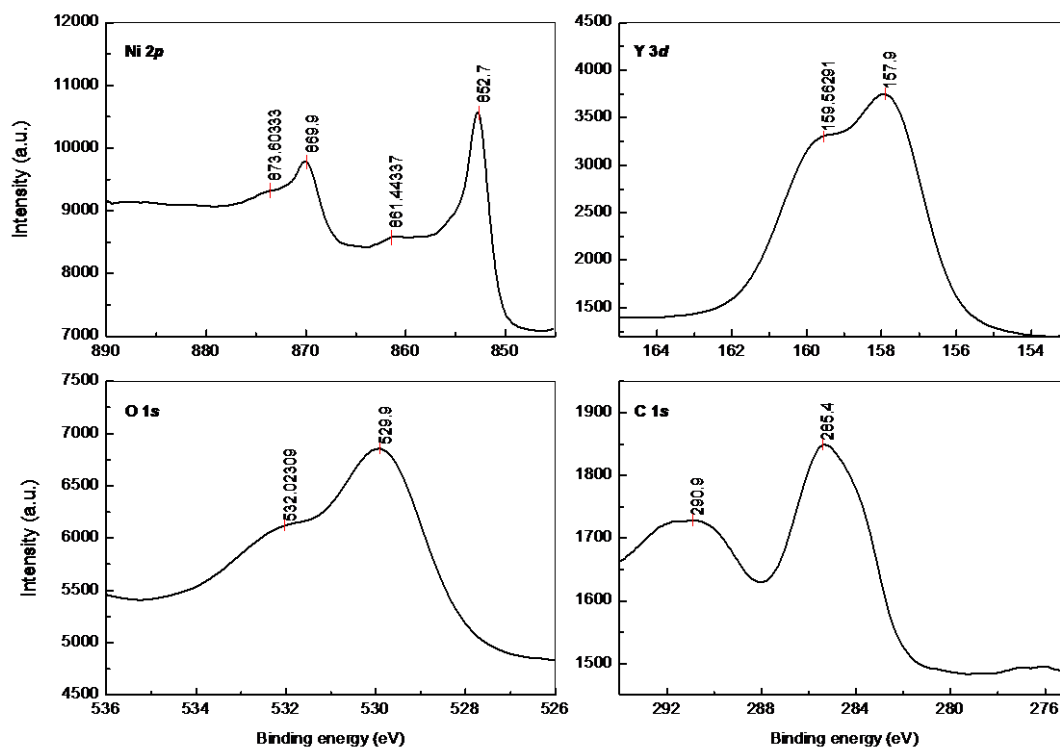


Figure 3.15 XPS spectra of Ni-Y₂O₃(2.5)623 catalyst.

3.8 Conclusion

In summary, the synthesis of Ni-Y₂O₃(x)T (x and T indicate the Ni/Y mole ratio and calcination temperature in Kelvin) catalysts were successfully prepared by coprecipitation, hydrothermal, calcination, and subsequent H₂ treatments (673 K). The XRD analysis showed the existence of Ni metal and yttrium oxide in the Ni-Y₂O₃ catalyst. The Ni-Y₂O₃(2.5)623 catalyst possesses the highest amount of H₂ uptake and acidic site which holds Ni⁰-Y₂O₃ boundaries effectively among the other investigated catalysts. The XPS analysis of that catalyst confirmed the presence of Ni(0) and Y₂O₃ as well. It exhibited the highest catalytic activity to the hydrogenolysis of FFR, FFA, and THFA by giving the highest yield of 1,5-PeD 29.8 %, 41.9 %, and 54.7 %, respectively, at the optimized reaction condition (2.0 MPa initial H₂ and 423 K) with 2-propanol as a solvent. Both FFR and FFA were hydrogenated giving THFA prior to the 1,5-PeD formation through ring opening of tetrahydrofuran ring selectively. The adsorption of THFA onto that catalyst surfaces from FTIR evaluation confirmed the deprotonation of OH group giving the preferable 1,5-PeD product. Utilizing of THP2M and DHP2O as substrates indirectly validated the proposed mechanism for the direct ring opening of THFA to 1,5-PeD selectively. Increasing the catalyst loading amount for 0.1 g catalyst, Ni-Y₂O₃(2.5)623, at the optimized condition yielded 1,5-PeD up 87.8% with 91.6% THFA conversion.

ABBREVIATIONS

FFR: furfural	2MF: 2-methylfuran	MeOH: methanol
FFA: furfuryl alcohol	2-HY-THP: 2-hydroxytetrahydropyran	EtOH: ethanol
THFA: tetrahydrofurfuryl alcohol	DHP2O: dihydropyran-2-one	2-PrOH: 2-propanol
1,5-PeD: 1,5-pentanediol	1,6-HDO: 1,6-hexanediol	1-BuOH: 1-butanol

1,4-PeD, 1,4-pentanediol THP2M: tetrahydropyran-2-methanol 2-BuOH: 2-butanol
1,2-PeD, 1,2-pentanediol THF: tetrahydrofuran

Notes

Some of the results in this chapter has been published as follows “H. W. Wijaya, T. Kojima, T. Hara, N. Ichikuni and S. Shimazu, Synthesis of 1,5-Pentanediol by Hydrogenolysis of Furfuryl Alcohol over Ni-Y₂O₃ Composite Catalyst, *ChemCatChem*, 2017, **9**, 2869–2874.” as part of a Special Issue on the Catalytic Conversion of Biomass.

REFERENCES

- 1 R. Mariscal López, P. Maireles-Torres, M. Ojeda, I. Sadaba and M. López Granados, *Energy Environ. Sci.*, 2016, **9**, 1144–1189.
- 2 Y. Song, W. Li, M. Zhang and K. Tao, *J. Fuel Chem. Technol.*, 2006, **34**, 483–486.
- 3 S. Iqbal, X. Liu, O. F. Aldosari, P. J. Miedziak, J. K. Edwards, G. L. Brett, A. Akram, G. M. King, T. E. Davies, D. J. Morgan, D. K. Knight and G. J. Hutchings, *Catal. Sci. Technol.*, 2014, **4**, 2280.
- 4 Y. Nakagawa, M. Tamura and K. Tomishige, *Catal. Surv. from Asia*, 2015, **19**, 249–256.
- 5 H. Liu, Z. Huang, F. Zhao, F. Cui, X. Li, C. Xia and J. Chen, *Catal. Sci. Technol.*, 2016, **6**, 668–671.
- 6 B. Zhang, Y. Zhu, G. Ding, H. Zheng and Y. Li, *Green Chem.*, 2012, **14**, 3402–3409.
- 7 T. Mizugaki, T. Yamakawa, Y. Nagatsu, Z. Maeno, T. Mitsudome, K. Jitsukawa and K. Kaneda, *ACS Sustain. Chem. Eng.*, 2014, **2**, 2243–2247.

- 8 D. Götz, M. Lucas and P. Claus, *React. Chem. Eng.*, 2016, **1**, 161–164.
- 9 H. Liu, Z. Huang, H. Kang, C. Xia and J. Chen, *Chinese J. Catal.*, 2016, **37**, 700–710.
- 10 P. Werle, M. Morawietz, S. Lundmark, K. Sörensen, E. Karvinen and J. Lehtonen, in *Ullmann's Encyclopedia of Industrial Chemistry*, 2012, vol. 2, pp. 263–284.
- 11 K. Huang, Z. J. Brentzel, K. J. Barnett, J. A. Dumesic, G. W. Huber and C. T. Maravelias, *ACS Sustain. Chem. Eng.*, 2017, **5**, 4699–4706.
- 12 S. Koso, I. Furikado, A. Shima, T. Miyazawa, K. Kunimori and K. Tomishige, *Chem. Commun.*, 2009, 2035.
- 13 K. Tomishige, Y. Nakagawa and M. Tamura, *Green Chem.*, 2017, **19**, 2876–2924.
- 14 M. Chia, Y. J. Pagán-Torres, D. D. Hibbitts, Q. Tan, H. N. Pham, A. K. Datye, M. Neurock, R. J. Davis, J. A. Dumesic, Y. J. Pag, Y. J. Pagán-Torres, D. D. Hibbitts, Q. Tan, H. N. Pham, A. K. Datye, M. Neurock, R. J. Davis and J. A. Dumesic, *J. Am. Chem. Soc.*, 2011, **133**, 12675–12689.
- 15 J. Guan, G. Peng, Q. Cao and X. Mu, *J. Phys. Chem. C*, 2014, **118**, 25555–25566.
- 16 H. Liu and D. He, *Int. J. Hydrogen Energy*, 2011, **36**, 14447–14454.
- 17 H. Liu, H. Wu and D. He, *Fuel Process. Technol.*, 2014, **119**, 81–86.
- 18 G. B. Sun, K. Hidajat, X. S. Wu and S. Kawi, *Appl. Catal. B Environ.*, 2008, **81**, 303–312.
- 19 M. Pospisil and P. Kanokova, *J. Therm. Anal. Calorim.*, 1999, **58**, 77–88.
- 20 P. D. Vaidya and V. V Mahajani, *Ind. Eng. Chem. Res.*, 2003, **42**, 3881–3885.

- 21 S. M. Gates, J. N. Russell and J. T. Yates, *Surf. Sci.*, 1986, **171**, 111–134.
- 22 M. Choura, N. M. Belgacem and A. Gandini, *Macromolecules*, 1996, **29**, 3839–3850.
- 23 S. Liu, Y. Amada, M. Tamura, Y. Nakagawa and K. Tomishige, *Green Chem.*, 2014, **16**, 617.
- 24 S. Koso, N. Ueda, Y. Shinmi, K. Okumura, T. Kizuka and K. Tomishige, *J. Catal.*, 2009, **267**, 89–92.
- 25 Z. Wang, B. Pholjaroen, M. Li, W. Dong, N. Li, A. Wang, X. Wang, Y. Cong and T. Zhang, *J. Energy Chem.*, 2014, **23**, 427–434.
- 26 Y. Nakagawa and K. Tomishige, *Catal. Today*, 2012, **195**, 136–143.
- 27 S. Liu, Y. Amada, M. Tamura, Y. Nakagawa and K. Tomishige, *Catal. Sci. Technol.*, 2014, **4**, 2535–2549.
- 28 P. Panagiotopoulou, N. Martin and D. G. Vlachos, *J. Mol. Catal. A Chem.*, 2014, **392**, 223–228.
- 29 T. Kratochwil, M. Wittmann and J. Küppers, *J. Electron Spectros. Relat. Phenomena*, 1993, **65**, 609–617.
- 30 K. Chen, S. Koso, T. Kubota, Y. Nakagawa and K. Tomishige, *ChemCatChem*, 2010, **2**, 547–555.
- 31 T. Buntara, S. Noel, P. H. Phua, I. Melian-Cabrera, J. G. De Vries and H. J. Heeres, *Angew. Chemie - Int. Ed.*, 2011, **50**, 7083–7087.
- 32 S. P. Burt, K. J. Barnett, D. J. McClelland, P. Wolf, J. A. Dumesic, G. W. Huber and I. Hermans, *Green Chem.*, 2017, **19**, 1390–1398.
- 33 G. A. M. Hussein and B. C. Gates, *J. Catal.*, 1998, **176**, 395–404.
- 34 A. P. Kilimov, M. A. Svechnikova, V. I. Shevchenko, V. V. Smirnov, S. B.

- Zotov and F. V. Kvasnyuk-Mudryi, *Chem. Heterocycl. Compd.*, 1967, **3**, 467–471.
- 35 A. P. Kilimov, M. A. Svchnikova, V. I. Shevchenko, V. V. Smirov, S. B. Zotov and F. V. Kvasnyuk-Mudryi, *Chem. Heterocycl. Compd.*, 1969, **5**, 156–159.
- 36 N. Li and K. Yanagisawa, *J. Solid State Chem.*, 2008, **181**, 1738–1743.
- 37 Y. Uwamino, T. Ishizuka and H. Yamatera, *J. Electron Spectros. Relat. Phenomena*, 1984, **34**, 67–78.
- 38 R. C. Plaza, J. D. G. Durán, A. Quirantes, M. J. Ariza and A. V. Delgado, *J. Colloid Interface Sci.*, 1997, **194**, 398–407.

Chapter 4

Improvement of Ni-Y₂O₃ catalyst by the addition of ruthenium to accelerate the C-O bond cleavage

ABSTRACT. A Ni-Y₂O₃ catalyst containing ruthenium (Ru/Ni-Y₂O₃) was synthesized and applied to the hydrogenolysis of tetrahydrofurfuryl alcohol (THFA) to produce 1,5-pentanediol (1,5-PeD), which showed superior catalytic performance over that of the Ni-Y₂O₃ catalyst itself. The optimized ruthenium-containing catalyst, which was prepared by impregnation of 1.0 wt. % ruthenium in Ni-Y₂O₃, showed high catalytic activity for producing 1,5-PeD, giving an 86.5% yield at 93.4% conversion of THFA under 2.0 MPa of H₂ at 423 K after 40 hours. The formation of Ru-Ni⁰-Y₂O₃ boundaries was proposed to accelerate the C-O bond scission of the tetrahydrofuran ring to give 1,5-PeD.

4.1 Introduction

Recently, a multi-step catalytic conversion from a furfural feedstock to 1,5-PeD involving hydrogenation and dehydration–hydration–hydrogenation processes was modelled from a techno-economic analysis point of view.¹ The authors suggested that the transformation of THFA through 2-hydroxytetrahydropyran formation previously obtained from dehydration (γ -Al₂O₃ catalyst) and hydration processes is a preferable route, giving 1,5-PeD up to 80% for overall yield from furfural.^{1,2} Schniepp and Geller pioneered that reaction using activated alumina and then copper chromite.³ Modified noble metal catalysts, especially Rh–ReOx/C, have demonstrated the best results, with 1,5-PeD yields up to 94.2% from THFA.^{4–6} The Brønsted acidic metal oxide modifiers ReOx and MoOx are essential to binding the oxygen atoms (ether and hydroxyl groups) of THFA and breaking a C–O bond to give the pentanediol products.^{7,8} To modify the Ni catalyst while preserving hydrogen molecule dissociation, our group has successfully added yttrium or lanthanum to facilitate the scission of the C–O bond, giving 1,5-PeD from FFR, FFA, and THFA.^{9,10} Encouraged by this result, the improvement of the Ni–Y₂O₃ catalyst is an important approach to accelerating the selective C–O bond cleavage of the tetrahydrofuran ring to give 1,5-PeD. To achieve that goal, the exploration for the addition of relatively economical noble metal such as ruthenium into the Ni–Y₂O₃ catalyst has been evaluated in this study. Although the hydrogenolysis of THFA to 1,5-PeD is mostly catalyzed employing noble metal-based catalysts, our nickel-based catalyst showed the comparable catalytic performance according to the results described in this chapter. Since the hydrogenolysis of THFA to 1,5-PeD is mostly catalyzed employing noble metal-based catalysts. The boundary of Ni⁰–Y₂O₃ is

known to be responsible for C-O bond scission¹⁰, and the Ru-Ni bimetallic catalyst is known to be highly active for hydrogenation¹¹⁻¹⁴; however, their combination could enhance the C-O bond cleavage of the THFA ring, giving 1,5-PeD rather than 1,2-pentanediol. We expect that modification of Ni-Y₂O₃, Ni-Y₂O₃(2.5)-623 catalyst particularly, with ruthenium could accelerate hydride formation on the catalyst surface to then attack the C-O bond of the tetrahydrofuran ring, i.e., the Ru-Ni⁰-Y₂O₃ boundaries could facilitate C-O bond cleavage.

4.2 Experimental procedure

4.2.1 Preparation of ruthenium modified Ni-Y₂O₃ catalyst

The unreduced Ni-Y₂O₃(2.5)623 sample, Ni/Y mol ratio equal 2.5, was prepared according to our previous report (Chapter 3 also).⁹ Typically, a 21 mL of 0.49 M Y(NO₃)₃ was added to 30 mL of 0.86 M Ni(NO₃)₂. A 3.1 M NaOH solution was added dropwise to a pH 13.2 for the solution mixture. After stirring for 1 h, the slurry solution was transferred into a Teflon vessel of a hydrothermal bomb and aged at 423 K for 24 h. Then, the precipitate was filtered and washed with hot distilled water until pH of the filtrated mother liquor was neutral. The light green powder was obtained after drying under vacuum overnight. The powder was calcined at 623 K with a heating rate of 5 K·min⁻¹ and annealed for 5 h in air.

The ruthenium was added to the calcined Ni-Y₂O₃ sample by impregnation method. A calcined Ni-Y₂O₃ powder was dispersed in ethanol and then added a small amount of RuCl₃·xH₂O (x ≈ 2) to obtain feeding amount 0.6, 0.8, 1.0, 3.0, and 5.0 at wt. %. The solution mixture was stirred at room temperature overnight then heated at 363 K for 8 h. All samples were treated with hydrogen treatment at 673 K for 3 h before using for catalytic hydrogenolysis. The catalyst was denoted *n* Ru/Ni-Y₂O₃,

where $n = \text{wt. \%}$ (weight %) of Ru feeding amount. The catalysts were characterized by FTIR and XRD so far. Bulk Ni-Ru(2.5) catalyst was prepared with the similar procedure of Ni-Y₂O₃(2.5)623 catalyst by using RuCl₃. x H₂O ($x \approx 2$) instead of yttrium precursor. Similarly, the 1.0M/Ni-Y₂O₃ catalyst (M = Ca, Fe, Co, Cu, and Sn) was prepared with corresponding metal salt (Ca(NO₃)₂.4H₂O, Fe(NO₃)₃.9H₂O, Co(NO₃)₂.4H₂O, CuCl₂.2H₂O, and SnCl₂) instead of RuCl₃.

A physical mixing between the unreduced Ni-Y₂O₃ and 1.0Ru/Y₂O₃ samples was prepared at 1:1 ratio using the agate mortar. Then, the mixture was treated with hydrogen gas at 673 K in the H₂ treatment apparatus before used as catalyst (Ni-Y₂O₃+1.0Ru/Y₂O₃) for hydrogenolysis of THFA.

4.2.2 Catalytic hydrogenolysis of THFA

Catalytic reaction was carried out in the stainless-steel autoclave (30 mL) equipped with a magnetic stirrer, pressure gauge, inserted glass vessel, and automatic temperature control apparatus. The reactor was connected to a hydrogen cylinder of the reaction pressure. In a typical reaction, the catalyst (0.05 g) was placed in a glass vessel together with a magnetic stirrer, 2-PrOH (3 mL), *trans*-decahydronaphthalene (0.07 g) and THFA (1.0 mmol). The glass vessel was inserted into the autoclave with 2.0 MPa H₂ gas and heated at 423 K for 24 h. After the reaction, the autoclave was cooled, the gas released slowly, the mixture was centrifuged, and then the liquid solution product was analyzed using GC equipped with a flame ionization detector (FID) and a capillary column (BAC Plus 1, 30 m \times 0.32 mm).

4.2.3 Characterization of ruthenium modified Ni-Y₂O₃ catalyst

All Ru modified Ni-Y₂O₃ catalysts were characterized by Powder X-ray diffraction (XRD) Miniflex 600 Rigaku with Cu as monochromatic source K α radiation ($\lambda =$

1.5444 nm). XRD operated at 40 kV and 15 mA with solar slit 1.25 deg., scan step 5 deg./min. and using a Ni $K\beta$ filter. The particle size of yttrium oxide and Ni(0) was estimated by using the Scherrer equation after analyzing some parameters of XRD data such as slit correction, Lorentz polarization correction, background subtraction, and $K\alpha_2$ elimination by using the Integral Intensity Calculation program. Isotherm N_2 adsorption-desorption measurements were taken using a Belsorp Max (BEL Japan). The samples were outgassed by evacuation at 200 °C for 2 h prior to analysis. Data were collected at liquid nitrogen boiling temperature (77 K). The surface area was calculated by the BET (Brunauer-Emmett-Teller) method with data collected at relative pressures between 0.06 and 0.2. Total pore volume and average pore diameter pore size were calculated with the BJH (Barrett Joyner-Halenda) method and DA method using the adsorption isotherm. Thermal gravimetric analyses (TGA) were performed on a Rigaku Thermal Analysis system (Thermo plus Evo TG 8120 apparatus) under N_2 gas flow (250 mL/min) using Pt pans in the range room temperature to 500 °C (5 °C/min). The hydrogen adsorption of the catalysts was evaluated by using hydrogen treatment apparatus line with 300 Torr H_2 gas and placed the tube containing sample in the ice bath (273 K). The NH_3 -TPD was performed on BELCAT-M machine under He gas flow, mixture of 5.23 vol.% NH_3 /He gas and a thermal conductivity detector for gas analysis.

4.3 Result and discussion

4.3.1 Screening of the third metal addition on the Ni- Y_2O_3 catalyst

The Ni- $Y_2O_3(2.5)623$ catalyst has been employed in hydrogenolysis of THFA giving the highest yield of 1,5-PeD up to 54.7% among the other investigated catalysts. The improvement of Ni- Y_2O_3 catalyst (a new notation for Ni- $Y_2O_3(2.5)623$

catalyst for simplification purpose) for accelerating C-O bond cleavage of tetrahydrofuran ring is critical to gain the high yield of 1,5-PeD. The screening of the addition of small amount third metal such as Ca, Fe, Co, Cu, Ru, and Sn to Ni-Y₂O₃ was prepared with the same procedure and loading amount correspond to their salt precursors. Their catalytic performance in hydrogenolysis was carried at the optimized reaction condition for the Ni-Y₂O₃ catalyst as shown in Table 4.1. All the third metal addition not only maintain the 1,5-PeD selectivity but also suppressed the 1-BuOH formation. Among the other screened third metal addition, the addition of Ru enhanced both conversion of THFA and yield of 1,5-PeD up to 80.8% and 74.9%, respectively. The hydrogenolysis of THFA over ruthenium added Ni-Y₂O₃ catalyst will be studied in this chapter to figure out the role of Ru addition, the optimized reaction condition, and reaction mechanism.

Table 4.1 Screening the third metal addition on the Ni-Y₂O₃ catalyst for hydrogenolysis of THFA.

Entry	Catalyst	Conv. (%)	Yield (%)		
			1,5-PeD	1,2-PeD	1-BuOH
1	Ni-Y ₂ O ₃	59.8	54.7	0.0	2.3
2	1.0Ca/Ni-Y ₂ O ₃	18.7	18.7	0.0	0.0
3	1.0Fe/Ni-Y ₂ O ₃	11.3	11.3	0.0	0.0
4	1.0Co/Ni-Y ₂ O ₃	29.6	25.3	0.0	1.4
5	1.3Cu/Ni-Y ₂ O ₃	26.7	24.9	0.0	0.9
6	1.0Ru/Ni-Y ₂ O ₃	80.8	74.9	0.0	1.7
7	1.0Sn/Ni-Y ₂ O ₃	27.6	26.2	0.0	1.0

^a *Reaction conditions*: Reduced catalyst (0.05 g), THFA (1.0 mmol), *trans*-decahydronaphthalene (0.07 g), 2-propanol (3 mL), 423 K, initial H₂ pressure (2.0 MPa), for 24 h. Conversion and yield were determined by GC using the internal standard technique.

4.3.2 Ruthenium modified Ni-Y₂O₃ catalyst properties

The FTIR spectra of the catalysts exhibited similar absorption bands, as shown in Figure 4.1. The presence of hydroxyl groups on the surface of the Ni-Y₂O₃ and Ru-containing catalysts was assigned as OH stretching (broad peak 3400 cm⁻¹), OH bending (1630, 1508, and 1384 cm⁻¹), Y-OH bending (800 cm⁻¹), and Y-O vibration (600-300 cm⁻¹) bands. The FTIR spectra of catalysts showed a quietly similar adsorption band as shown in Figure 4.1.¹⁵ Moreover, the Y-O vibration mode shifted to lower wavenumbers (464 to 458 cm⁻¹) in all the Ru-containing catalysts. Thermogravimetric analysis of the 1.0Ru/Ni-Y₂O₃ catalyst under an N₂ flow showed a mass loss below 473 K of only approximately 3.3%, which could be assigned to a dehydration process. This result indicates that Ru was highly dispersed and had weak interactions with Y₂O₃.

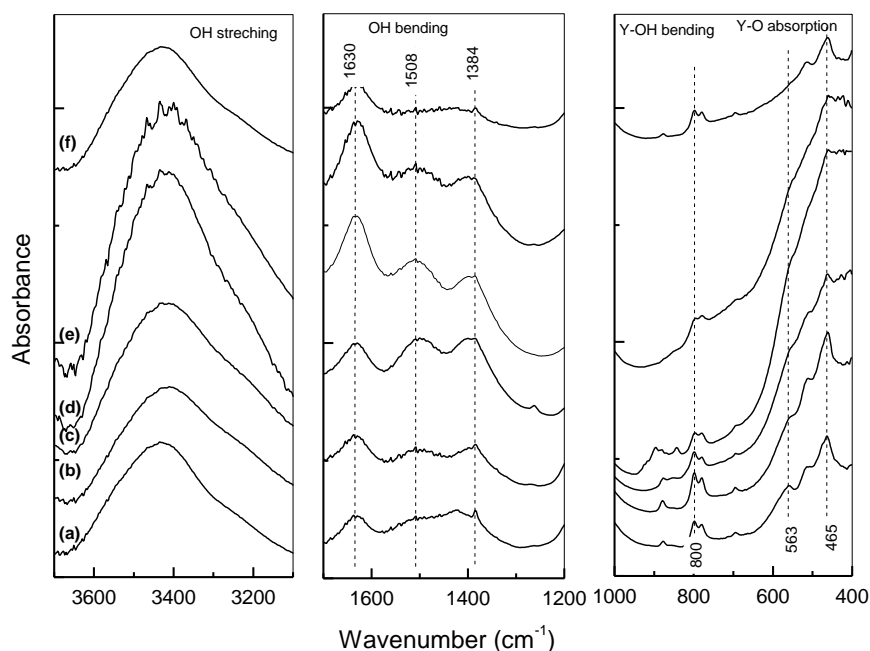


Figure 4.1. FTIR spectra of (a) Ni-Y₂O₃, (b) 0.6Ru/Ni-Y₂O₃, (c) 0.8Ru/Ni-Y₂O₃, (d) 1.0Ru/Ni-Y₂O₃, (e) 3.0Ru/Ni-Y₂O₃, (f) 5.0Ru/Ni-Y₂O₃.

The addition of Ru into the Ni-Y₂O₃ catalyst was successfully accomplished by an impregnation method and subsequent H₂ treatment at 673 K. The XRD patterns of the Ru-containing catalysts with various amounts of Ru are shown in Figure 4.2 (A). Diffraction peaks from Ni metal ($2\theta = 44.4, 51.7, \text{ and } 76.3$) were observed in all the Ru-containing samples. Meanwhile, the diffraction peaks of Ru species were not detected owing to the low content ($\leq 5 \text{ wt. } \%$) and high dispersion of Ru. The hydrogen treatment at 673 K was necessary to form zero valent Ni and Ru.^{16,17} The peaks from Ni metal were sharp in the samples containing 3.0-5.0 wt. % of ruthenium, indicating the agglomeration of Ru-Ni bimetallic species.¹⁸ The strongest diffraction peaks at approximately 44° for both Ni (111) and Ru (101) are very close and are superimposed in the bimetallic systems because the metals crystallize with a similar structure, and they have fairly similar ionic radii (Ni: 1.25 Å and Ru: 1.34 Å).¹⁹ The intensity of the easily observed Y₂O₃ diffraction peak at $2\theta = 29.2$ decreased with increasing Ru content. This change may correspond to the dispersion of ruthenium on the Y₂O₃, and the FTIR spectra corroborated this hypothesis, as a shift in the Y-O absorption band to lower wavenumbers ($464 \text{ to } 458 \text{ cm}^{-1}$) was observed for all the Ru-containing catalysts (Figure 4.1). In addition, the mesoporous hysteresis loop of the Ni-Y₂O₃ catalyst gradually dissipated, as shown in Figure 4.4(A), and the Ru-containing catalysts had a lower BET surface area than that of the Ni-Y₂O₃ catalyst, as listed in Table 4.2.

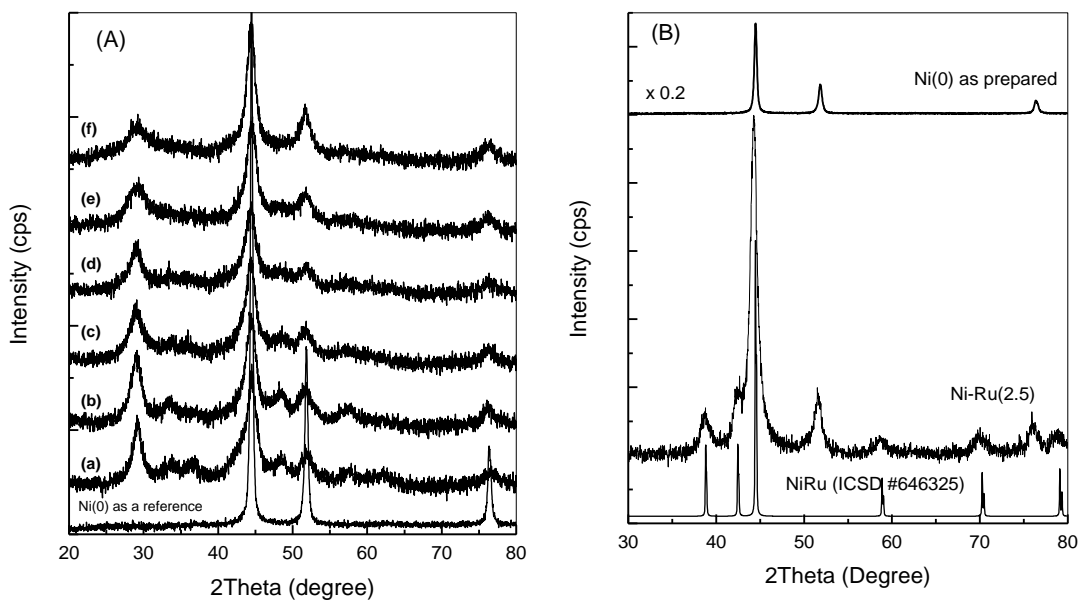


Figure 4.2. (A) The XRD pattern of (a) Ni-Y₂O₃, (b) 0.6Ru/Ni-Y₂O₃, (c) 0.8Ru/Ni-Y₂O₃, (d) 1.0Ru/Ni-Y₂O₃, (e) 3.0Ru/Ni-Y₂O₃, (f) 5.0Ru/Ni-Y₂O₃. (B) Ni-Ru(2.5) catalyst.

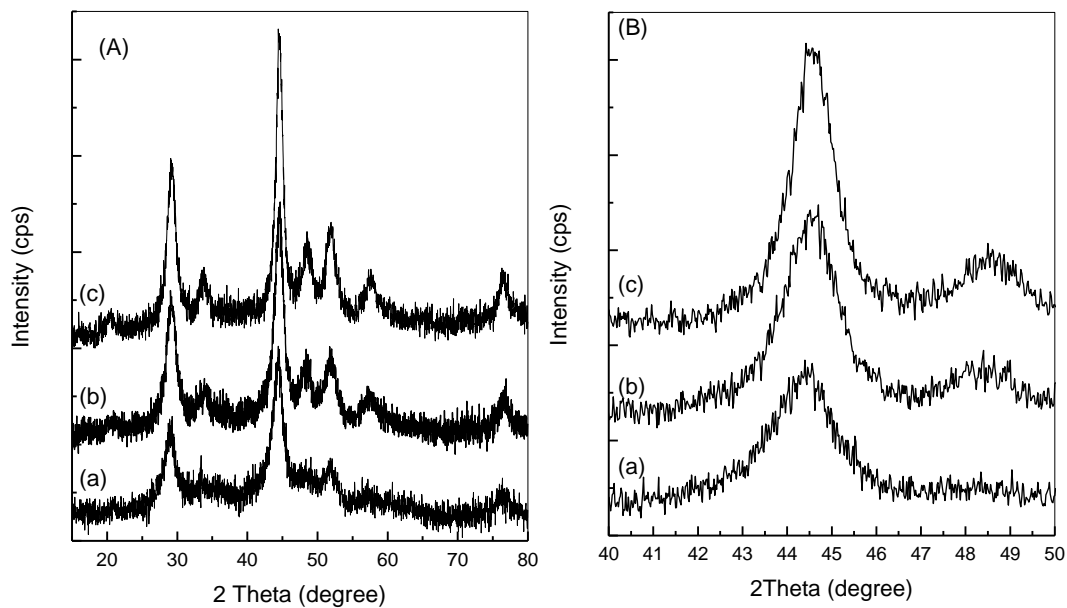


Figure 4.3 (A) XRD pattern of 1.0Ru/Ni-Y₂O₃ at different H₂ treatment temperature (a) 673 K, (b) 723 K, and (c) 773 K. (B) Enlarged view of XRD patterns within 2θ 40° to 50°.

Increasing the H₂ treatment temperature (in the range 673 to 773 K) of 1.0Ru/Ni-Y₂O₃ catalyst had been investigated as depicted in Figure 4.3(A). The crystallinity of

Ni(0) and Y₂O₃ gradually increased by increasing H₂ treatment temperature at higher than 673 K. The enlarged view (Figure 4.3(B)) revealed a shifted peak of Ni(111) to the higher 2θ regarding Ni-Ru bimetallic or NiRu alloy formation at the higher temperature. The catalytic reaction for those catalysts was then evaluated for the hydrogenolysis of THFA to 1,5-PeD.

The physicochemical properties of Ru/Ni-Y₂O₃ catalysts are listed in Table 4.2. The BET surface area of Ni-Y₂O₃ lowered because of the Ru addition and insignificantly changed for Ru/Ni-Y₂O₃ catalyst by altering Ru feeding amount. The high dispersion of Ru over Ni-Y₂O₃ catalyst could correspond to it. The H₂ uptake which only absorbed on Ni(0) not only corroborated those properties but also informed a better dispersion of Ni(0) by the addition of Ru. The 1.0Ru/Ni-Y₂O₃ catalyst showed the highest H₂ uptake among Ru/Ni-Y₂O₃ catalysts while at 5.0 wt. % Ru had the lowest one owing to the rich of Ru. Garcia et al., proven that H₂ chemisorption on NiRu_x corresponds to Ni(0) not ruthenium metal.¹⁸ In addition, increasing H₂ treatment temperature more than 673 K lowered the amount of H₂ uptake and BET surface area of those catalyst (1.0Ru/Ni-Y₂O₃-723 and 1.0Ru/Ni-Y₂O₃-773 catalysts) probably due to the formation bimetallic Ni-Ru or NiRu alloy intensely, sintering regarding to their XRD patterns (Figure 4.3) and dissipating mesoporous hysteresis loop on their N₂ adsorption-desorption properties (Figure 4.4(B)). The amount of acidic site is calculated from NH₃-TPD measurement which shows three different strength at around 450 K, 621 K, and 862 K. A total acidity of catalysts shows the addition of ruthenium did not increase the acidity as listed in Table 4.2. The 1.0Ru/Ni-Y₂O₃ holds the highest H₂ uptake and total acidic amount compare to other ruthenium feeding amount. Increasing H₂ treatment temperature

significantly lowered the total acidic amount of 1.0Ru/Ni-Y₂O₃ catalyst. It means the presence of ruthenium on the Ni-Y₂O₃ catalyst which indicated to forming Ni-Ru bimetallic species significantly enhance the amount of hydrogen uptake while keeping the acidic site of the catalyst.

Table 4.2 Physicochemical properties of the Ru/Ni-Y₂O₃ catalyst.

Catalyst	H ₂ uptake ^[a] ($\mu\text{mol}/\text{g cat.}$)	S_{BET} (m^2/g)	Langmuir (m^2/g)	Acidity ^[b] (mmol/g)
Ni-Y ₂ O ₃	154.6	74.1	61.8	1.103
0.6Ru/Ni-Y ₂ O ₃	158.4	68.7	59.7	0.347
0.8Ru/Ni-Y ₂ O ₃	173.9	66.7	61.9	0.335
1.0Ru/Ni-Y ₂ O ₃	235.2	59.4	51.9	0.862
3.0Ru/Ni-Y ₂ O ₃	134.3	45.5	38.6	0.203
5.0Ru/Ni-Y ₂ O ₃	109.2	66.5	56.7	0.386
1.0Ru/Ni-Y ₂ O ₃ -723	231.9	53.7	48.4	0.316
1.0Ru/Ni-Y ₂ O ₃ -773	252.7	48.4	45.3	0.258

[a] measured at 273 K and after corrected with H₂ physisorption. [b] Calculated from NH₃-TPD measurement as a total amount of NH₃ desorption at elevated temperature from 373-1073 K.

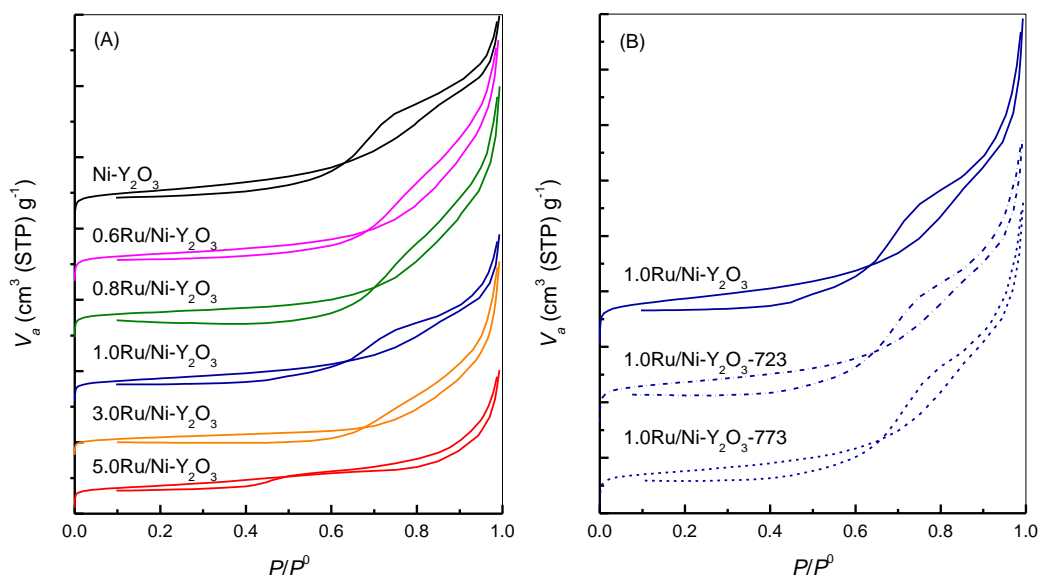


Figure 4.4 (A) The N₂ adsorption-desorption properties of (A) $n\text{Ru}/\text{Ni-Y}_2\text{O}_3$ ($n = \text{wt. \% Ru}$) after H₂ treatment at 673 K. (B) 1.0Ru/Ni-Y₂O₃ at different H₂ treatment temperature.

4.3.3 Catalytic hydrogenolysis of THFA

The initial screening of the catalysts was conducted in the hydrogenolysis of THFA to give 1,5-PeD under pressurized hydrogen, i.e., 2.0 MPa and 423 K, as shown in Table 4.3. We performed our investigation with reduced Ru/Y₂O₃ and unreduced Ru/Ni-Y₂O₃ catalysts, but neither case produced 1,5-PeD (entries 1-2). The product 2-methyltetrahydrofuran (1.3% yield) was detected, particularly in entry 2. The dispersion of Ni (16 wt. %) and Ru (1 wt. %) on as-prepared Y₂O₃ (imp(16Ni1.0Ru)-Y₂O₃ catalyst), which was synthesized by co-impregnation and then hydrogen treatment at 673 K, did not produce 1,5-PeD under the same reaction conditions (entry 3). The Ni-Ru(2.5) catalyst composed of Ni⁰ and NiRu alloy (ICSD #646325), as shown in Figure 4.2(B), was not active for C-O cleavage of the tetrahydrofuran ring (entry 11). The physical mixing catalyst (Ni-Y₂O₃(2.5)+1.0Ru/Y₂O₃) which treated with H₂ gas at 673K only resulted in 10.5% yield of 1,5-PeD (entry 14). The reduced Ni-Y₂O₃ catalyst having Ni⁰-Y₂O₃ boundaries and the highest amount acidic site was active in the cleavage of the C-O bond of THFA to give 1,5-PeD in up to 54.7% yield (entry 4). The above experimental results indicate that the ruthenium species, Ru-Ni bimetallic and NiRu alloy did not facilitate the C-O bond cleavage of the tetrahydrofuran ring under this reaction condition.

It is generally known that Ru and Ni metals are active in hydrogenation through activation and dissociation of hydrogen molecules. Obviously, the Ru-Ni bimetallic is more active than its monometallic counterparts for the hydrogenation of C=C bonds, such as the hydrogenation of benzene to cyclohexane under 5.3 MPa of H₂ at 60 °C.¹¹⁻¹³ To our delight, the addition of a small amount of ruthenium (1.0 wt. %)

into Ni-Y₂O₃ significantly enhanced the catalytic activity for this reaction after 24 h, giving a 74.9% yield of 1,5-PeD (Table 4.3, entry 5). Prolonging the reaction time to 40 h slightly increased the conversion of THFA to 93.4%, giving an 86.5% yield of 1,5-PeD (Table 4.3, entry 6). Only 1-butanol (1-BuOH) as a by-product was detected in our catalytic reaction conditions. Thus, the addition of a small amount of ruthenium (1.0 wt. %) enhanced the ring opening of THFA to give 1,5-PeD through hydrogenolysis of the C-O bond. The highest H₂ uptake property which deals with Ru-Ni bimetallic formation and the well-maintained acidic site which correlated with Ni⁰-Y₂O₃ boundaries of 1.0Ru/Ni-Y₂O₃ catalyst is responsible for forming Ru-Ni⁰-Y₂O₃ boundaries

Table 4.3 Catalytic hydrogenolysis of THFA to 1,5-PeD.^a

Entry	Catalyst	Conv. (%)	Yield (%)	
			1,5-PeD	1-BuOH
1	1.0Ru/Y ₂ O ₃	0.0	0.0	0.0
2	1.0Ru/Ni-Y ₂ O ₃ ^b	5.4	0.0	0.0
3	Imp(16Ni1.0Ru)-Y ₂ O ₃	0.0	0.0	0.0
4	Ni-Y ₂ O ₃	59.8	54.7	2.3
5	1.0Ru/Ni-Y ₂ O ₃	80.8	74.9	1.7
6	1.0Ru/Ni-Y ₂ O ₃ ^c	93.4	86.5	2.4
7	0.8Ru/Ni-Y ₂ O ₃	71.0	69.2	1.8
8	0.6Ru/Ni-Y ₂ O ₃	68.3	58.9	0.8
9	3.0Ru/Ni-Y ₂ O ₃	34.5	27.4	1.2
10	5.0Ru/Ni-Y ₂ O ₃	39.7	23.3	0.7
11	Ni-Ru(2.5)	0.0	0.0	0.0
12	Ni-Y ₂ O ₃ +1.0Ru/Y ₂ O ₃	10.5	10.5	0.0
13	1.0Ru/Ni-Y ₂ O ₃ -723 ^d	62.7	60.0	1.0
14	1.0Ru/Ni-Y ₂ O ₃ -773 ^e	59.6	55.5	0.0

^a Reaction conditions: All catalysts were calcined at 623 K and then H₂ treatment at 673 K (0.05 g), THFA (1.0 mmol), *trans*-decahydronaphthalene (0.07 g), 2-propanol (3 mL), 423 K, initial H₂ (2.0 MPa), for 24 h. ^b without H₂ treatment. ^c 40h. ^d H₂ treatment at 723 K. ^e H₂ treatment at 773 K. Conversion and product yields were determined by GC using the internal standard technique.

The presence of the Ru-Ni bimetallic species in the 1.0Ru/Ni-Y₂O₃ catalyst enhanced the C-O bond cleavage compared to that of the Ni-Y₂O₃ catalyst. Such cooperative activity could not be achieved with the Ru-Ni bimetallic species, which suggests that the prominent role of the Ru-Ni bimetallic species was in accelerating the dissociation of hydrogen molecules.

Furthermore, the effect of the Ru content variation was investigated, as shown in Table 4.3 (entries 7-10). A ruthenium feeding amount of 0.6-0.8 wt. % (0.6Ru/Ni-Y₂O₃ and 0.8Ru/Ni-Y₂O₃ catalysts) significantly enhanced the catalytic activity, but the activity was still lower than that of the 1.0Ru/Ni-Y₂O₃ catalyst. In contrast, the yield of 1,5-PeD significantly dropped to 27.4% and 23.3% when 3.0Ru/Ni-Y₂O₃ and 5.0Ru/Ni-Y₂O₃ were utilized, respectively. Larger Ru contents (>1.0 wt. % Ru) corresponded to greater dispersion of the Ru metal on the Ni-Y₂O₃ and Y₂O₃ surface. In addition, the Ru-Ni bimetallic species was considerably enriched at higher Ru contents since the surface was mainly covered with Ni, as confirmed by the XRD patterns shown in Figure 4.2(e)-(f). The yield of 1,5-PeD catalyzed by 0.3Ru/Ni-Y₂O₃ was nearly 2-fold lower than that catalyzed by Ni-Y₂O₃; the excess Ru metal likely poisoned the Ni⁰-Y₂O₃ boundary, resulting in deactivation of the C-O bond cleavage reaction, and the Ru-Ni species was not active. This hypothesis was also corroborated by the decreasing surface area and H₂ uptake upon further Ru addition (Table 4.2). These results suggest that a Ru-Ni⁰-Y₂O₃ boundary, which was quite active in C-O bond hydrogenolysis, was effectively produced in the 1.0Ru/Ni-Y₂O₃ catalyst, as evidenced by the highest catalytic activity corresponding to a 74.9% yield of 1,5-PeD.

Ru-Ni bimetallic catalysts have been reported to be more active than the corresponding monometallic catalysts in several catalytic hydrogenations, such as that of acetonitrile, benzene, naphthalene, and other aromatic compounds.^{11-14,18,20} An electron donation effect from Ru to Ni (ligand effect) was also proven, which contributed to the specific catalytic enhancement. A higher Ru content would enhance the Ru-Ni bimetallic dispersion and the catalytic activity. The hydrogen uptake (hydrogen chemisorption) of the 1.0Ru/Ni-Y₂O₃ catalyst at 298 K showed the highest value among the investigated catalysts, as shown in Table 4.2. The hydrogen uptake of Ru metal was confirmed to be negligible in accordance with the results of previous studies.^{18,21} The study of Chen et al. on the structure-activity of Ru-Ni bimetallic species revealed that Ru-Ni alloy and segregated Ru-Ni bimetallic species were more active than Ru clusters on Ni.¹² It is very likely that the amount of H₂ uptake, especially H₂ chemisorption, was related to the Ni⁰ dispersion, and this dispersion also effectively enhanced the Ru-Ni⁰-Y₂O₃ boundaries, which are crucial to C-O bond scission.

The above explanation indirectly suggests that Ru-Ni bimetallic is not responsible for C-O bond cleavage of tetrahydrofuran ring. By assuming the H₂ treatment at a higher temperature (723 K and 773 K) enriches the Ru-Ni bimetallic or RuNi alloy formation which is revealed by a shifted peak of Ni(111) to the higher 2θ the higher H₂ treatment temperature (Figure 4.3). Increasing the crystallinity of both Ni⁰ and Y₂O₃ caused decreasing the surface area and H₂ uptake (Table 4.2) of 1.0Ru/Ni-Y₂O₃ catalyst, in consequence, the yield of 1,5-PeD was lower than that 74.9% (Table 4.3, entries 13-14). Although, the elevated temperature of H₂ treatment (> 673 K) was beneficial for obtaining Ru-Ni bimetallic. Seemingly, it was detrimental for Ru-Ni⁰-

Y₂O₃ boundaries formation which is crucial for accelerating the H species formation as well as C-O bond cleavage of tetrahydrofuran ring.

Ru-Ni bimetallic catalysts have been reported to be more active than the corresponding monometallic catalysts in several catalytic hydrogenations, such as that of acetonitrile, benzene, naphthalene, and other aromatic compounds.^{11-13,18,20,22} An electron donation effect from Ru to Ni (ligand effect) was also proven, which contributed to the specific catalytic enhancement. A higher Ru content would enhance the Ru-Ni bimetallic dispersion and the catalytic activity. The hydrogen uptake (hydrogen chemisorption) of the 1.0Ru/Ni-Y₂O₃ catalyst at 298 K showed the highest value among the investigated catalysts, as shown in Table 4.2. The hydrogen uptake of Ru metal was confirmed to be negligible in accordance with the results of previous studies.^{18,21} The study of Chen et al. on the structure-activity of Ru-Ni bimetallic species revealed that Ru-Ni alloy and segregated Ru-Ni bimetallic species were more active than Ru clusters on Ni.¹² It is very likely that the amount of H₂ uptake, especially H₂ chemisorption, was related to the Ni⁰ dispersion, and this dispersion also effectively enhanced the Ru-Ni⁰-Y₂O₃ boundary, which is crucial to C-O bond scission.

The effect of the initial H₂ pressure and reaction temperature on the course of THFA hydrogenolysis over the 1.0Ru/Ni-Y₂O₃ catalyst was investigated, as shown in Table 4.4. The investigated initial H₂ pressures between 1.5 – 3.0 MPa at 423 K resulted in comparable yields of 1,5-PeD. The bimetallic Ru-Ni species did not improve heterolytic hydrogen molecule dissociation. However, the production of 1-BuOH increased considerably to a 4.4% yield for reaction at high temperature (443 K). The catalytic reaction was effectively carried out under an initial H₂ pressure of

2.0 MPa at 423 K in our catalytic reaction system. Nevertheless, the C-O bond hydrogenolysis could still proceed at 1.5 MPa H₂ and a mild reaction temperature (403 K), giving a modest yield of 1,5-PeD.

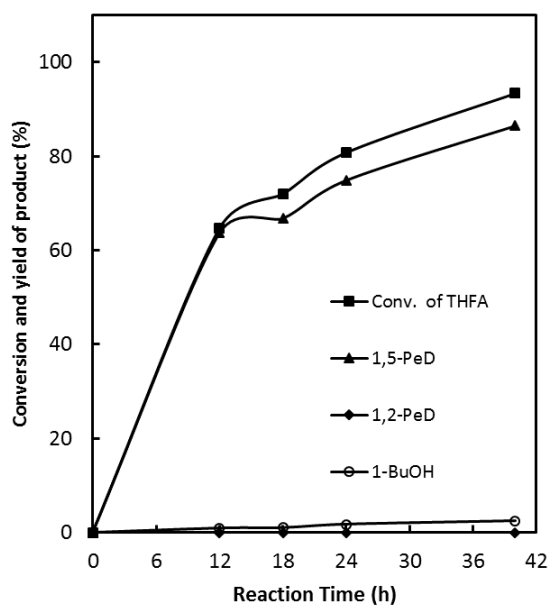
Table 4.4 Hydrogenolysis of THFA to 1,5-PeD over 1.0Ru/Ni-Y₂O₃ catalyst at various reaction condition.

Entry	P _{H₂} (MPa)	T (K)	Conv. (%)	Yield (%)	
				1,5-PeD	1-BuOH
1	1.5	423	65.9	64.1	1.5
2	2.0	423	80.8	74.9	1.7
3	3.0	423	72.0	71.7	Trace
4	2.0	403	43.4	39.5	0.0
5	2.0	433	73.9	68.2	2.6
6	2.0	443	75.3	71.2	4.1

Reaction conditions: 1.0Ru/Ni-Y₂O₃-623 catalyst (0.05 g), THFA (1.0 mmol), *trans*-decahydronaphthalene (0.07 g), 2-propanol (3 mL), 423 K, initial H₂ (2.0 MPa), for 24 h. Conversion and product yields were determined by GC using the internal standard technique.

4.3.4 Time course

A ruthenium content of 1.0 wt. % in Ni-Y₂O₃ to form the 1.0Ru/Ni-Y₂O₃ catalyst resulted in a better catalytic performance than that of the other investigated catalysts and Ni-Y₂O₃ itself. Figure 4.5 shows the time course for the hydrogenolysis of THFA to 1,5-PeD using the 1.0Ru/Ni-Y₂O₃ catalyst. During the first 12 h, 1,5-PeD was produced in up to 63.7% yield, which was two times higher than that obtained with the Ni-Y₂O₃ catalyst (Table 4.3, entry 4). Unfortunately, the hydrogenolysis was moderately sluggish from 12 to 40 h. The selectivity of 1,5-PeD over 1-BuOH formation obviously decreased upon prolonging the reaction time. After 24 h at the same reaction conditions, 1-BuOH was obtained (2.5% yield) when 1,5-PeD was used as the substrate. This reveals that adding Ru to Ni-Y₂O₃ accelerated C-O bond scission and prevented the formation of 1-BuOH.



Reaction conditions: 1.0Ru/Ni-Y₂O₃ catalyst, (0.05 g), THFA (1.0 mmol), *trans*-decahydronaphthalene (0.07 g), 2-propanol (3 mL), 423 K, and initial H₂ (2.0 MPa). Conversion and product yields were determined by GC using the internal standard technique.

Figure 4.5 Time course for 1,5-PeD formation from THFA using 1.0Ru/Ni-Y₂O₃ catalyst.

4.3.5 Reusability test

The reusability of the catalysts was tested by using the used catalyst which was recovered by centrifugation, washing with a solvent, and then drying in vacuum. The catalytic activity of the used catalyst for the second run drastically decreased giving 18.1% yield of 1,5-PeD with 19.4% THFA conversion at the same reaction condition. Compared with the fresh catalyst, the XRD patterns and thermogravimetric analysis as shown in Figure 4.6 informed that agglomeration of catalyst and remained organic compound on the catalyst surface could be exploited for this result. Refer to the Chapter 3 section 3.7 that the Ni⁰-Y₂O₃ boundary is easily poisoned by diol compound and Ni-Y₂O₃ catalyst is easily agglomerated, the Ru-Ni⁰-Y₂O₃ boundaries could be noted having a similar property regarding its catalytic activity.

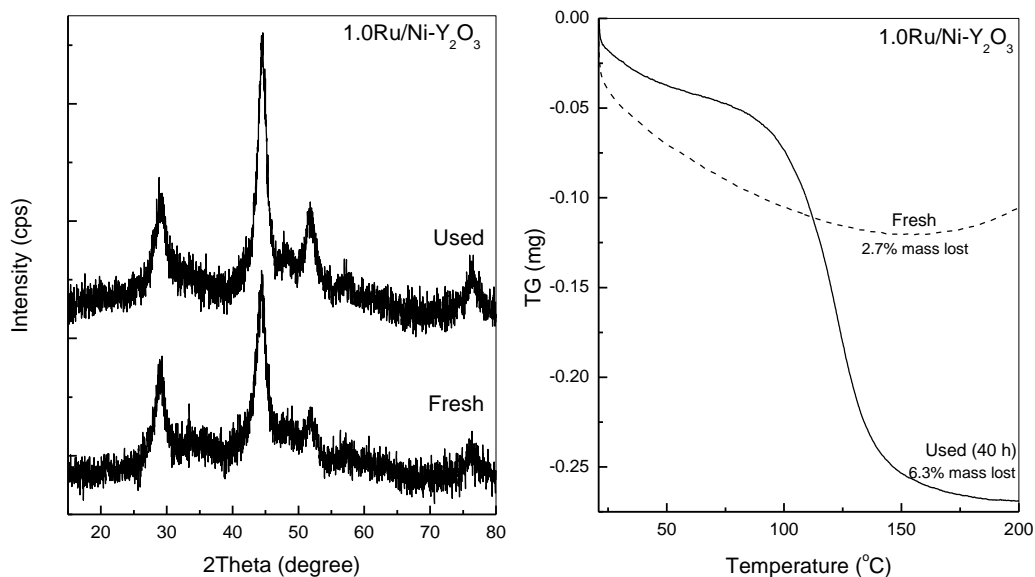


Figure 4.6. The XRD pattern (left) and thermogravimetric graph (right) of fresh and used 1.0Ru/Ni-Y₂O₃ catalyst.

4.3.6 FT-IR study of the absorbed THFA

The adsorption of THFA vapor on Ni-Y₂O₃(2.5)-623 catalyst (recently noted as a Ni-Y₂O₃ catalyst) was evaluated in Chapter 3. The same procedure was applied for the adsorption of THFA on 1.0Ru/Ni-Y₂O₃ catalyst and the results were depicted in Figure 4.7. The vibrational assignments are quietly similar with the adsorption of THFA on Ni-Y₂O₃ catalysts (Figure 3.12). The yttrium oxide of Ni-Y₂O₃(2.5)623 catalyst can be coordinated by THFA through hydroxyl group (CH₂OH) on the catalyst surface. Then the absorbed THFA can be easily attacked by hydride species from Ni metal or Ni-Ru bimetallic surface giving 1,5-PeD with high selectivity. The same mechanism or interaction of THFA forming 1,5-PeD with high selectivity can be applied as illustrated in Figure 4.8.

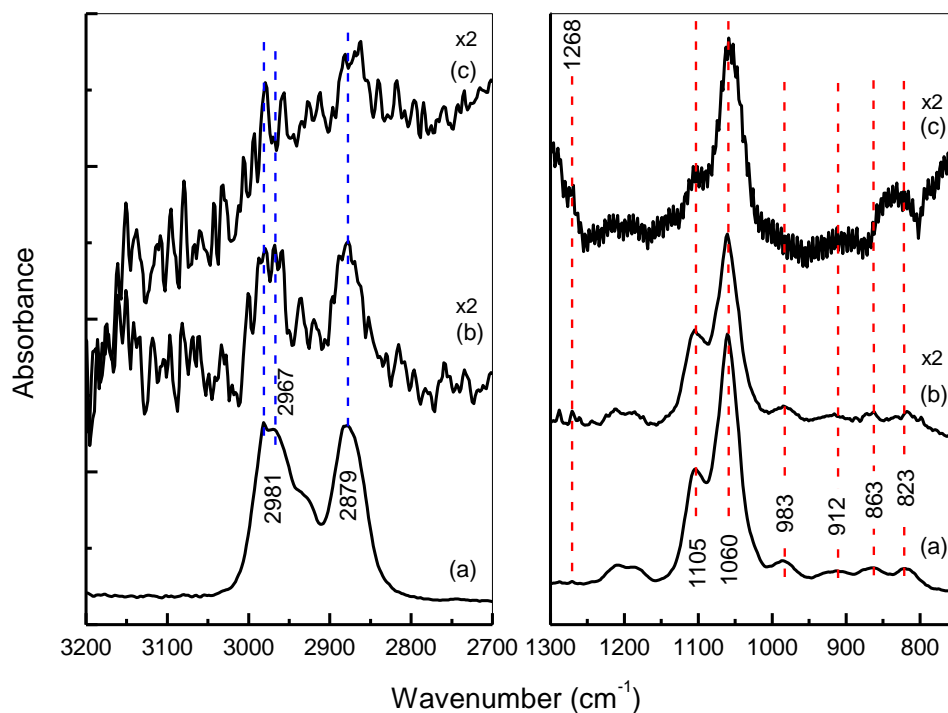


Figure 4.7 Background-substituted FT-IR spectra of (a) THFA vapor, the adsorbed THFA on 1.0Ru/Ni-Y₂O₃ (b) at room temperature and (c) after heated at 423 K.

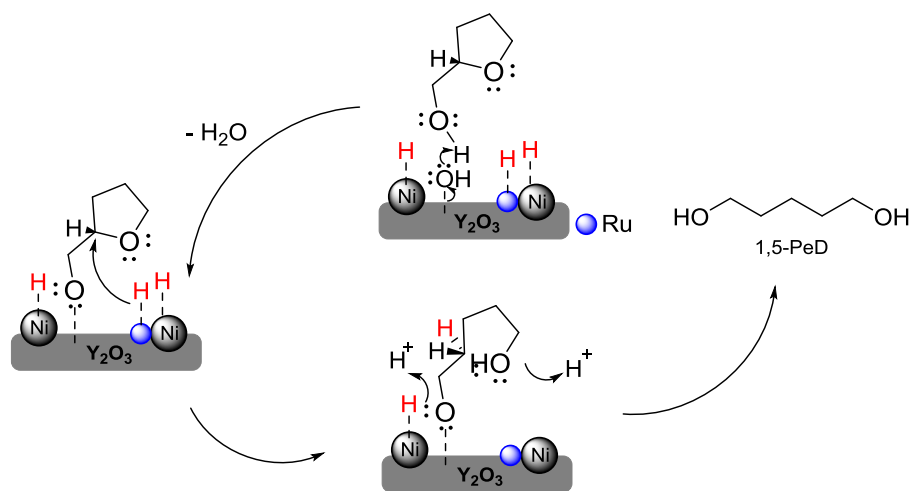
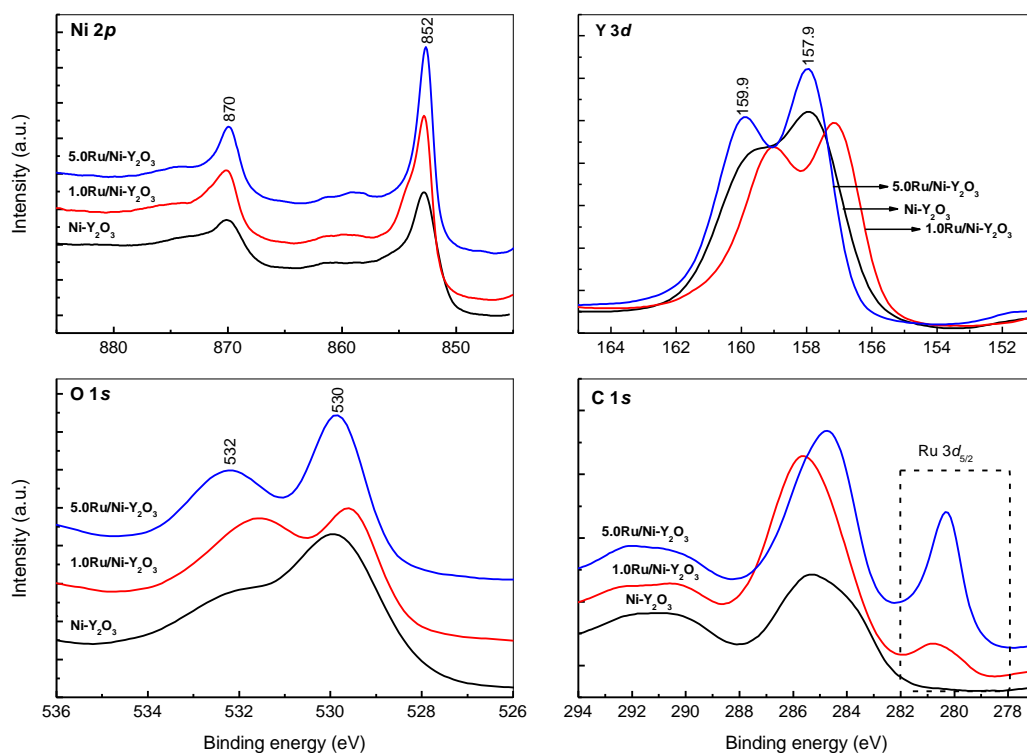


Figure 4.8 Illustrated of the proposed reaction mechanism for selective hydrogenolysis of THFA to 1,5-PeD over 1.0Ru/Ni-Y₂O₃ catalyst.

4.3.7 XPS analysis of Ru/Ni-Y₂O₃ catalysts

Ru species of 1.0Ru/Ni-Y₂O₃ and 5.0Ru/Ni-Y₂O₃ catalysts were investigated by XPS as shown in Figure 4.9. The XPS of Ni-Y₂O₃ discussed in section 3.8 (page 72)

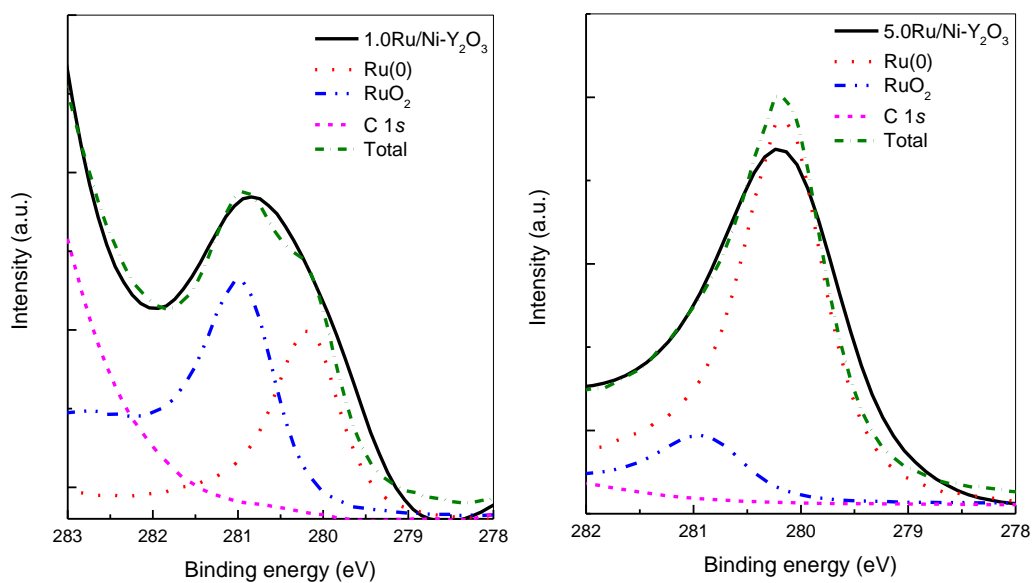
was also shown for the comparison. The surface components of Ni-Y₂O₃ catalyst did not change of Ni(0) and Y₂O₃ species by the addition of ruthenium except for Ru species and chloride. Binding energy (BE) of Y(3*d*_{3/2}) and Y(3*d*_{5/2}) at 159.6 eV and 157.9 eV was indicated the presence of yttrium oxide species.^{23,24} The O(1*s*) BE at 529.9 eV was also confirmed for yttrium oxide. The chloride (BE at 199 eV for Cl(1*s*)) and carbonate (BE at 532.0 eV for O(1*s*) and 290.0 eV for C(1*s*)) species could be assigned as impurities from ruthenium salt and air, respectively. The BE in C(1*s*) area around 280 eV was definitely the highlight of Ru species existence.²⁵ The estimated atomic content of Ru increased with the increasing Ru feeding amount.



	Ru 3<i>d</i>_{5/2}	Ni 2<i>p</i>_{3/2}	Y 3<i>d</i>_{5/2}	O 1<i>s</i>	C 1<i>s</i>	Cl 1<i>s</i>
5.0Ru/Ni-Y ₂ O ₃	1.2	14.2	33.4	24.6	22.4	2.7
1.0Ru/Ni-Y ₂ O ₃	0.3	14.2	29.7	24.9	29.6	1.3
Ni-Y ₂ O ₃	—	12.5	36.2	31.3	20.1	—

Figure 4.9 XPS spectra of Ni-Y₂O₃ (black line), 1.0Ru/Ni-Y₂O₃ (red line), and 5.0Ru/Ni-Y₂O₃ (blue line) catalysts. The bottom table listed the atomic percentage of samples.

The chemistry for Ru on the Ni-Y₂O₃ surface was delicate matters, consisting of more than one oxidation states and overlaying peaks as shown in Figure 4.10. The deconvoluted signal at that peaks revealed the BE energy as 280.9 and 280.1 eV which were assigned for RuO₂ and Ru, respectively.²⁵ From these XPS study, Ru(0) and RuO₂ were present on the surfaces of both 1.0Ru/Ni-Y₂O₃ and 5.0Ru/Ni-Y₂O₃ catalysts. The 1.0Ru/Ni-Y₂O₃ catalyst possessed a higher percentage RuO₂ than Ru(0). On the contrary, the 5.0Ru/Ni-Y₂O₃ catalyst had a higher Ru(0) than RuO₂. The high amount of Lewis acidic site and H₂ uptake of 1.0Ru/Ni-Y₂O₃ were corroborated with RuO₂ (Lewis acidic) and Ru(0) based on the observed results. Obviously, the ring opening of THFA enhanced with an excellent THFA conversion of 93.4% and 1,5-PeD yield of 86.5% over that catalyst.



	% Ru(0)	% RuO ₂
5.0Ru/Ni-Y ₂ O ₃	84.6	15.4
1.0Ru/Ni-Y ₂ O ₃	44.1	55.9

Figure 4.10 XPS spectra deconvolution of 1.0Ru/Ni-Y₂O₃ (left), and 5.0Ru/Ni-Y₂O₃ (right) catalysts at Ru binding energy region. The bottom table listed the percentage of Ru species.

4.3.8 Ring opening of cyclic ether to terminal diols

Hydrogenolysis of THFA at the optimized reaction condition (2 MPa H₂ and 423 K for 24 h) selectively produced 1,5-PeD in particular by using 1.0Ru/Ni-Y₂O₃ catalyst which formed the highest yield of 1,5-PeD in this study. Its selectivity corresponds to THFA adsorption through OH group deprotonation and weakly interaction of oxygen tetrahydrofuran ring on the catalyst surface. Transformation of tetrahydropyran-2-methanol (THP2M) was considered to have succeeded. At the optimized reaction condition, the 1.0Ru/Ni-Y₂O₃ catalyst catalyzed the formation of 1,6-hexanediol (1,6-HDO) up to 28% yield in 32% THP2M conversion. The GC-MS analysis also confirmed tetrahydropyran and 2-methyltetrahydropyran as by-products. It confirmed the high selectivity of 1.0Ru/Ni-Y₂O₃ catalyst in the C-O bond cleavage of THFA and THP2M to give corresponding terminal diols.

4.4 Conclusion

In summary, the addition of ruthenium into Ni-Y₂O₃ catalyst was successfully conducted by impregnation method and subsequent H₂ treatment at 673K. The XPS analysis reveals that Ru(0) and RuO₂ was present on the of 1.0Ru/Ni- Y₂O₃ and 5.0Ru/Ni- Y₂O₃ catalysts. The addition of ruthenium influenced the formation of Ru-Ni⁰-Y₂O₃ boundaries which is effectively formed in the 1.0Ru/Ni- Y₂O₃ catalyst. Increasing Ru feeding amount at higher than 1.0 wt. %. decelerated the 1,5-PeD formation owing to the lack of Ru-Ni⁰-Y₂O₃ boundary formation. The C-O bond cleavage of tetrahydrofuran ring of THFA over 1.0Ru/Ni- Y₂O₃ catalyst accelerated two times faster than the Ni-Y₂O₃ catalyst. The direct formation of terminal diols from the hydrogenolysis of THFA as well as THP2M Ru/Ni-Y₂O₃ catalyst validated

the selectivity of Ru-Ni⁰-Y₂O₃ boundaries on the C-O bond cleavage to give corresponding terminal diol.

ABBREVIATIONS

FFR: furfural	1-BuOH: 1-butanol
FFA: furfuryl alcohol	2-HY-THP: 2-hydroxytetrahydropyran
THFA: tetrahydrofurfuryl alcohol	2-PrOH: 2-propanol
1,5-PeD: 1,5-pentanediol	1,6-HDO: 1,6-hexanediol
1,2-PeD, 1,2-pentanediol	THP2M: tetrahydropyran-2-methanol

Notes

Some results have been published as follows: H. W. Wijaya, T. Hara, N. Ichikuni and S. Shimazu, Hydrogenolysis of Tetrahydrofurfuryl Alcohol to 1,5-Pentanediol over a Nickel-Yttrium Oxide Catalyst Containing Ruthenium, *Chem. Lett.*, 2018, **47**, 103–106.

REFERENCES

- 1 K. Huang, Z. J. Brentzel, K. J. Barnett, J. A. Dumesic, G. W. Huber and C. T. Maravelias, *ACS Sustain. Chem. Eng.*, 2017, **5**, 4699–4706.
- 2 Z. J. Brentzel, K. J. Barnett, K. Huang, C. T. Maravelias, J. A. Dumesic and G. W. Huber, *ChemSusChem*, 2017, **10**, 1351–1355.
- 3 L. E. Schniepp and H. H. Geller, *J. Am. Chem. Soc.*, 1946, **68**, 1646–1648.
- 4 S. Koso, I. Furikado, A. Shima, T. Miyazawa, K. Kunimori and K. Tomishige, *Chem. Commun.*, 2009, 2035.
- 5 Y. Nakagawa, M. Tamura and K. Tomishige, *Catal. Surv. from Asia*, 2015, **19**, 249–256.
- 6 K. Tomishige, Y. Nakagawa and M. Tamura, *Green Chem.*, 2017, **19**, 2876–2924.

- 7 M. Chia, Y. J. Pagan-Torres, D. Hibbitts, Q. Tan, H. N. Pham, A. K. Datye, M. Neurock, R. J. Davis and J. A. Dumesic, *J. Am. Chem. Soc.*, 2011, **133**, 12675–12689.
- 8 J. Guan, G. Peng, Q. Cao and X. Mu, *J. Phys. Chem. C*, 2014, **118**, 25555–25566.
- 9 H. W. Wijaya, T. Kojima, T. Hara, N. Ichikuni and S. Shimazu, *ChemCatChem*, 2017.
- 10 H. W. Wijaya, T. Sato, H. Tange, T. Hara, N. Ichikuni and S. Shimazu, *Chem. Lett.*, 2017, **46**, 744–746.
- 11 L. Zhu, L. Zheng, K. Du, H. Fu, Y. Li, G. You and B. H. Chen, *RSC Adv.*, 2013, **3**, 713.
- 12 L. Zhu, M. Cao, L. Li, H. Sun, Y. Tang, N. Zhang, J. Zheng, H. Zhou, Y. Li, L. Yang, C. J. Zhong and B. H. Chen, *ChemCatChem*, 2014, **6**, 2039–2046.
- 13 L. Zhu, J. Zheng, C. Yu, N. Zhang, Q. Shu, H. Zhou, Y. Li and B. H. Chen, *RSC Adv.*, 2016, **6**, 13110–13119.
- 14 L. Zhu, S. Shan, V. Petkov, W. Hu, A. Kroner, J. Zheng, C. Yu, N. Zhang, Y. Li, R. Luque, C.-J. Zhong, H. Ye, Z. Yang and B. H. Chen, *J. Mater. Chem. A*, 2017, **5**, 7869–7875.
- 15 G. A. M. Hussein and B. C. Gates, *J. Catal.*, 1998, **176**, 395–404.
- 16 C. Crisafulli, S. Scirè, S. Minicò and L. Solarino, *Appl. Catal.*, 2002, **225**, 1–9.
- 17 C. Crisafulli, S. Scirè, R. Maggiore, S. Minicò and S. Galvagno, *Catal. Letters*, 1999, **59**, 21–26.
- 18 P. Braos-García, C. García-Sancho, A. Infantes-Molina, E. Rodríguez-Castellón and A. Jiménez-López, *Appl. Catal. A Gen.*, 2010, **381**, 132–144.

- 19 J. M. Rynkowski, T. Paryjczak and M. Lenik, *Appl. Catal. A, Gen.*, 1995, **126**, 257–271.
- 20 J. Zhang, J. Teo, X. Chen, H. Asakura, T. Tanaka, K. Teramura and N. Yan, *ACS Catal.*, 2014, **4**, 1574–1583.
- 21 T. Miyata, M. Shiraga, D. Li, I. Atake, T. Shishido, Y. Oumi, T. Sano and K. Takehira, *Catal. Commun.*, 2007, **8**, 447–451.
- 22 L. Zhu, S. Shan, V. Petkov, W. Hu, A. Kroner, J. Zheng, C. Yu, N. Zhang, Y. Li, R. Luque, C.-J. Zhong, H. Ye, Z. Yang and B. H. Chen, *J. Mater. Chem. A*, 2017.
- 23 Y. Uwamino, T. Ishizuka and H. Yamatera, *J. Electron Spectros. Relat. Phenomena*, 1984, **34**, 67–78.
- 24 R. C. Plaza, J. D. G. Durán, A. Quirantes, M. J. Ariza and A. V. Delgado, *J. Colloid Interface Sci.*, 1997, **194**, 398–407.
- 25 Y. Kaga, Y. Abe, H. Yanagisawa, M. Kawamura and K. Sasaki, *Surf. Sci. Spectra*, 1999, **6**, 68.

Chapter 5

Summary

Transformation of biomass-derived furfural (FFR) and its hydrogenated product to 1,5-pentanediol (1,5-PeD) through hydrogenolysis C-O bond has been conducted using Ni-La or Ni-Y catalyst. The modification of Ni catalyst with Y produced the high yield of 1,5-PeD. Lately, we had a glimpse of our studies as follow:

1. The Ni-Y₂O₃ and Ni-La(OH)₃ catalysts which were synthesized by coprecipitation, hydrothermal, and the hydrogen treatment showed promise as catalysts for the hydrogenolysis of FFR to 1,5-PeD (2.0 MPa H₂, 423 K,). Both catalysts exhibited remarkably high selectivity for producing 1,5-PeD from the hydrogenolysis of FFR, particularly starting from THFA. The results emphasized the essential role of the Ni⁰-Y₂O₃ or Ni⁰-La(OH)₃ boundary in executing C-O bond cleavage selectively as a key step in 1,5-PeD formation.
2. Enhancing of Ni-Y catalyst preparation which was calcined prior to H₂ treatment and denoted as Ni-Y₂O₃(x)T (x and T indicate the Ni/Y mole ratio and calcination temperature in K) improved their catalyst properties and catalytic performance.

The catalysts were successfully prepared by coprecipitation, hydrothermal, calcination, and later H₂ treatments. The Ni-Y₂O₃(2.5)623 catalyst has the highest amount of H₂ uptake and acidic site which holds a Ni⁰-Y₂O₃ boundary effectively among the other investigated catalysts. The XPS analysis of that catalyst confirmed the presence of Ni(0) and Y₂O₃ as well. That catalyst showed the highest catalytic activity to the hydrogenolysis of FFR, FFA, and THFA by giving the highest yield of 1,5-PeD 29.8 %, 41.9 %, and 54.7 %, respectively, at the optimized reaction condition (2.0 MPa initial H₂ and 423 K) with 2-propanol as a solvent. Both FFR and FFA were hydrogenated giving THFA prior to the 1,5-PeD formation through ring opening of tetrahydrofuran ring selectively. The adsorption of THFA onto that catalyst surfaces from FTIR evaluation confirmed the deprotonation of OH group giving the preferable 1,5-PeD product. Increasing the catalyst loading amount for 0.1 g catalyst, Ni-Y₂O₃(2.5)623, at the optimized condition effectively gave 1,5-PeD up 87.8% with 91.6% THFA conversion.

3. The addition of ruthenium into Ni-Y₂O₃ catalyst was successfully conducted by impregnation method and later H₂ treatment at 673K. The addition of ruthenium influenced the formation of Ru-Ni⁰-Y₂O₃ boundaries which is effectively formed in the 1.0Ru/Ni- Y₂O₃ catalyst. Increasing Ru feeding amount at higher than 1.0%wt. decelerated the 1,5-PeD formation owing to the lack of Ru-Ni⁰-Y₂O₃ boundary formation. The C-O bond cleavage of tetrahydrofuran ring of THFA over 1.0Ru/Ni- Y₂O₃ catalyst accelerated two times faster than the Ni-Y₂O₃ catalyst. The XPS study on that catalyst confirmed the existence of Ru(0) and RuO₂ on the surface of the Ni-Y₂O₃ catalyst. FT-IR study of the absorbed THFA on 1.0Ru/Ni-Y₂O₃ catalyst conclude that the interaction of THFA was occurred

through the OH deprotonation and followed by the attacking of hydride species on Ni(0) or bimetallic NiRu surface.

4. Transformation of tetrahydropyran-2-methanol (THP2M) to 1,6-hexanediol (1,6-HDO) was also experimented using Ni-Y₂O₃(2.5)623 and 1.0Ru/Ni- Y₂O₃ catalysts at the optimized reaction condition (2 MPa, 423 K). Both catalysts yielded the high selectivity of 1,6-HDO with a small amount of tetrahydropyran and 2-methyltetrahydropyran. It assumes that the similar reaction mechanism of the ring opening of THFA can be applied for the ring of THP2M giving 1,6-HDO.

Bibliography

PERSONAL DATA

Name : Husni Wahyu Wijaya
Gender : Male
Address : Jl. Mayjen Sungkono V1/11 Malang, East Java, Indonesia
Email : husni.wahyu.fmipa@um.ac.id and husniwahyu@gmail.com
Date of birth : October 1st, 1984
Nationality : Indonesia
Occupation : Lecturer at Chemistry Department, State University of Malang (*Universitas Negeri Malang*), Indonesia.

FORMAL EDUCATION

Bachelor in chemistry (S. Si.) and education of chemistry (S.Pd), State University of Malang (*Universitas Negeri Malang*), Indonesia.
Sept. 2003 to Sept. 2009.

Master of science (M. Si.) in Chemistry, Bandung Institute of Technology (*Institute Teknologi Bandung*), Indonesia.
Sept. 2010 to Oct. 2012.

Ph.D. in Applied Chemistry and Biotechnology Department, Chiba University, Japan.
April. 2015 to March. 2018.

RECENT PUBLICATIONS

1. H. W. Wijaya, T. Sato, H. Tange, T. Hara, N. Ichikuni and S. Shimazu, Hydrogenolysis of Furfural into 1,5-Pentanediol by Employing Ni-M (M = Y or La) Composite Catalysts, *Chem. Lett.*, 2017, **46**, 744–746.

2. H. W. Wijaya, T. Kojima, T. Hara, N. Ichikuni and S. Shimazu, Synthesis of 1,5-Pentanediol by Hydrogenolysis of Furfuryl Alcohol over Ni-Y₂O₃ Composite Catalyst, *ChemCatChem*, 2017, **9**, 2869–2874.
3. H. W. Wijaya, T. Hara, N. Ichikuni and S. Shimazu, Hydrogenolysis of Tetrahydrofurfuryl alcohol to 1,5-Pentanediol over a Nickel-Yttrium Oxide Catalyst Containing Ruthenium, *Chem. Lett.*, 2018, **47**, 103-106..

CONFERENCES

1. Husni Wahyu Wijaya, Takayoshi Hara, Nobuyuki Ichikuni, Shogo Shimazu. Catalytic activities of metal oxide (M = Y and La) promoted Ni catalysts in 1,5-pentanediol production from hydrogenolysis of furfural. **Chemical Society of Japan (CSJ): The 96th Annual Meeting 2016**, March 24- 27th, 2016, Doshisha University (Kyotanabe Campus), Japan.
2. Husni Wahyu Wijaya, Takayoshi Hara, Nobuyuki Ichikuni, Shogo Shimazu. Catalytic performance of yttrium oxide promoted Ni catalyst for 1,5-pentanediol production from hydrogenolysis of biomass-derived furfural. **International Symposium on Catalytic Conversions of Biomass (ISCCB 2016)**, June 27-30th, 2016, Taipei, Taiwan.
3. Husni Wahyu Wijaya, Takayoshi Hara, Nobuyuki Ichikuni, Shogo Shimazu. Hydrogenolysis of furfuryl alcohol in various alcohol solvents by Ni-Y₂O₃ catalyst. **The Catalysis Society of Japan (CatSJ): The 118th Catalysis Society Meeting**, September 21- 23th, 2016, Iwate University, Japan.